הטכניון – מכון טכנולוגי לישראל
Technion – Israel Institute of Technology

ספריות הטכניון
The Technion Libraries

בית הספר ללימודי מוסמכים ע"ש ארווין וג'ואן ג'ייקובס
Irwin and Joan Jacobs Graduate School

איפיון על-נוזליות ב- ^4He

ניר גוב

איפיון על-נוזליות ב- ^4He

חיבור על מחקר

לשם מילוי חלקי של הדרישות לקבלת תואר
דוקטור לפילוסופיה

ניר גוב

הוגש לסנאט הטכניון - מכון טכנולוגי לישראל
סיון תשנ"ח חיפה יוני 1998

לריקי ולהורי
באהבה

מחקר זה נעשה בפקולטה לפיסיקה בהדרכתו של פרופ. אריק אקרמן.

אני מודה לו על הנחייתו ותמיכתו במהלך המחקר.

ברצוני להודות למשה חביליו על השיחות המועילות ועזרה במהלך העבודה.

תודתי לטכניון על התמיכה הכספית הנדיבה בהשתלמותי.

תוכן עניינים

רשימת ציורים

תקציר

הליום 4 (^4He) על-נוזל הינו תופעה קוונטית מאקרוסקופית. על ידי קרור ההליום מתחת לטמפרטורה קריטית $T_\lambda=2.17^oK$ בלחץ-רווית-אדים (Saturated-Vapor-Pressure SVP) הנוזל הופך מנוזל נורמלי לעל-נוזל בעל תכונות קוונטיות כדוגמת העדר חיכוך וצמיגות, והולכת חום אינסופית ללא דיפוזיה. התנהגות העל-נוזל ניתנת לתיאור מאקרוסקופי תוך התחשבות התרמודינמיקה ובהידרודינמיקה היחודיות שלו. התאוריה המאקרוסקופית הזו נקראת "המודל הדו נוזלי" בו מפורק העל-נוזל לשני רכיבים: רכיב נורמלי (בעל צפיפות מסה ρ_n) המתנהג כנוזל רגיל בעל צמיגות ומכיל את כל האנטרופיה של העל-נוזל. בנוסף ישנו רכיב על-נוזלי (בעל צפיפות מסה ρ_s) שאינו מכיל אנטרופיה. שני הרכיבים בעלי מהירויות זרימה בלתי-תלויות המסומנות ב- v_n ו- v_s כאשר מהירות הרכיב העל-נוזלי מוגבלת להיות אי-רוטציונית. משוואות הרציפות עבור שני הרכיבים הן:

$$\rho = \rho_n + \rho_s \,, \vec{J} = \rho_n \vec{v}_n + \rho_s \vec{v}_s \qquad (1)$$

כאשר $\vec{J}$ הוא זרם הצפיפות הכולל ו- ρ היא הצפיפות הכוללת. מ-(1) ברור שבעל-נוזל ישנם שני גדלים תרמודינמים נוספים (על פני המצב בנוזל הרגיל) המתארים את מצב הנוזל והם: ρ_s ו- v_s.

תאוריה זו שפותחה ע"י לנדאו וחלטניקוב נותנת תאור טוב של ההידרודינמיקה והתרמודינמיקה של העל-נוזל כל עוד לא קרבים לטמפרטורת מעבר הפאזה.

בכדי לתאר את תלות ρ_n ושאר הגדלים התרמודינמים בטמפרטורה יש לדעת את ספקטרום האנרגיה של האקסיטציות האלמנטריות (קוואזי-חלקיקים) של העל-נוזל. נתון זה נמדד בד"כ ע"י ניסויים של פיזור אי-אלסטי של ניוטרונים, ותאוריות מיקרוסקופיות מנסות לחשב אותו.

התאור התאורטי המיקרוסקופי של העל-נוזל החל עם עבודתו של בוגוליובוב. תוצאת עבודה זו היתה תאור מקורב בשיטת שדה-ממוצע (Mean Field) של גז בוזה עם אינטראקציות חלשות (Weakly Interacting Bose Gas). נמצא שלגז זה יש ספקטרום פונוני (ז"א לינארי בתנע קטן) בדומה ל- ^4He על-נוזל. אין בתאוריה זו התאמה כמותית למהירות הקול הנמדדת והיא נכונה כל

עוד אחוז החומר שבתנע אפס (מוגדר 'אחוז העיבוי' כ- Condensate Fraction) הינו כמעט 100%, בעוד שבהליום- 4 על-נוזל אחוז זה הוא בערך 10% ב- T=0.

התאוריה הבאה לחישוב ספקטרום האקסיטציות הינה של פיינמן. ע"י שיקולי סימטריה של פונקציית הגל, הניח פיינמן את הצורה הבאה עבור פונקציית הגל של המצב המעורר של העל-נוזל:

$$\psi(\bar{R}_1 \ldots \bar{R}_n) = \left(\sum_{i=1}^{n} e^{i\bar{k}\cdot\bar{R}_i}\right)\varphi_0 = \rho_k^+|\varphi_0\rangle \qquad (2)$$

כאשר $\bar{R}_i$ הוא וקטור המקום של אטום i, φ_0 היא פונקציית הגל של מצב היסוד ו- ρ_k^+ הוא טרנספורם פוריה של אופרטור היצירה של הצפיפות. ההנחה היא שכל הקורלציות הסבוכות על-פני מרחקים קצרים בין האטומים בשל אינטראקצית גלעין-קשית (Hard Core) ביניהם אינן משתנות בשל האקסיטציה ונשארות כבמצב היסוד. לפיכך האקסיטציה אינה אלא שינוי צפיפות או פונון. ע"י שימוש בעיקרון מינימום של האנרגיה וסימטריית הזזה מתקבל הספקטרום הבא:

$$\varepsilon(k) = \frac{\hbar^2 k^2}{2mS(k)} \qquad (3)$$

כאשר m היא מסה אטומית ו- S(k) היא מקדם- המבנה הסטטי (Static structure factor) בוקטור-גל k, כפי שנמדד ע"י פיזור ניוטרונים. ביטוי (3) נותן התאמה איכותית לתוצאות הניסויים כאשר הוא משחזר את התכונות הבאות: ספקטרום לינארי (נקרא פונון) בוקטור-גל קטן $k\to 0$, ומינימום (נקרא רוטון) סביב $k \approx 1.9\,\text{Å}^{-1}$. מבחינה כמותית הביטוי נותן בערך פי-שניים מהערך הניסויי. בכדי לשפר את ההתאמה לניסוי נעשו ניסיונות בהם השתמשו בפונקציות-גל וריאציוניות מסובכות יותר מ- (2). המשותף לניסיונות אלו שמוסיפים בהם מבנה מקומי מורכב יותר, ז"א קורלציות בין-אטומיות נוספות על אלו שבמצב היסוד. בניסיונות אלו, שהחלו בעבודתם של פיינמן וכהן מאבדים את ההסבר הפיזיקלי של העירורים כשינויי צפיפות. ניתן בשיטה זו לקרב די-טוב את הספקטרום הנמדד אבל במחיר אובדן ההבנה של מהות העירורים.

אחרי הקדמה לנושא על-נוזליות ב- ^{4}He (פרק 1), אנו בוחנים את ה- ^{4}He על-נוזל משני אספקטים:

1) בפרק 2 נעקוב אחר התאור ההידרודינמי המקובל של העל-נוזל כפי שהוא בא לידי ביטוי בתגובה של העל-נוזל לשינויים חיצוניים. לשם כך משתמשים בתאורית התגובה-הלינארית

(Linear Response). בתאור זה ישנם מספר שאלות שאינן פתורות לגבי הקשר בין ההגדרות של צפיפות הרכיב העל-נוזלי (ρ_s) ואחוז העיבוי (n_0 Condensate fraction). אנו מוצאים שישנה תכונה של העל-נוזל שלא הודגשה ושנובעת מההגדרות הנ"ל, והיא שבצינור אינסופי ישנן קורלציות תנע-תנע לא-אלכסוניות אפילו בגבול התרמודינמי (שבו המערכת היא אינסופית בכל מימדיה). עובדה זו מצביעה על הימצאות ספונטנית של סירקולציה על-נוזלית סביב ציר הצינור. זוהי מערבולת קוונטית (Quantized Vortex). ע"י מיפוי הבעיה לזו של חלקיק טעון בשדה מגנטי ניצב, אנו מגיעים למסקנה שהעל-נוזל בצינור הינו במצב של 'פרומגנט-קוהרנטי':

$$L_z, L_- = L_x - iL_y \text{ כאשר } \rho_s / \rho = \langle L_z \rangle / \hbar, \quad n_0 = \left|\langle L_- \rangle\right|^2 / \hbar \langle L_z \rangle \text{ אופרטורים של תנע-}$$

זויתי ו- ρ היא הצפיפות הכוללת. מכאן שכדי להגדיר את המצב העל-נוזלי יש צורך ב- ρ_s וב- n_0 גם יחד. חישובים נומריים מראים שקיומה של מערבולת קוונטית לאורך הציר של צינורות יכולה להסביר תוצאות ניסויים של מהירות קריטית בעל-נוזל, ומחזקים את המסקנה שלנו שמערבולת כזו נוצרת באופן ספונטני.

אנו מוצאים שהאקסיטציות של המערבולת הקוונטית מקיימות משוואת שרודינגר ומקבלים קשר בין אחוז העיבוי והמבנה הפנימי של העל-נוזל ושל מרכז המערבולת הקוונטית (Vortex-Core). ספקטרום האקסיטציות הללו שמתקבל מתאים לתוצאות ניסויים המופיעים בספרות.

לבסוף באמצעות ספקטרום האקסיטציות של המערבולת הקוונטית אנו מגדירים פרמטר חסר יחידות ששולט במעבר מעל-נוזל למבודד כתוצאה מאי-סדר. פרמטר כזה הוגדר ע"י תאולס (Thouless) עבור מעבר מוליך-מבודד במתכת ובאמצעותו ניתן למצוא את המימד הקריטי שמתחתיו כל אי-סדר יגרום למיקום החלקיק (Localization) ולמצב מבודד. עבור הולכה חשמלית מימד זה הינו 2. אנו מוצאים שהמימד הקריטי עבור העל-נוזליות הוא אפס כך שרק בגאומטריה ממוקמת (Dot geometry=zero dimension) אין על-נוזליות. תוצאה זו מתאימה לתוצאות חישובים נומריים במימדים 1 ו- 2 בהם נמצא שיש על-נוזליות כל עוד האי-סדר חלש מספיק. גם בניסויים נמצא שבמערכות חד- ודו-מימדיות יש על-נוזליות.

2) בפרק 3 אנו מציאים תיאור חדש לספקטרום האנרגיה של האקסיטציות האלמנטריות של ה- ^4He על-נוזל. אנו מניחים שבנוסף לשינויי הצפיפות שהציע פיינמן ישנם בעל-נוזל אופני-עירור

Characterization of Superfluidity of ^{4}He.

NIR GOV

Characterization of Superfluidity of ^{4}He.

RESEARCH THESIS

SUBMITTED IN PARTIAL FULFILMENT OF THE REQUIREMENTS
FOR THE DEGREE OF DOCTOR OF PHILOSOPHY

BY

NIR GOV

SUBMITTED TO THE SENATE OF THE TECHNION-ISRAEL INSTITUTE OF TECHNOLOGY
SIVAN 5758 HAIFA JUNE 1998

To Riki and my parents.

This research was carried out in the Physics Department of the Technion under the supervision of Prof. Eric Akkermans.

I wish to thank Prof. Eric Akkermans for the supervision and support during the research.

I wish to thank Moshe Havilio for usefull discussions and encouragement.

The generous financial support of the Technion is gratefully acknowledged.

Contents

List of Figures

Abstract

In this thesis we have attempted to further our understanding of the phenomenon of superfluid ^{4}He. The phenomenon of superfluidity in ^{4}He is an example of a macroscopic quantum effect where the bulk matter has quantum features, such as zero-viscosity, quantized circulation etc. These features appear as the ^{4}He is cooled bellow a critical temperature $T_\lambda \simeq 2.17^oK$ (at Saturated Vapor Pressure (S.V.P.)), where it changes from a normal fluid to the superfluid phase. The subject has been intensively studied both experimentally and theoretically for 50 years, but still has many unexplained aspects, two of which are studied in this work:

1) One is to follow the conventional hydrodynamic definition of the superfluid as it appears in the response to external perturbations using linear-response theory [1], [2]. In this description there are some unresolved question as to the relation between the definitions of the superfluid-component density (ρ_s) and the condensate-fraction (n_0). We find that there is an overlooked property of the superfluid which follows from the above definitions and is that in a infinitely long tube there is off-diagonal momentum-momentum response even in the thermodynamic limit. We point out that this can be physically interpreted as signaling the occurance of a spontaneous circulation (quantized-vortex) along the tube's axis. Using an analogy with the commutation relations of a charged particle in a magnetic field we are led to the conclusion that the superfluid is a 'coherent-ferromagnet' phase where: $\rho_s/\rho = \langle L_z \rangle /\hbar, n_0 = \frac{|\langle L_- \rangle|^2}{\hbar \langle L_z \rangle}$ (L_z,$L_- = L_x - iL_y$ are the angular momentum operators where the tube axis is in the z-direction, ρ is the total density). Both ρ_s and n_0 are needed to define the superfluid phase. We also find a Schrodinger-like equation for the excitation modes of the quantized-vortex and relate the condensate-fraction to the internal structure of the fluid and of the vortex-core. Finally, using the vortex-modes' excitation spectrum that we have found we define a Thouless-like dimensionless parameter that controls the transition from superfluid to insulator due to disorder. We find a critical dimension of zero and give some physical comments on its relation to numerical and exprimental results.

2) The elementary excitation spectrum (phonon-roton branch) of the superlfuid ^{4}He has been a long-standing theoretical problem. This spectrum allows the calculation of the thermodynamic properties of the superfluid [3] and is measured by neutron-scattering experiments [52]. Since the pioneering work of Feynman [5] which proposed that the excitations are simple density fluctuations, there has been many improvements [6], [7], but at the price that the physical nature of the excitation is lost in the complicated variational wavefunction used. We propose a new description of the energy spectrum based on the assumption that in addition to the Feynman density excitations, there exist localized modes for which quantum statistical effects are importnat. These two modes are hybridized in a way reminiscent of the case of excitons in dielectric crystals [8]. This analogy allows us to write an effective Hamiltonian which we diagonalise using a Bogoliubov transformation. The resulting

spectrum of the phonon-roton branch comes out as half the energy of the Feynman excitation and compares well with the experimental results at S.V.P. and high pressure. We are also able to give an analytic expression for the scattering-intensity of the excitation as a function of the wavevector k, which agrees very well wuth the experimental results. We also predict another type of excitation which we interpret as the intrinsic vortex-loop excitation of the superfluid whose energy agrees with both critical-velocity and Raman scattering experiments. Finally we extend this theory to include a Fermi-Dirac excitation to describe the 'multiparticle'-excitation branch at higher energy.

List of symbols

Symbol	Meaning
ρ_s	Superfluid density
n_0	Condensate fraction
L_i	Angular momentum in direction i
ρ	Total density
k	Wavevector
ρ_n	Normal component density
T_λ	Transition temperature
$\overrightarrow{v_s}$	Superfluid velocity
$\overrightarrow{v_n}$	Normal component velocity
$\overrightarrow{J}$	Total momentum-density current
F	Free energy
$\overrightarrow{w}$	Relative internal velocity
$a_i^\dagger, a_i$	Creation and anihilation operators at site i
t_{ij}	Hopping amplitudes
U_{ij}	Interatomic potentials
μ_{dis}	Random on-site disorder
d	Dimension
μ	Chemical potential
p	Momentum
N_0	Condensate number
T	Temperature
m	Atomic mass
ψ	Wavefunction
Ψ	Condensate-wavefunction or superfluid order-parameter
$\theta(r)$	Superfluid phase
$\rho_k^\dagger$	Density fluctuation creation operator
φ_0	Ground-state wavefunction
$S(k)$	Static structure factor
λ_T	Thermal de-Brogli wavelength
W	Winding-length
$\varepsilon(k)$	Feynman energy-spectrum
E_0,$\hbar\omega_0$	Localized mode bare energy
χ''_{ij}	Imaginary part of the momentum-momentum susceptibility
$\chi_{ij}(k\omega)$	Real part of the momentum-momentum susceptibility

Symbol	Meaning
ω	Frequency
ω_0	Superfluid vortex rotation frequency
ω_c	Cyclotron frequency
B_z	magnetic field
$a_d, a_d^\dagger$	Circulation anihilation/creation operators
V_x, V_y	Magnetic velocity components
b	Radial length scale
V	Specific volume
$\overrightarrow{A}$	Vector potential
n	Particle number operator
f	Superfluid to condensate ratio
$\overrightarrow{J_l}$	Total longitudinal current density
η_{ij}	Viscosity tensor
ξ	Vortex displacement
z	Average number of nearest-neighbors
a	Vortex core radius
P	Pressure
t	Reduced temperature
n_v	Vortex density
Δ	Roton minimum energy
H	Hamiltonian
$Z(k)$	Single-particle scattering intensity
ΔE_0	Reduction in ground-state energy

Chapter 1

Introduction

1.1 Hydrodynamic description of superfluid ^{4}He

The superfluid phase of ^{4}He is achieved by cooling the normal-liquid phase below a transition temperature $T_\lambda = 2.17^oK$ at saturated-vapor-pressure (SVP). The phase diagram is shown in Fig.1.1. This phase is distinguished from the normal-liquid phase by having no apparent viscosity and having infinite thermal conductivity. A first theoretical description of the superfluid was proposed by Landau (1941). This hydrodynamic description of superfluid ^{4}He (known as the 'Two Fluid Model' (TFM)) is summarized in several reviews [9], [1], [2], [10], and was developed by Landau and Khalatnikov [3]. In this model the liquid consists of two interpenetrating liquids, a normal fluid and a superfluid, each with its own density and velocity fields. The superfluid fraction of the fluid does not contain any entropy and its mass density is ρ_s. This part of the fluid can have only irrotational flow with velocity $\overrightarrow{v_s}$. The normal component contains all the entropy of the liquid and has velocity $\overrightarrow{v_n}$ and density ρ_n such that the local density and momentum current density are:

$$\rho = \rho_n + \rho_s \qquad \overrightarrow{J} = \rho_n \overrightarrow{v_n} + \rho_s \overrightarrow{v_s} \tag{1.1}$$

where ρ is the total density.

The normal component is due entirely to the low-lying excitations or quasiparticles of the superfluid. It goes to zero at T=0 and becomes the entire density at T_λ, with the superfluid component having oposite behavior. Landau was able to express the normal component density ρ_n in terms of the thermally excited quasiparticles:

$$\rho_n(T) = \int \frac{d^3p}{(2\pi)^3} \frac{p^2}{3} \left[-\frac{\partial N(\varepsilon_p)}{\partial \varepsilon_p} \right] \tag{1.2}$$

where $N(\varepsilon_p) = \left(e^{\varepsilon_p / k_B T} - 1 \right)^{-1}$ is the Bose distribution function and ε_p is the excitation spectrum. Similarly he obtained the other thermodynamic quantities of the superfluid and by fitting to the experimental results was able to predict the approximate shape of the excitation spectrum even before it was directly measured.

The response of the superfluid to an external perturbation is therefore different from that of a normal fluid. In fact there appear long-range momentum-momentum

correlations in the superfluid, which are absent in the normal phase. The superfluid therefore has two additional thermodynamic quantities that describe its equilibrium state (1.1): the superfluid density and velocity ρ_s, $\overrightarrow{v_s}$. The free energy F depends on the relative internal velocity between the two components: $\overrightarrow{w} \equiv \overrightarrow{v_n} - \overrightarrow{v_s}$, in the form: $\partial^2 F/\partial w^2 = \rho_s/\rho$. In particular there can be metastable equilibrium states where the superfluid and the normal components have different velocities.

Since the superfluid velocity is irrotational it can be written as:

$$\overrightarrow{v_s} \equiv \frac{\hbar}{m}\overrightarrow{\nabla}\theta(r) \tag{1.3}$$

where $\theta(r)$ is some single-valued function which describes the phase of the complex order parameter at each point. The free energy therefore depends on the phase gradients, and a global phase relation between different points in the fluid describes the superfluid state. Due to the single-valued condition the phase can change by an integral number of 2π when going around a line-defect (vortex-core) where $\rho_s = 0$ and the phase $\theta(r)$ is undefined. This leads to vortices with quantized circulation around them, which are a unique feature of the superfluid.

1.2 Superfluid-insulator transition due to disorder

The problem of the superfluid transition in the presence of disorder has been treated previously [11]. It is concerned with the effects of a static random (disorder) potential which can lead, if sufficiently strong, to the localization of the atoms thereby destroying the superfluidity. Upon localization the atoms become randomly trapped and form a random solid called a Bose-glass.

The typical Hamiltonian studied in this respect is of the Hubbard form (see for example [11]):

$$H = -\sum_{i,j} t_{ij}\left(a_i^\dagger a_j + c.c.\right) + \frac{1}{2}\sum_{i,j} U_{ij} n_i (n_j - \delta_{ij}) - \sum_i \mu_i n_i \tag{1.4}$$

where the anihilation/creation operators $a_i^\dagger, a_i$ are of an atom at site i, t_{ij} are the hopping amplitudes (which maybe random but always positive), U_{ij} is the interatomic potential with the condition of hard-core repulsion built into the $n_i(n_j - \delta_{ij})$ factor ($n_i = a_i^\dagger a_i$). The last term is the random on-site disorder potential usually taken as uniformly distributed in the interval $[-\mu_{dis}, \mu_{dis}]$. This Hamiltonian describes lattice bosons that can move from site to (unoccupied) site and feel a pairwise interaction between them. This is a reasonable approximation of the superfluid where it is believed usually that the atomic interaction is weak and can be taken as a summation of pair interaction.

This Hubbard model is different from the continuum superfluid as even at zero-disorder it can become a Mott-insulator (solid) for strong enough interaction U and commensurate filling of the lattice. This insulator has the atoms in some periodic crystal solid. We are not interested in this transition but in the disorder-induced transition so we will concentrate on incommensurate filling where this problem is absent.

Calculating numerically the superfluid fraction from models like (1.4) in d=1,2 dimensions it was found that [12] (at T=0):

a) The value of ρ_s is reduced due to disorder so that it is less than the total density ρ.

b) There is a critical disorder μ_{dis} where the superfluid component goes to zero. It is not clear what are the critical exponents of this transition, and it has no physical realization at the moment.

c) This transition occurs for all dimensions $d \geq 1$.

In the above treatment it is still not clear as to the role of the superfluid quantized-vortices in the disorder driven transition and their possible effects on the critical exponents.

We shall go beyond the above mentioned numerical work and shall consider these questions using the approach of Thouless [40] on the problem of electron localization in disordered metals. The idea is to compare the energy change of an electronic level in response to changing the system size, to the energy gap between levels. If this ratio is such that it decreases with the system size then we can conclude that in the thermodynamic limit the electron is most likely in a localized state. The problem is to find such a dimensionless ratio that captures the physics of the energy levels of the system. For the metal-insulator transition this is the dimensionless conductance $g = G/(e^2/h)$, where G is the conductance.

1.3 Microscopic description of superfluid ^{4}He

The microscopic theory of superfluid ^{4}He starts with the works of Boguliubov [14] and Pitaevski [15] for the Weakly Interacting Bose Gas (WIBG). It is assumed there that the interactions between the atoms can be described by summation over pairwise interactions only:

$$\begin{aligned} H_{pair} &= \sum_i \frac{p_i^2}{2m} + \frac{1}{2}\sum_{i,j} V(r_i - r_j) \\ &= \sum_p \left(\frac{p^2}{2m} - \mu\right) C_p^\dagger C_p + \frac{1}{2}\sum_{qkk'} V(q) C_{k-q}^\dagger C_{k'+q}^\dagger C_k C_{k'} \end{aligned} \tag{1.5}$$

where (in the plane-wave representation) $C_p^\dagger, C_p$ are Bose creation/anihilation operators of ^{4}He atoms, μ is the chemical potential and the interaction $V(r)$ is taken to be of the Lennard-Jones form for the hard-core part and a r^{-6} van der Waals attraction. The assumption now is that the interactions are weak so that we are close to the Ideal Bose Gas situation where at T=0 all the atoms occupy the zero-momentum energy level (the condensate) $N_0 = C_0^\dagger C_0$. The effect of creating or anihilating an atom from the condensate makes a negligible change to the eigenstate and is approximated by:

$$\begin{aligned} C_0^\dagger |N_0\rangle &= (N_0+1)^{1/2} |N_0+1\rangle \simeq (N_0)^{1/2} |N_0\rangle \\ C_0 |N_0\rangle &= (N_0)^{1/2} |N_0-1\rangle \simeq (N_0)^{1/2} |N_0\rangle \end{aligned} \tag{1.6}$$

The next step is to isolate the $k = 0$ terms in the Hamiltonian so we finally get the Bogoliubov Hamiltonian:

$$H_B = \sum_p \left(\varepsilon_p + N_0 V(0)\right) C_p^\dagger C_p + \frac{1}{2} N_0 \sum_q V(q) \left(C_q^\dagger + C_{-q}\right) \left(C_{-q}^\dagger + C_q\right) \qquad (1.7)$$

This Hamiltonian can be diagonalized by using the mean field approximation and shows that the elementary excitation spectrum changes from the quadratic form of the Ideal Bose Gas (IBG) to a linear sound-like form in the long wavelength limit ($k \to 0$). This qualitative change is important since the excitation spectrum of the superfluid ^{4}He does have a linear (phonon) form with a sound velocity given by the slope, but there is no quantitative agreement with experiment. The limitation of the WIBG approach is that it treats the atomic interaction as a weak perturbation of the gas, while ^{4}He is a dense liquid with strong interactions (hard-core). In particular this theory is valid as long as the depletion of the condensate fraction due to the interactions is small: $n_0 = N_0/N \simeq 1$ (N is the total number of particles), while in the superfluid ^{4}He it is ~ 0.1 at T=0.

The Bogoliubov theory emphasizes the importance of the Bose-Einstein condensate in the superfluid as it affects the excitation spectrum. It also introduces the concept of broken symmetry (1.6) and Off-Diagonal-Long-Range-Order (ODLRO) [16] which appears in the single-particle (reduced) density matrix $\rho_1(r, r') = \langle \psi(r) | \rho | \psi(r') \rangle$:

$$\begin{aligned} \left\langle C_0^\dagger(r) \right\rangle \quad &\equiv \quad \Psi^*(r) \neq 0, \qquad \langle C_0 \rangle \equiv \Psi(r) \neq 0 \\ &\Rightarrow \quad \lim_{|r-r'|} \rho_1(r, r') = \Psi^*(r)\Psi(r) \neq 0 \end{aligned} \qquad (1.8)$$

where $\psi(r)$ is the ground-state wavefunction of the liquid and $\rho = \sum_i |\psi_i(r)\rangle \langle \psi_i(r)|$ is the density matrix. We introduce the expectation value $\Psi(r)$ to distinguish from the operator for creation and anihilation of the ^{4}He atoms $\psi(r)$.

This means that the broken symmetry of the superfluid state can be identified with a complex scalar function $\Psi(r) = |\Psi(r)|\, e^{i\theta(r)}$, with the properties of the particle annihilation operator: $\Psi(r) = \langle \psi(r) \rangle$. In such a system there is a Bose-Einstein condensation of particles into the zero-momentum state (when there is zero superfluid velocity), with the condensate-fraction given by: $n_0 \equiv |\Psi|^2$. The phase $\theta(r)$ is identified as that given in the definition of the irrotational superfluid velocity (1.3). Even though the Bogoliubov theory is not correct for ^{4}He we assume that there exists an order-parameter $\Psi(r)$ with the above properties in the real superfluid.

Another approach was provided by Feynman [5] who assumes from symmetry requirements a simple variational wavefunction for the excited states of the superfluid. This wavefunction represents a single pure density fluctuation of wavevector k (a phonon):

$$\psi(\overrightarrow{R_1} ... \overrightarrow{R_n}) = \sum_i e^{i \overrightarrow{k} \cdot \overrightarrow{R}_i} \varphi_0 = \rho_k^\dagger |\varphi_0\rangle \qquad (1.9)$$

where $\overrightarrow{R_i}$ is the position of atom i , φ_0 is the ground-state wavefunction and $\rho_k^\dagger$ is the Fourier transform of the density operator. The guiding idea is that all the

complicated short-range correlations between the atoms due to their strong hard-core interactions are unchanged by the excitation and remain as in the ground-state φ_0.

Using a minimum energy calculation and translational invariance the excitation spectrum is:

$$\varepsilon(k) = \frac{\hbar^2 k^2}{2mS(k)} \tag{1.10}$$

where m is the atomic mass and $S(k)$ is the static form factor at wavevector k measured by neutron scattering experiments. The relation (1.10) reproduces the qualitative features of the phonon-roton excitation branch (Fig.1.2): the linear phonon spectrum at $k \to 0$ and the roton minimum around $k \simeq 1.9\mathring{A}^{-1}$. Quantitatively it gives approximately twice the value of the experimentally measured spectrum. In order to improve the agreement there have been various attempts using increasingly involved variational wavefunctions that have been suggested over the years [6], [7]. The most recent works manage to reproduce quite closely the experimental spectrum but at the price that the excitation does not represent anymore a pure density fluctuation. All these elaborate wavefunctions have in common a more localized structure in the excitation.

It has also been pointed out [17] that the role of the condensate fraction and therefore of the Bose-Einstein condensation is not crucial for the development of the Feynman result. In particular it has been noted [18] that the Feynman density fluctuation is similar to zero-sound in a normal (non-superfluid) system like ^{3}He. In fact above the transition temperature T_λ the Feynman expression fits quite well the broad excitation peak found in neutron scattering experiments [17]. We therefore conclude that the Feynman excitation does not capture the essence of the superfluid order.

Another shortcoming of the above treatments is that the quantized vortex excitations that are unique to the superfluid state are not explicitly described, only the sound-like density fluctuations. These vortices have cores of microscopic size and should therefore appear in any microscopic description of the superfluid. It is therefore still an open problem to give a quantitative theoretical description of the excitation spectrum of superfluid ^{4}He, its condensate fraction, quantized vortex excitations etc.

The excitation spectrum has also a high-energy 'multiparticle' branch which has much lower intensity than the phonon-roton branch (Fig.1.2). The usual treatment is to describe it as multiple excitations such as roton-pair, roton-maxon pair (maxon is the excitation at the first maximum of the single excitation spectrum) etc. This analysis does not give the continuous shape of this higher branch or its intensity.

Another approach to describing superfluid ^{4}He is through Path-Integral Monte-Carlo (PIMC) calculations [19]. This numerical procedure calculates for a finite number of atoms (up to 128) and finite temperature the many-body density matrix:

$$\rho(R, R'; \beta) = \left\langle R \left| e^{-\beta H} \right| R' \right\rangle = \sum_n e^{-\beta E_n} \psi_n^*(R) \psi_n(R') \tag{1.11}$$

where $\beta = 1/k_B T$, H is the total hamiltonian, and $|R\rangle$ stands for some spacial

arrangement of the atoms. This can be rewritten in terms of Path-Integrals where the inter-atomic interaction is taken as a simple two-body potential and the Bose permutations are taken over the atomic indices. The resulting calculation gives the specific heat c_v, the superfluid fraction ρ_s and reduction in zero-point-energy as functions of temperature with a good accuracy. From these calculations came a direct theoretical indication that the condensate-fraction at $T \to 0$ is $\sim 10\%$, and that there are long-range off-diagonal momentum-momentum correlations proportional to ρ_s (see I.1).

The superfluid phase is distinguished in these calculations from the normal phase by having macroscopic permutation-cycles of the atoms that span the entire system. These amount to a non-zero expectation value of the winding-number squared (Fig.1.3):

$$\rho_s/\rho = \frac{\langle W^2 \rangle}{\lambda_T^2}$$

where $\langle W^2 \rangle$ is the expectation value of the square of the length of paths that wind around the entire system (periodic boundary conditions) and $\lambda_T^2 = \hbar^2/2mk_BT$ is the thermal de-Brogli wavelength of the atoms.

Due to the hard-core interactions these permutation cycles cause long-range coherence in the fluid, that is the paths with the largest statistical weight in the calculation are those with straight parallel winding paths. The broken-symmetry appears when a particular direction of permutations is selected, which occurs in reality due to some external infinitesimal symmetry-breaking field. It is therefore seen from these calculations that the Bose statistics in ^{4}He is essential for the appearance of superfluidity, as are the short-range hard-core-induced correlations.

In the above work [19] using the PIMC approach it was not possible to calculate the excitation spectrum of the elementary quasiparticles in the superfluid.

1.4 The research subject

This work is divided into two main sections:

1) There are some points in the hydrodynamic description which we aim to clarify:

a) The connection between the superfluid fraction ρ_s and the condensate fraction $n_0 \equiv |\Psi|^2$:

A possible identification [9]: $\Psi(r) = \sqrt{\rho_s(r)}e^{i\theta(r)}$, with $\Psi(r)$ obeying Schrodinger's equation leads to the following hydrodynamic equations:

$$\begin{aligned} \frac{\partial \rho_s}{\partial t} + \nabla(\rho_s v_s) &= 0 \\ \frac{\partial v_s}{\partial t} + (v_s \cdot \nabla)\, v_s &= \nabla\left(\frac{\hbar^2}{2m^2}\frac{\nabla^2\sqrt{\rho_s}}{\sqrt{\rho_s}}\right) \end{aligned} \qquad (1.12)$$

These equations cannot be right, since from (1.12) follows that the superfluid density is conserved seperately from the total density. The true mass conservation equation of the TFM is (see (1.1)):

$$\frac{\partial \rho}{\partial t} + \nabla(\rho_s v_s + \rho_n v_n) = 0 \qquad (1.13)$$

Further, there are systems of low dimensionality ($d < 3$) where there is a superfluid fraction ($\rho_s > 0$) but appparently no condensate fraction ($n_0 = 0$). It is therefore not entirely clear how are these two quantities related and which is the essential one for the superfluid phenomenon.

b) Disappearance of superfluidity due to disorder :

We are particularly interested in the possibility of defining a scaling dimensionless parameter from which we can find the critical dimensionality below which any amount of disorder will destroy the superfluid phase. This is along the same lines as the Thouless treatment of the conductor-insulator transition in metals. There this is the dimensionless conductance which serves as the scaling parameter: $g = \sigma L^{d-2}/(e^2/\hbar)$, where σ is the conductivity, L is the system length, d is the dimensionality and e the electron's charge. In that case that the critical dimensionality above which there is an insulator-conductor transition is 2.

To answer those questions in the first section we analyze the hydrodynamic description of superfluidity as summarized in [2],[1]. We start our analysis with the usual operational definition of the superfluid component density ρ_s and show by analogy with the two-dimensional motion of a charged particle in a magnetic field, that it describes spontaneous circulation in a cylindrical geometry. Using this we propose a natural definition of the 'macroscopic-wavefunction' or complex-order-parameter Ψ (where: $n_0 = |\langle\Psi\rangle|^2$) in terms of angular momentum-like operators. We find that the order-parameter Ψ obeys the Schrodinger equation of a free particle. The equation is that of spin-wave modes of the vortex which are quadratic in the wavevector $\overrightarrow{k}$. We therefore obtain a description where:

$$\rho_s/\rho = \langle L_z \rangle /\hbar, \qquad n_0 = \frac{|\langle L_- \rangle|^2}{\hbar \langle L_z \rangle} \tag{1.14}$$

(where: $L_- \equiv L_x - iL_y$, L_j is the angular-momentum operator in the $\widehat{j}$ direction and ρ the mass density) for a cylinder along the z-axis. Both (ρ_s,n_0) are needed to describe the superfluid state and are related to each other. The situation is that of a coherent-ferromagnet, with a spontaneous circulation in the z-axis, but also a finite circulation in the xy-plane.

We give a physical interpretation for this spontaneous circulation by identifying it with the bosonic permutation-cycles of the path-integral calculation of Ceperley [19]. The superfluid lowers its kinetic zero-point-energy (z.p.e.) in this way, and we give a quantitative estimate for the change in the ground state energy. The superfluid is shown to correspond to an XY-model which is known to describe the superfluid transition. We further relate the condensate fraction n_0 to the internal structure of the superfluid and to the vortex-core size.

We give some experimental and numerical evidence for the spontaneous circulation in ^{4}He, especially in cylindrical geometries.

From the above description of the superfluid and considering essentially the vortex modes, we write a Thouless-like criterion for the superfluid-insulator transition due to disorder. Using the vortex-modes' excitation spectrum, we get that the critical dimensionality for the transition is zero, unlike for metal-insulator transition where it is two.

2) In the second section we develope a phenomenological theory that incorporates the hydrodynamic density fluctuations with vortex-core excitations into a microscopic Hamiltonian. This is done by proposing an effective Hamiltonian for the hybridization of the Feynman-phonon and a localized excitation (representing a microscopic vortex-core element). Within the dipolar approximation like the exciton-photon treatment [8], we find that the resulting excitation spectrum is very close to the experiment and given by the simple result:

$$E = \varepsilon(k)/2$$

where $\varepsilon(k)$ is the Feynman spectrum (1.10). The calculation uses as a free parameter the constant energy level of the localized excitation E_0. It turns out that the energy of the resulting spectrum is independent of the choice of E_0. This description allows us to calculate the condensate fraction and the reduction in the ground-state energy at zero temperature. Both quantities compare well with the experimental results at saturated-vapor-pressure (S.V.P.) and high pressure.

In addition we predict a new excitation branch of constant energy which we identify as the intrinsic vortex-loop excitation of the superfluid with energy $2E_0$. We find experimental indications for this excitation in Raman scattering [20] and critical-velocity experiments [21].

Finally, we propose a new approach for the calculation of the high-energy 'multiparticle' spectrum of the superfluid ^{4}He by treating it as an elementary excitation of a free vortex-core, which behaves like a fermion. We use a Dirac Hamiltonian to describe it, and its mean-field solutions give the spectrum and the scattering intensity. Both compare favorably with the experimental results.

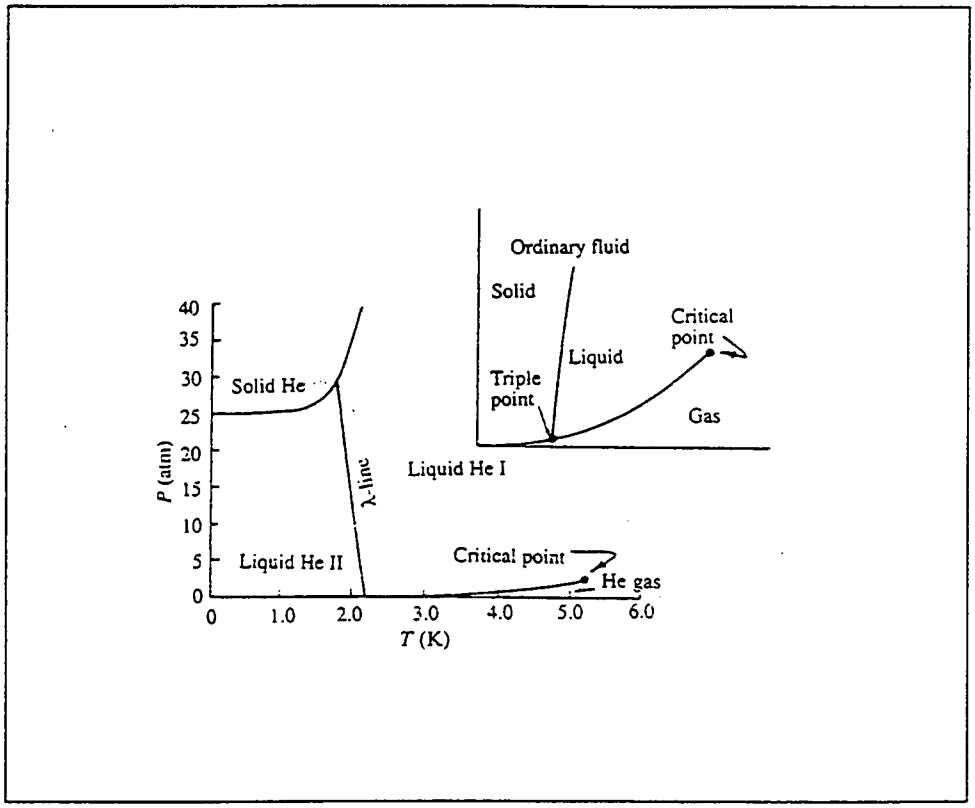

Figure 1.1: The P-T diagram for the condensed phases of ^{4}He contrasted to that of a normal liquid [17].

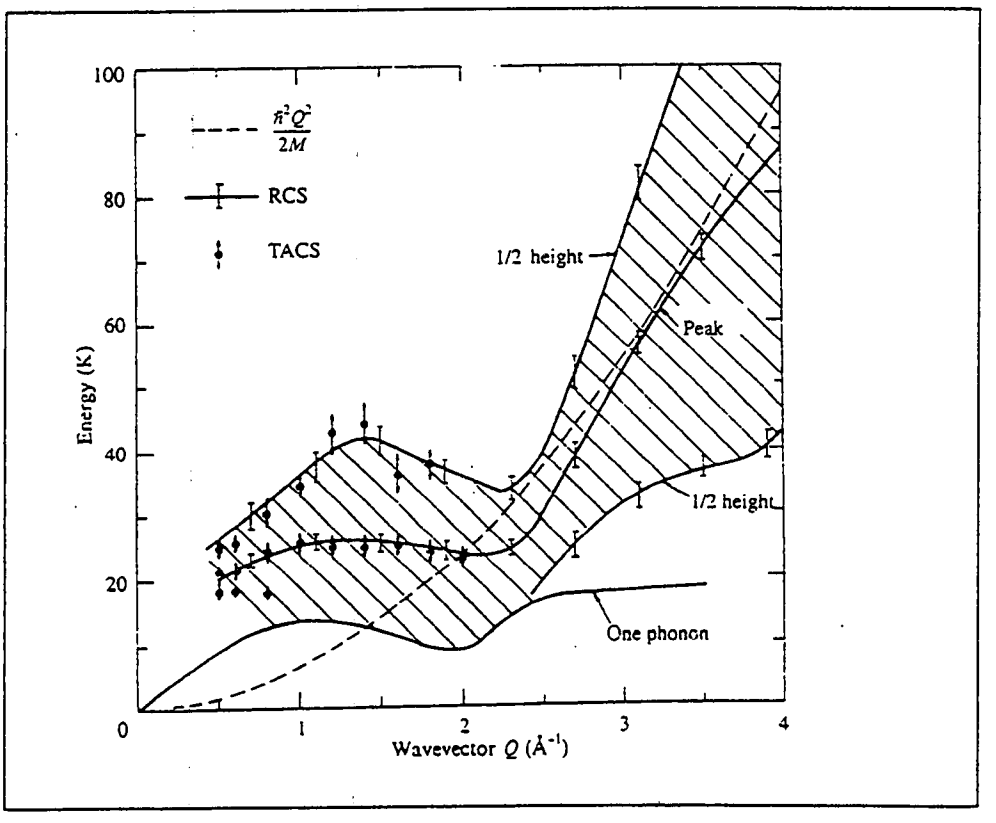

Figure 1.2: The excitation spectrum of superluid ^{4}He at $T = 1.1°K$ from inelastic neutron-scattering experiments [17].

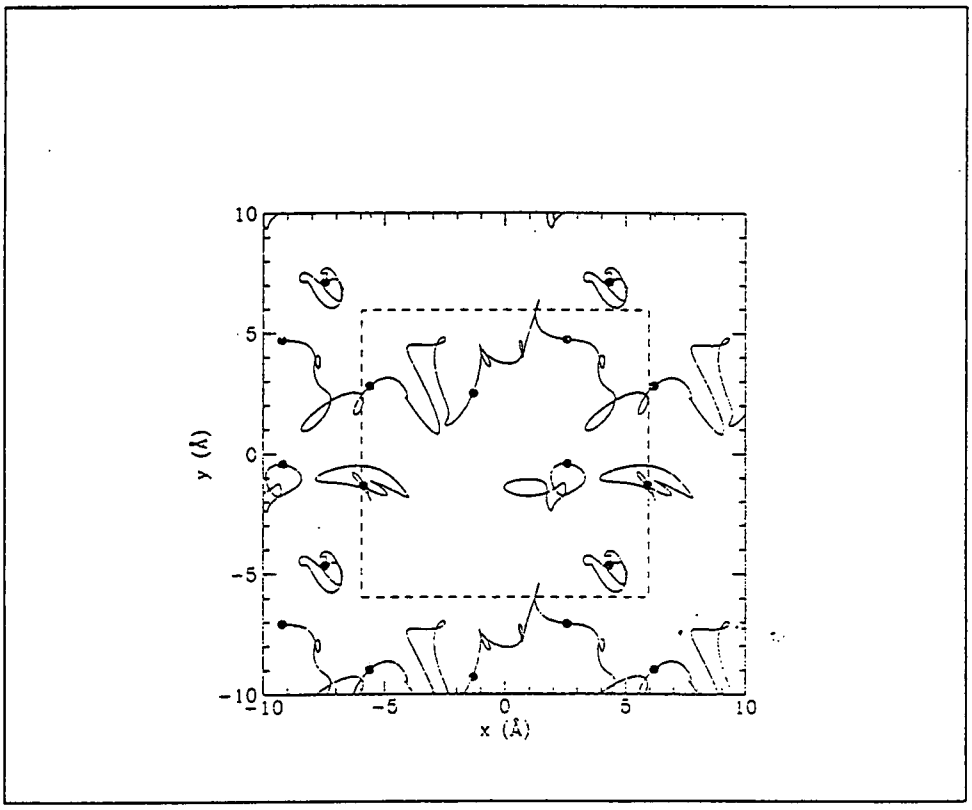

Figure 1.3: The trace of the paths of six ^{4}He atoms at $T = 0.75^oK$ in the Path-Integral Monte-Carlo calculations [19]. Three of the atoms are involved in an exchange which winds around the boundary in the x direction.

Chapter 2

Hydrodynamic description of superfluid ^{4}He

2.1 Introduction

We start with the conventional description of the superfluid through its linear response to external motion. In particular we want to investigate the momentum response of the superfluid to the motion of the walls of a long tube with velocity u. We begin by introducing the hydrodynamic definitions of the superfluid state [2], and then the contents of the section.

We define the superfluid state by the fact that the momentum density current sets up in the fluid as a response to the moving tube such that it is less than the entire fluid mass:

$$\vec{J} = \rho_n \vec{u} \qquad \rho_n \leq \rho \tag{2.1}$$

where the normal component density ρ_n is defined in the two-fluid-model described in the introduction and $\vec{u}$ is the velocity of the tube along its axis. Alternatively the expectation value of the momentum density is given by [2]:

$$\left\langle \overrightarrow{J(r)} \right\rangle_u = \frac{tre^{-\beta\left[H - \vec{P}\cdot\vec{u} + \frac{1}{2}Mu^2 - \mu N\right]} \overrightarrow{J(r)}}{tre^{-\beta\left[H - \vec{P}\cdot\vec{u} + \frac{1}{2}Mu^2 - \mu N\right]}} \tag{2.2}$$

where the mometum density operator is:

$$\overrightarrow{J(r)} = \frac{1}{2i}\left[\psi^\dagger(r)\left\{\vec{\nabla}\psi(r)\right\} - \left\{\vec{\nabla}\psi^\dagger(r)\right\}\psi(r)\right]$$

with $\psi(r), \psi^\dagger(r)$ the anihilation/creation operators of the ^{4}He atoms, and $\beta = 1/k_B T$. $\langle\rangle_u$ means the expectation value in the moving-tube condition, and using the equilibrium Hamiltonian given by:

$$H = \sum_i \frac{p_i^2}{2m} + \frac{1}{2}\sum_{i,j} v(r_i - r_j)$$

where $v(r_i - r_j)$ is the interatomic potential which is independent of the velocity of the tube.

The total momentum is given by: $\overrightarrow{P} = \int \overrightarrow{J(r)} dr$, and if we expand (2.2) to first order in u we get:

$$\langle J_z(r) \rangle_u = \langle J_z(r) \rangle + \beta \left[\langle J_z(r) P_z \rangle - \langle J_z(r) \rangle \langle P_z \rangle \right] u \tag{2.3}$$

where the tube axis defines the z-direction, and the expectation values on the r.h.s. are in the equilibrium system at rest ($u = 0$) where $\langle J_z(r) \rangle = 0$. Using linear response theory we get from (2.3):

$$\langle J_z(r) \rangle_u = \int dr' \int \frac{d\omega}{2\pi} \frac{\chi''_{zz}(r, r', \omega)}{\omega} u \tag{2.4}$$

where

$$\chi''_{ij}(r, r', \omega) = \int dt e^{i\omega(t-t')} \langle [J_i(rt), J_j(r't')] \rangle \tag{2.5}$$

By comparing (2.1) with (2.4) we get:

$$\rho_n = \lim_{k_x, k_y \to 0} \lim_{k_z \to 0} \int \frac{d\omega}{2\pi} \frac{\chi''_{zz}(k, \omega)}{\omega} = \lim_{k_x, k_y \to 0} \lim_{k_z \to 0} \chi_{zz}(k, \omega) \tag{2.6}$$

where we used:

$$\chi_{ij}(k\omega) = \int \frac{d\omega}{\pi} \frac{\chi''_{ij}(k\omega)}{\omega} \tag{2.7}$$

In addition there is in the superfluid a broken gauge-symmetry due to the Bose-Einstein condensation. This occurs when:

$$\langle \psi(r) \rangle = \sqrt{n_0} e^{i\theta(r)} \neq 0 \tag{2.8}$$

which means that there is fluctuating number of particles but a well defined global phase. This is identical to the case of a coherent-state in a quantum system. The definition (2.8) is the superfluid 'macroscopic wavefunction' or order-parameter. This is a complex scalar which is non-zero in the superfluid, except on the boundaries or along linear defects called vortex-cores. The superfluid velocity is non-rotational and given by the gradient:

$$\overrightarrow{v_s} = (\hbar/m) \nabla \theta(r)$$

The vortices in a superfluid are quantized so that around a vortex-core the phase $\theta(r)$ changes by an integral number of 2π, which causes a circulating superfluid.

In this chapter we shall develop the above definitions of the superfluid state. Our aim is to investigate the consistency of the above definitions of the superfluid and find their physical consequences. In particular we are interested in the phenomena of quantized vortices, effects of boundaries and destruction of superfluidity due to disorder.

In section 2.2 we find that in a long tube the superfluid has off-diagonal momentum-momentum response indicating the occurance of a spontaneous vortex along the tube axis. We propose a mapping of the superfluid to a 'coherent-ferromagnet'. From

this we develop the hydrodynamic susceptibilities of the superfluid (2.3) and show that it corresponds to broken time-reversal symmetry (2.4). Further results are the spectrum of the excitation modes of the vortex in a superfluid (2.5). We give some qualitative arguments for the physics behind the spontaneous vortex in a tube (2.6) and suggest a connection between the condensate-fraction (at T=0) and the spacial packing of the atoms (2.7). We then map this problem to an XY-spin model (2.8), compare with the results of Path-Integral Monte Carlo calculations (2.9) and vortex-ring theory (2.10). Some experimental and numerical evidence for such spontaneous vortex in a tube is presented in section 2.11.

Finally we define a Thouless-like criterion for the occurance of superfluidity as a localization problem (2.12,2.13).

We summarize the results in section 2.14.

2.2 The superfluid in a long cylinder - a coherent-ferromagnet

The phenomenological characterization of superfluidity is summarized in several reviews [2],[1]. It is still not clear though what is the connection between the operational definition of the superfluid-component ρ_s and the condensate fraction n_0. While the superfluid fraction is obtained from the off-diagonal momentum-momentum correlation function, the condensate is usually defined as the expectation value of the atomic annihilation/creation operator ψ: $n_0 \equiv |\langle\psi\rangle|^2$, or the magnitude of the 'condensate wavefunction' (order-parameter): $|\Psi| = \sqrt{n_0}$. It gives the macroscopic occupation of the lowest energy state, which in the thermodynamic limit (at T=0) is the zero momentum ($k = 0$) state.

The superfluid is usually defined operationally by the following physical circumstance:

The response of the fluid to an external velocity field (induced by moving the walls of the container) is dependant on the geometry. The susceptibility of the momentum density $\vec{J}$ to the external perturbation, i.e. the momentum-density correlation function, can be divided into longitudinal and transverse parts [1]:

$$\chi_{ij}(\vec{k}\,\omega) = \hat{k}_i\hat{k}_j\chi_l(k\omega) + \left(\delta_{ij} - \hat{k}_i\hat{k}_j\right)\chi_t(k\omega) \tag{2.9}$$

where: $\hat{k}_i \equiv \frac{k_i\hat{x}_i}{\left|\vec{k}\right|}$. This results from the three tensors that can be formed by the vector $\vec{k}$: δ_{ij}, k_ik_j and $\epsilon_{ijk}k_k$, where δ_{ij} is the Kronecker-delta and ϵ_{ijk} is the Levi-Civita tensor. Thus we can most generally write:

$$\chi_{ij}(\vec{k}) = A(k)\delta_{ij} + B(k)k_ik_j + C(k)\epsilon_{ijk}k_k$$

but $C(k) = 0$ since $\chi_{ij}(\vec{k})$ is even under parity, so we are left with the first two terms as in (2.9). The longitudinal component is parallel to $\vec{k}$ while the transverse

component is perpendicular [2]:

$$\sum_i k_i \left(\hat{k}_i \hat{k}_j\right) = k_j, \sum_i k_i \left(\delta_{ij} - \hat{k}_i \hat{k}_j\right) = 0$$

We now observe two different physical ways to take the (hydrodynamic) limit $\overrightarrow{k} \to 0$ (Fig.2.1):

1) In a closed tube the entire fluid moves with the container, by mass conservation. This situation is achieved by taking the 'plane'-limit:

$$\lim_{k_z \to 0} \left[\lim_{k_x, k_y \to 0} \chi_{ij}(\overrightarrow{k}) \right]$$

If we look at the component: $i = j = z$, then we have:

$$\lim_{k_z \to 0} \left[\lim_{k_x, k_y \to 0} \chi_{zz}(\overrightarrow{k}) \right] = \chi_l(k) \equiv \rho \tag{2.10}$$

where we used:

$$\lim_{k_z \to 0} \lim_{k_x, k_y \to 0} \frac{k_z k_z}{k^2} = 1$$

This result (2.10) corresponds to the mass conservation and follows from the usual f-sum rule.

2) The open tube, in the z-direction is achieved by taking the 'wire'-limit:

$$\lim_{k_x, k_y \to 0} \left[\lim_{k_z \to 0} \chi_{ij}(\overrightarrow{k}) \right]$$

If we consider motion along the tube axis, only the normal component is dragged with the walls so we have:

$$\lim_{k_x, k_y \to 0} \left[\lim_{k_z \to 0} \chi_{zz}(\overrightarrow{k}) \right] = \chi_t(k) \equiv \rho_n$$

where we used:

$$\lim_{k_x, k_y \to 0} \lim_{k_z \to 0} \frac{k_z k_z}{k^2} = 0$$

The susceptibility matrix is therefore:

$$\chi_{ij}(\overrightarrow{k}) = \rho_n \delta_{ij} + \rho_s \hat{k}_i \hat{k}_j \tag{2.11}$$

where: $\rho_s \equiv \rho - \rho_n$. The result (2.11) should be contrasted with the normal fluid behavior where both the longitudinal and transverse components of the susceptibility equal to ρ.

We summarize the response in the two limits and in the different directions:

		Wire limit	Plane limit
$\underline{i = j}$:	$i = j = z$	ρ_n	ρ
	$i = j = x, y$	ρ	ρ_n
$\underline{i \neq j}$:	$i = z, j = x, y$	0	0
	$i = x, j = y$	ρ_s	0

The top two rows in the table are the usual characteristics of a superfluid which we have demanded. In addition we find that the superfluid displays the other peculiarity:

$$\lim_{k_x,k_y\to 0}\left[\lim_{k_x\to 0}\chi_{xy}(\overrightarrow{k})\right]=\rho_s \tag{2.12}$$

To get (2.12) the limit of $k_x, k_y \to 0$ can be taken as:

$$k_x \equiv \alpha k_y \Rightarrow \lim_{k_x,k_y\to 0}\left[\lim_{k_x\to 0}\chi_{xy}(\overrightarrow{k})\right]=\rho_s\frac{2\alpha}{(1+\alpha^2)} \tag{2.13}$$

with the maximum given by $\alpha = \pm 1$, i.e. when the x and y limits are isotropic, which gives (2.12). This result is unexpected because it means that a perturbation in the x-direction produces a response in the y-direction. The sign of α is the sign of the vorticity of the response, or spontaneous vortex which we shall now introduce.

What is the physical meaning of the off-diagonal response (2.12) in the wire-limit ? We interpret this as pointing out the underlying vortex structure of the superfluid in this geometry. We shall explore now the consequences of (2.12) and its interpretation.

We shall be using [1]:

$$\int\frac{d\omega}{\pi}\frac{\chi''_{xy}(k\omega)}{\omega}=\chi_{xy}(k\omega) \tag{2.14}$$

where χ''_{xy} is the imaginary part of the susceptibility given by the Fourier-transform of:

$$\chi''_{ij}(\overrightarrow{r}t,\overrightarrow{r'}t')=\left\langle\frac{1}{2\hbar}\left[J_i(\overrightarrow{r}t),J_j(\overrightarrow{r'}t')\right]\right\rangle \tag{2.15}$$

i.e.

$$\frac{1}{2\hbar}\left\langle\left[J_i(\overrightarrow{r}t),J_j(\overrightarrow{r'}t')\right]\right\rangle(k,\omega)=\int d^dr e^{-ikr}\int dt e^{iwt}\left\langle\left[J_i(\overrightarrow{r}t),J_j(0,0)\right]\right\rangle$$

and the bra-ket is the expectation value:

$$\langle X\rangle=\frac{tr\left[e^{-\beta(H-\mu N)}X\right]}{tr\left[e^{-\beta(H-\mu N)}\right]}$$

with H the grand-canonical ensemble Hamiltonian and μ the chemical potential. The $\langle\rangle(k,\omega)$ means the time and space Fourier transform of the the expectation value.

Assuming that only one frequency (ω_0) gives the dominant contribution to the integral (2.14) at a certain radius from the central axis of the tube, we get from (2.14) and (2.15):

$$\begin{aligned}\chi''_{xy}(k\omega) &\simeq \pi\delta(\omega-\omega_0)\frac{1}{\hbar}\langle[J_x,J_y]\rangle(k\omega)\\ &\Rightarrow \langle[J_x,J_y]\rangle(rt)\simeq i\hbar\omega_0\rho_s\frac{\rho}{m}\end{aligned} \tag{2.16}$$

where we use: $\int d^3k \equiv \rho/m \equiv V^{-1}$ (V - specific volume), and take the equal time and place commutation. We shall take the commutators of operators to be non-zero only on equal sites so that the space Fourier-transform will only multiply or divide the expression by the specific volume. The above assumption of a single dominant frequency means that we consider the case where there is a vortex-like structure in the superfluid such that at each radius from the central core the atoms circulate with a definite angular velocity ω_0 (Fig.2.2). We take the time correlations of the rotational motion as the only important momentum-momentum correlation in the fluid, i.e. only the superfluid circulation.

It might be interesting to compare this with the case of a ferromagnet where: $\chi_{xy}(k\omega) = 0$ for the magnetization susceptibility, although there is also: $\chi''_{xy}(k\omega) \neq 0$. The ferromagnet is the $\omega_0 = 0$ limit of the superfluid case, since a domain of ordered spins in the z-direction have no natural frequency (or vortex structure). The antisymmetric response of the magnetization averages over time ($t \to \infty$) to zero.

This result highlights that the momentum-density operators $J_{x,y}$ in the two perpendicular directions do not commute. This is reminiscent of the results for a two-dimensional charged particle in a perpendicular magnetic field [22]. In that case the components of the particle velocity in the plane obey:

$$[V_x, V_y] = -i\hbar\omega_c/m \tag{2.17}$$

where $\omega_c = qB_z/m$, B_z the magnetic field perpendicular to the plane and q is the charge of the particle. The velocity associted with the particle is given by:

$$\overrightarrow{V} = \frac{1}{m}(\overrightarrow{P} - q\overrightarrow{A}) \tag{2.18}$$

where $\overrightarrow{A}$ is the vector potential such that: $\overrightarrow{B} = \overrightarrow{\nabla} \times \overrightarrow{A}$.

By comparison with (2.16) we see that in the superfluid case the role of the external magnetic field is played by the superfluid-fraction ρ_s/ρ with the sign of the magnetic field played by the sign of α in (2.13). So we can make the identifications:

$$\omega_c \equiv \frac{\rho_s}{\rho}\omega_0, \overrightarrow{J} \equiv \rho\overrightarrow{V} \tag{2.19}$$

where ω_0 will be shown to be independent of ρ_s. Using (2.19) we can equate (2.17) with (2.16). As we shall see due to the vortex structure in the superfluid the frequency ω_0 depends on the radius from the vortex-core. The superfluid at each radius is therefore mapped to a two-dimensional charged particle moving in a different uniform perpendicular field. The non-zero superfluid fraction behaves as a spontaneous magnetic field, again similar to a ferromagnet. Further, this magnetic problem can be solved using a mapping to a two-dimensional harmonic oscillator (in the gauge $\overrightarrow{A}(r) = -\frac{1}{2}\overrightarrow{r} \times \overrightarrow{B}$):

$$V_x = -\frac{i\omega_c}{2\gamma}(a_d - a_d^\dagger), V_y = \frac{\omega_c}{2\gamma}(a_d + a_d^\dagger) \tag{2.20}$$

where $a_d, a_d^\dagger$ are anihilation and creation operators of right (or left) circulation quanta (the direction depends on the sign of B_z), and $\gamma \equiv \sqrt{\frac{m\omega_c}{2\hbar}}$. These operators obey Bose commutation relations. The z-component of the angular momentum in this case is given by: $L_z = \hbar(a_d^\dagger a_d)$.

It is customary to define for the superfluid a complex-scalar order-parameter, which corresponds to the condensate-wavefunction, Ψ. Since in the two-dimensional magnetic problem there is a mapping to an harmonic oscillator which has Bose creation/anihilation operators and the ^{4}He is a Boson we are led to the following assumption: The superfluid wavefunction or order-parameter creation and annihilation operators are to be identified with the Bose-circulation operators:

$$a_d \equiv \Psi, a_d^\dagger \equiv \Psi^\dagger \tag{2.21}$$

where it is understood that the magnetic field of the equivalent charged-particle problem depends on the radius from the vortex-core axis.

We shall now use the mapping (2.21) to write the superfluid wavefunction in terms of the dynamical quantities of the circulation. The operators $a_d, a_d^\dagger$ are given in terms of the velocity associated with the 2d particle in the magnetic field:

$$a_d = i\frac{\gamma}{\omega_c}V_-, a_d^\dagger = -i\frac{\gamma}{\omega_c}V_+ \tag{2.22}$$

where $V_\pm = V_x \pm iV_y$.

If we now define $\omega_0 \equiv \hbar/2mb^2$, where b is a length of the order of the tube radius, we get from (2.21) and (2.22):

$$\Psi = mbV_-\frac{1}{\hbar\sqrt{\rho_s/\rho}}, \Psi^\dagger = mbV_+\frac{1}{\hbar\sqrt{\rho_s/\rho}} \tag{2.23}$$

We see that $mbV_\pm$ has units of angular-momentum, so that the result (2.16) can be recast in terms angular momentum operators:

$$L_i \equiv J_i Vb \Rightarrow [L_x, L_y] = i\hbar^2\frac{\rho_s}{\rho} \tag{2.24}$$

We therefore get that in the wire-limit there is a spontaneous angular momentum in the z-direction per atom given by:

$$[L_x, L_y] = -iL_z \Rightarrow \langle L_z\rangle = \hbar\frac{\rho_s}{\rho} \tag{2.25}$$

where the bra-ket means the expectation value in the ground-state.

We can then rewrite (2.23) as:

$$\left[\Psi, \Psi^\dagger\right] = 1, \Psi = L_-\frac{1}{\hbar\sqrt{\rho_s/\rho}}, \Psi^\dagger = L_+\frac{1}{\hbar\sqrt{\rho_s/\rho}} \tag{2.26}$$

This identification is similar to the Holstein-Primakof transformation done in a ferromagnetic system from the spin to Bose operators. This transformation is valid

as long as the total system spin (here angular momentum) is large, that is a macroscopic number of ordered spins. Here this restriction translates to a macroscopic condensate or superfluid fraction. We see that the Bose commutation relation of the superfluid wavefunction (2.26) is to be identified with the 'ferromagnetic' order (2.25).

The usual definition of the superfluid condensate is that of a coherent state:

$$\langle [n, \Psi] \rangle = -\langle \Psi \rangle = -|\Psi_0| \tag{2.27}$$

where: $n \equiv \Psi^\dagger \Psi$ is the particle number operator which is here normalized to one, and $|\Psi_0|$ is a real number, so that the condensate fraction is: $n_0/n = n_0 = |\Psi_0|^2$. The operators in (2.26) are taken per atom and dividing by V we obtain density operators.

Eqs. (2.27) and (2.26) give:

$$\langle L_+ \rangle = \langle L_- \rangle = \hbar |\Psi_0| \sqrt{\frac{\rho_s}{\rho}} \tag{2.28}$$

We therefore arrive to the relations:

$$\begin{aligned} \rho_s/\rho &= \langle L_z \rangle / \hbar, \qquad n_0 = \frac{|\langle L_- \rangle|^2}{\hbar \langle L_z \rangle} \\ &\Rightarrow \quad (\rho_s/\rho)/n_0 = |\langle L_z \rangle|^2 / |\langle L_- \rangle|^2 \end{aligned} \tag{2.29}$$

The situation in the wire-limit of a spontaneous single-quantized vortex along the z-direction allows therefore to define the superfluid and condensate fractions in terms of the expectation values of the angular-momentum operators.

This case is different from a usual ferromagnet in that we have a 'coherent-ferromagnet' (2.28):

$$L_- |\alpha\rangle = \alpha |\alpha\rangle \neq 0 \tag{2.30}$$

where the eigenvalue α depends on time as: $\alpha(t) = \alpha(0) \exp(\pm i\omega t)$, $\hbar\omega \equiv \langle H \rangle$.

This means that the 'superfluid atoms' behave as a coherent-state of a two-dimensional harmonic oscillator. Each 'superfluid-atom' is like a wave-packet of mass $m\rho_s/\rho$, with a time-dependent position along the circular trajectory. The coherent-ferromagnet has a macroscopic magnetization vector that has a constant z-component and an xy-component that precesses with constant (r-dependent) angular velocity. Both components (ρ_s,n_0) are therefore needed to define the superfluid state.

We can compare the Complete-Set-of-Commuting-Observables (CSCO) of a usual ferromagnet and of our superfluid 'coherent ferromagnet':

Ferromagnet: (L_z, L^2, H), Superfluid: $(L_z, L^2, L_\pm)$, where the commutation of $(L_z, L_\pm)$ is satisfied only approximately. These two cases of ferromagnets are due to the fact that the operators (L_z, L^2) that just describe the angular coordinates do not constitute a CSCO and have to be complemented by an additional operator that will remove the radial degeneracy [22].

2.3 Hydrodynamic susceptibilities

The spontaneous circulating currents J_x, J_y are superfluid currents since they are non-zero in an equilibrium state. These currents can be defined as:

$$\overrightarrow{J_{x,y}} \equiv \overrightarrow{v_s}\rho_s \tag{2.31}$$

with the superfluid velocity defined as:

$$\overrightarrow{v}_s \equiv \frac{\hbar}{m}\overrightarrow{\nabla}\theta = \frac{\hbar\overrightarrow{k}}{m}\frac{\Psi}{|\Psi_0|} \tag{2.32}$$

where the condensate wave-function is: $\Psi(r,t) = |\Psi_0|\exp(i\theta(r,t))$, and we performed a Fourier transform where k is the wavevector of the velocity of the circulating current.

Due to the circulating superfluid currents around the vortex, each atom has a kinetic energy:

$$\langle H_{kin}\rangle = \frac{\hbar^2k^2}{2m}\frac{\rho_s}{\rho} \tag{2.33}$$

where k is the wavevector of the momentum of the superfluid in its motion around the vortex.

From (2.24),(2.26),(2.31) we see that the definition (2.32) of the superfluid velocity operator follows:

$$v_{s-} \equiv L_-/\left(mb\frac{\rho_s}{\rho}\right) = \frac{\hbar}{m}\frac{1}{b\sqrt{\rho_s/\rho}}\Psi = V_-/\left(\rho_s/\rho\right) \tag{2.34}$$

where V_- is the velocity operator in the equivalent magnetic problem as defined in (2.23). Comparing with (2.32) we have arrive at the relation between the superfluid and condensate fractions:

$$f \equiv \frac{\rho_s}{\rho}/n_0 = \frac{1}{(bk)^2} \tag{2.35}$$

We find that f is some finite numerical factor, we know its value at T=0 when $\frac{\rho_s}{\rho} = 1$: $f(T=0) \simeq 10$ for ^{4}He.

In the usual quantum mechanical treatment we get for the probability current density and velocity:

$$\overrightarrow{J} = \frac{\hbar}{2i}\left(\psi\overrightarrow{\nabla}\psi^* - \psi^*\overrightarrow{\nabla}\psi\right) \Rightarrow \overrightarrow{v} \equiv \frac{\hbar}{2mi}\left(\psi\overrightarrow{\nabla}\psi^* - \psi^*\overrightarrow{\nabla}\psi\right)/\psi^*\psi \tag{2.36}$$

which is different from (2.32). We see explicitly that the superfluid velocity (2.32) is undefined if $\langle\Psi\rangle = |\Psi_0| = 0$, while the usual quantum-probability velocity (2.36) is still well-defined.

We now rewrite down the kinetic energy Hamiltonian per atom around the vortex (2.33):

$$H = \frac{1}{2}\frac{\rho_s}{\rho}mv_s^2 = \frac{1}{2\frac{\rho_s}{\rho}m}\left(VJ_{xy}\right)^2 = \frac{1}{2\frac{\rho_s}{\rho}mb^2}L_{xy}^2 = f\frac{\hbar^2k^2}{2m}\left(\Psi^\dagger\Psi + \Psi\Psi^\dagger\right) \tag{2.37}$$

where: $L_{xy}^2 = L_x^2 + L_y^2 = (L_+L_- + L_-L_+)/2$, and we used the definitions (2.26) and (2.35), V being the specific volume.

From (2.37) we write down the energy spectrum of the 'spin-waves' (magnon) that arise due to the 'ferromagnetic' structure (2.25):

$$\frac{dL_\pm}{dt} = \pm i\omega(k)L_\pm, \qquad \omega(k) = \frac{R}{V\langle L_z\rangle}k^2$$

where:

$$R \equiv \frac{1}{k^2}V\int\frac{d\omega}{\pi}\omega\chi''_{L_+,L_-}(k\omega) = \frac{V}{\hbar^2k^2}\langle[[L_+,H],L_-]\rangle = \frac{V}{(bk)^2}\frac{\rho_s}{\rho}\frac{\hbar^2}{2m} \quad (2.38)$$

$$= Vf\frac{\rho_s}{\rho}\frac{\hbar^2}{2m} \quad (2.39)$$

where we used:

$$\int\frac{d\omega}{\pi}\omega^n\chi''_{A_iA_j}(r,r',\omega) = \left\langle\frac{1}{\hbar}[[...[A_i(rt),H/\hbar]...,H/\hbar],A_j(r't)]\right\rangle$$

We therefore get:

$$\omega(k) = \frac{\hbar k^2}{2m}f = \omega_0 \quad (2.40)$$

The equation of motion for the angular momentum (and Ψ) is therefore:

$$\frac{dL_\pm}{dt} = \pm i\frac{\hbar k^2}{2m}fL_\pm \Rightarrow \frac{d\Psi}{dt} = -i\frac{\hbar k^2}{2m}f\Psi \quad (2.41)$$

Equation (2.41) is just the Schrodinger equation up to the factor f. It is important to notice that we obtained a Schrodinger-like equation due to the ferromagnetic nature of the superfluid state. We also notice that for the Ideal-Bose-Gas $f = 1$ and the equation is just the Schrodinger equation for a free non-interacting particle, as it should be.

The susceptibilities can now be calculated using the definition (2.14) and (2.38) using the Bogoliubov inequality for the ferromagnetic case [1]:

$$\int\frac{d\omega}{\pi}\frac{\chi''_{L_-L_-}(k\omega)}{\omega} = \chi_{L_-L_-}(k\omega) \geq \frac{\left|\int\frac{d\omega}{\pi}\chi''_{L_+,L_-}(k\omega)\right|^2}{\int\frac{d\omega}{\pi}\omega\chi''_{L_+,L_-}(k\omega)} \quad (2.42)$$

We can make this into an equality by calculating the bound on the denominator, which is given by (2.38):

$$\Rightarrow \chi_{L_-L_-} = \frac{|\langle L_z\rangle|^2}{(k^2R/V)} = \frac{2mV\hbar^2(\rho_s/\rho)^2}{\hbar^2k^2f\rho_s/\rho} = \frac{2mV|\Psi_0|^2}{k^2} \quad (2.43)$$

Similar results follow for the susceptabilities: $\chi_{L_+L_+}, \chi_{L_z-L_z}, \chi_{L_yL_y}$. We see that the susceptibility diverges in the thermodynamic limit $k \to 0$, meaning that the

spontaneous vortex can flip its axis in any direction without resistance in the infinite system. Without a boundary and pinning this is expected for a superfluid vortex.

Using the identities: (2.26),(2.24),(2.31) and (2.32) we obtain from (2.43):

$$\chi_{J_sJ_s} = \rho_s, \qquad \chi_{v_sv_s} = \rho_s^{-1}, \qquad \chi_{\Psi\Psi} = \frac{|\Psi_0|^2 (m/\hbar)^2}{\rho_s k^2} \tag{2.44}$$

where we used: $J_s^2 = J_{xy}^2 = J_x^2 + J_y^2$ etc. so that the factor 2 from (2.43) cancels out.

Alternatively, we can derive these identities directly from the Hamiltonian (2.37). For example, for the last identity in (2.44):

From the Bogoliubov inequality:

$$\chi_{\Psi\Psi} \geq \frac{\left|\int \frac{d\omega}{\pi} \chi''_{n\Psi}\right|^2}{\int \frac{d\omega}{\pi} \omega \chi''_{nn}}$$

we have:

$$\left|\int \frac{d\omega}{\pi} \chi''_{n\Psi}\right|^2 = \frac{|\Psi_0|^2}{\hbar^2} V^2, \qquad \int \frac{d\omega}{\pi} \omega \chi''_{nn} = V \frac{|\Psi_0|^2}{\hbar^2} \left[[\Psi, H], \Psi^\dagger\right] = V \frac{\rho_s}{\rho} \frac{k^2}{m} \tag{2.45}$$

$$\Rightarrow \quad \chi_{\Psi\Psi} = \frac{|\Psi_0|^2 (m/\hbar)^2}{\rho_s k^2}$$

where we again change the inequality to an equality by calculating the bound on the denominator.

Now the definitions of ρ_s in (2.12) and (2.35) are consistent if we can find that the superfluid current couples with the total longitudinal current in a form:

$$\lim_{k\to 0} \chi_{J_lJ_s} = \rho_s \tag{2.46}$$

where J_l is the total longitudinal current and J_s is the superfluid current density (which in the xy plane is just J_{xy}). If this follows from the relation (2.35) then the relation (2.12) is consistent with there being only one variable with long-range correlations in the superfluid. We write the longitudinal and transverse momentum-momentum susceptibility [1] as:

$$\begin{aligned} \chi_l(k) &= \chi_{J_lJ_s} \chi^{-1}_{J_sJ_s} \chi_{J_sJ_l} + \sum ..... \\ \chi_t(k) &= 0 + \sum ..... \end{aligned}$$

where the sum $\sum .....$ is the part that contributes equally to $\chi_l(k)$ and $\chi_t(k)$ as $k \to 0$. From (2.44) we know that: $\chi^{-1}_{J_sJ_s} = \rho_s^{-1}$. The longitudinal excess is therefore given by (from (2.12)):

$$\rho_s = \lim_{k\to 0} \chi_{J_lJ_s} \chi^{-1}_{J_sJ_s} \chi_{J_sJ_l}$$

which is our desired result if (2.46) is true, as we shall now prove.

We use (2.41) for the field Ψ , to get the following modified continuity equation:

$$m\frac{\partial n}{\partial t} + \overrightarrow{\nabla}.\overrightarrow{J_l} = 0 \tag{2.47}$$

where: $\overrightarrow{J_l} \equiv f\overrightarrow{J_0}, \overrightarrow{J_0} = \frac{1}{2i}\left(\Psi\overrightarrow{\nabla}\Psi^\dagger - \Psi^\dagger\overrightarrow{\nabla}\Psi\right)$.

If we use (2.47) and the definition of J_l, we get:

$$\chi_{J_lJ_s} = \frac{1}{V}\int\frac{d\omega}{\pi}\frac{\chi''_{J_lJ_s}}{\omega} \Rightarrow \chi_{J_lJ_s} = \frac{m}{Vk}\int\frac{d\omega}{\pi}\chi''_{nJ_s}$$

where J_l is now a current density. Using the definitions (2.31) and (2.32) gives:

$$\chi_{J_lJ_s} = \rho_s\frac{1}{V\Psi_0}\hbar\int\frac{d\omega}{\pi}\chi''_{n\Psi} = \rho_s$$

where we used (2.27), i.e. $\int\frac{d\omega}{\pi}\chi''_{n\Psi} = V\Psi_0/\hbar$. This is the required result (2.46).

We see that while the superfluid current becomes a zero-operator at T_λ , the total current remains a constant (assuming that as $T \to T_\lambda$, $f \to const.$, see Fig.2.3):

$$J_s = \hbar k\frac{\rho_s}{\rho} \to_{\frac{\rho_s}{\rho}\to 0} 0 \qquad J_l = f\hbar k \to_{\frac{\rho_s}{\rho}\to 0} \hbar k(\times const.)$$

Let us examine the definition of the number operator. If written in terms of the angular momentum operators we have:

$$n \equiv \Psi^\dagger\Psi = L_+L_-\frac{1}{\hbar^2\frac{\rho_s}{\rho}} \tag{2.48}$$

In (2.25) we saw that the superfluid fraction can be interpreted as the fraction of atoms with $\langle L_z\rangle = \hbar$ ($|l=1, m=1\rangle$) while the rest have zero angular momentum ($|l=0, m=0\rangle$). We count using L_+L_- only the fraction with $\langle L_z\rangle = \hbar$, so that divided by $\frac{\rho_s}{\rho}$ we will get the total density.

From the mean-field treatment of ferromagnetism we get that the susceptibility in the magnetized direction diverges at the critical temperature like:

$$\chi_{S_zS_z} \propto \frac{1}{T-T_c} \tag{2.49}$$

By analogy we expect for the superfluid that the angular momentum in the $\hat{z}$-direction will have a divergent susceptibility too, at the transition temperature. This corresponds to divergent density of vortices, which is expected at the superfluid transition according to vortex-loop models of the transition [23]. In particular, in two dimensions there is the result [24], that the vortex density ρ_v diverges below the transition like (2.49). We therefore have:

$$\chi_{L_zL_z} \sim \chi_{\rho_s\rho_s} \propto \rho_v \propto \frac{1}{T-T_c} \tag{2.50}$$

This Curie-type behavior (2.50) comes from mean-field but is found to be generally true in experiments on ferromagnetic systems.

2.4 Broken time-reversal symmetry

The commutation relations we have found for the superfluid transverse currents, and the dynamical equation (2.41), result in the following anti-symmetric relations:

$$\frac{dJ_x}{dt} = f\frac{\hbar^2 k^2}{2m} J_y, \qquad \frac{dJ_y}{dt} = -f\frac{\hbar^2 k^2}{2m} J_x \tag{2.51}$$

These are the set of equations that occurs for the coordinates of a vortex with zero core size in an incompressible liquid [25]. This can also be written in the form of an anti-symmetrical viscosity tensor η_{ij} [26]:

$$\frac{\partial J_i}{\partial t} = -\eta_{ij}\nabla_j^2 J_j$$

where: $\eta_{ij} = -\eta_{ji}$. In [26] such a situation is identified with broken time-reversal symmetry (TRS). It occurs in the Quantum Hall effect, the Magnus force in a superconductor etc. Just as in the QHE the anti-symmetric response (2.12) implies no-dissipasion, which in the superfluid means that only the superfluid component circulates with zero viscosity and quantized circulation.

We shall now see that in the coherent-ferromagnet/superfluid the TRS is broken:

The broken rotational symmetry in the x, y-axes is produced by: $\langle L_z \rangle \neq 0$. In addition we demand the coherence criterion: $\langle L_+ \rangle \neq 0$. This further breaks the rotational symmetry around the z-axis, leaving the system with no rotational symmetry. The precession of the circulation in the xy-plane now has a time-dependent angle, and together with the sign of $\langle L_z \rangle$ defines an imaginary motion along a screw in space. Such a motion is unique and is different from the motion along the same screw in the opposite direction, if time is reversed.

As seen in (2.30) the time dependence of $\langle L_\pm \rangle$ has a specific sign in the exponent. This time dependence is reversed under time-reversal.

We see therefore the connection between the superfluid density ρ_s and the condensate fraction n_0. The non-zero superfluid density ρ_s causes off-diagonal momentum-momentum correlations (2.12). This means broken TRS and such a state can be choosen as a coherent-state for the system, which leads to Off-Diagonal-Long-Range-Order (ODLRO) [27] and therefore a finite n_0.

2.5 Vortex modes

In ferromagnets it is known that the spin-wave excitations (2.40) have a spectrum which is quadratic in k. The result (2.41) is similar to that of Hall [28], where he finds that for the vortex displacement ($\xi = x + iy$ is the vortex displacement vector if the vortex axis is along the z-direction) in an incompressible liquid:

$$\frac{d\xi}{dt} = \pm i\frac{\hbar k^2}{2m}\mu\xi \tag{2.52}$$

where $\mu \equiv \ln(d/a)$, a is the core radius and d is related to the average vortex spacing from neighboring vortices or boundaries. There is some confusion as to

the meaning of d in μ, but the experimental results for oscillating vortices between parallel plates in superfluid ^{4}He give [28]: $\mu \sim 9.5 \pm 0.5$.

If we compare (2.52) and (2.41) we find that:

1) At the temperatures of the experiments in [28] we have: $\rho_s/\rho \simeq 1$, so that we predict from (2.35):

$$f \simeq 1/n_0 = \mu \Rightarrow n_0 \simeq 10.5 \pm 0.5\%$$

This value agrees with the experimental result for n_0 [29], so that our relation (2.41) is supported.

2) We can identify the 'macroscopic wavefunction' Ψ with the vortex core displacement ξ.

The result (2.40) is a mode of the vortex in the superfluid, distinct from the other hydrodynamic modes of the first and second sounds. In particular only the vortex-mode frequency (2.40) depends explicitly on the condensate fraction through the factor f, unlike the case of first and second sounds

$$\omega_1 = kc_1 = k\left(dP/d\rho\right)^{1/2}, \qquad \omega_2 = kc_2 = k\left(-\frac{\rho_s}{\rho_n}\frac{\partial T}{\partial(1/s)}\right)^{1/2}$$

where P is the pressure, T the temperature and s the specific entropy. In none of these thermodynamic quantities does the condensate fraction appear explicitly. In [30] it is stated that there is no experimental property of the superfluid that is directly dependent on the value of n_0. The vortex modes are therefore a prediction of an experimental observation directly dependent on n_0.

We can plot the function $f(T)$ using the experimental measurements of $\rho_s(T)/\rho$ and $n_0(T)$ [29], in Fig.2.3. We see that $f(T)$ is approximately constant up to $\sim 2^oK$. Close to the transition the lack of accurate measurements prohibits the calculation. We also plot the result of the formula of [31]:

$$f(T) = \frac{1-\rho_n(T)/\rho}{1-\rho_n(T)T/\rho T_\lambda}\frac{1}{n_0} \tag{2.53}$$

where n_0 is taken at T=0. This formula gives also an approximately constant $f(T)$, and at the transition temperature it gives $f(T_\lambda) = f(0)$.

In [28] it is mentioned that the factor μ in (2.52) does not change much with temperature, just as we expect if we equate it with $f(T)$.

2.6 Spontaneous circulation in a cylinder

Our interpretation is that the superfluid in the wire-limit has a remnant vortex structure in the thermodynamic limit. This means that there is a non-zero circulation in the ground-state. We now give a qualitative argument why the superfluid develops such a spontaneous circulation in a cylinder when the thermodynamic limit is taken (wire-limit).

In the normal fluid (and superfluid) the kinetic energy of the atoms at low T is predominantly the zero-point-energy (z.p.e.) given by:

$$E_k \simeq \frac{\hbar^2}{mV^{2/3}} \tag{2.54}$$

where V is the specific volume of an atom.

In order to reduce their z.p.e. the ^{4}He atoms become delocalized below the superfluid transition temperature. Due to their hard-core repulsion this delocalization is not homogeneous but the atoms form 'permutation' paths with their neighboring atoms. This appears clearly in the Path Integral Monte-Carlo (PIMC) calculations of Ceperley et al. [19]. In these calculations the atoms are taken as point particles with the true inter-atomic potential and Bose permutations. It is found that below the superfluid transition the atoms tend to form longer permutation-cycles that reduce their z.p.e.. Due to the hard-core repulsion the largest weight will be given to paths that are straight, i.e. where the atoms in neighboring paths are at constant distance from each other.

In a finite volume these permutation-loops span the system, with the largest weight given to a configuration of loops where the atoms take part in the straightest loops possible. In a closed cylinder there are two extreme cases (Fig.2.4): 1) straight paths along the axis, not including the end surfaces or 2) circular paths leaving out a central 'vortex-core'. Since the loops have to be closed the first option of axial-paths cannot occur, unlike the case of a torus. We are left with the spontaneous axial-vortex that will remain if we now extend the cylinder to infinity along its axis. As mentioned in [19] the superfluid order parameter is due to spontaneous breaking of the symmetry of the motion along these paths. This means that an infinitesimal external force selects the sign of the spontaneous vortex, and the Bose exchanges occur in one particular direction.

The z.p.e. of an atom along such a circular path is less then (2.54) since in one particular direction it is delocalized with kinetic energy proportional to the path's radius, i.e. given by (2.37). If there are z nearest-neighbors then the energy per superfluid atom, taking part in such a permutation cycle, is given by:

$$E_k' \simeq \frac{\hbar^2}{mV^{2/3}} + \frac{1}{2m}k^2 L_{xy}^2 \frac{1}{|\Psi_0|^2} - \frac{\hbar^2}{mV^{2/3}} \cdot \frac{\rho_s}{\rho}\frac{1}{z} \rightarrow_{k\rightarrow 0} \frac{\hbar^2}{mV^{2/3}}\left(1 - \frac{\rho_s}{\rho}\frac{1}{z}\right) \qquad (2.55)$$

where the first term is the zero-point-energy of the normal liquid, the second term is the kinetic energy due to the superfluid circulation and the last term is the part of the original z.p.e. now replaced by the circulation.

Since in the thermodynamic limit the second term vanishes ($k \rightarrow 0$), we are left with the first and last terms. The reduction in the ground-state energy per ^{4}He atom can therefore be approximated as (T=0, $z \simeq 8.0 \pm 1$ [32]):

$$\Delta E \sim E_k \cdot 1/z \simeq \frac{\hbar^2}{mV^{2/3}} \cdot 1/z \simeq 15^oK \cdot 0.125 = 1.88 \pm 0.1^oK \qquad (2.56)$$

which is of the order of the measured result [29]: $\sim 2.5 \pm 0.5^oK$. The average number of nearest-neighbors is found from neutron scattering where the spacial correlation function $g(r)$ is calculated as the Fourier transform of the static structure factor $S(k)$.

The total change in kinetic energy due to the presence of a straight vortex at T=0, in a cylinder of radius R and length L is:

$$E_T = \int \frac{1}{2}\rho_s v_s^2 d^3r - \int \frac{1}{z} E_k \frac{\rho_s}{m} d^3r \qquad (2.57)$$

$$= \pi L \frac{\rho}{m} \left(\frac{\hbar^2}{m} \ln (R/a) - \frac{1}{z} E_k R^2 \right)$$

where $v_s = \hbar/mr$, a is the vortex-core radius which is equal to the atomic separation and we take $\rho_s = \rho$ (T=0). The first term is the additional kinetic energy of the circulation while the second term is the z.p.e. reduction. The change in total kinetic energy (2.57) is negative if:

$$\frac{1}{z} E_k R^2 > \frac{\hbar^2}{m} \ln (R/a)$$

which for the values at saturated-vapor-pressure is always the case for all $R > 4\mathring{A}$ (we take: $a \simeq 2.9\mathring{A}$). So we conclude that for all macroscopic cylinders the kinetic energy is reduced due to the presence of a vortex.

An additional argument for the spontaneous vortex along the axis of a long cylinder is based on the symmetry of the superfluid order-parameter Ψ, which is a complex scalar. The zeros or defects of such an order-parameter of the lowest dimension are vortex-cores, which are one-dimensional lines of either infinite length or curled-up into vortex-loops.

Now the walls of the container are surfaces where the superfluid order-parameter vanishes. They are therefore 'vortex-sheets' made up of a dense arrangement of parallel vortex-cores with uniform vorticity. In a cylinder there are two different possibilities: straight parrallel vortices along the z axis, and circular vortex-loops along the circumference. The first possibility induces a vortex along the axis, while the second causes a linear current along the axis. The second possibility is ruled out by mass conservation in a cylinder with closed ends. The single axial vortex seems therefore to be a more natural possibility in an infinite cylinder.

By comparison, in a slab geometry any vortex-structure of the permutation cycles can first be transported to infinity when $k_{x,y} \to 0$, leaving a uniform fluid in the thermodynamic limit.

We point out that the argument based on the PIMC calculations shows the important effect of the hard-core interactions between the atoms. In a non-interacting Ideal Bose Gas (IBG) the weights of the paths have no advantage for straight paths, so the atoms are homogeneously spread-out throughout the volume, and no vortex arises.

2.7 Condensate fraction and vortex-core structure

We have shown in section II that the reduction in z.p.e. in the superfluid depends on $1/z$ where z is the average number of nearest-neighbors ((2.55),(2.56)). But at T=0 a fraction n_0 of atoms are in the $k = 0$ state, that is with zero z.p.e.. We therefore have the relation

$$n_0 \simeq 1/z \tag{2.58}$$

Therefore at s.v.p. and T=0 we have (using $z \simeq 8 \pm 1$) $n_0 = 12.5 \pm 1\%$, which is in the range of the measured values [29]. We thus propose that the condensate fraction at T=0 is determined by the short-range structure of the superfluid.

A longitudinal current $J_l \equiv fJ_0$ (2.47) along the axis of the cylinder is produced by the circulation (condensate wave-function):

$$\Psi = Ae^{ikz} \Rightarrow \overrightarrow{J_l} = fA^2\hbar k\hat{z} \tag{2.59}$$

where A is some constant. This is the form of a wavefunction of a free particle of momentum k in the z-direction. The circulation is thus constant along the tube but the vortex line has the shape of a helix since we saw in (2.52) that the condensate wavefunction can be identified with the vortex-core displacement. This means that the phase of the circulation changes linearly along the z-axis. We therefore see that a 'wiggling' vortex produces a net mass flow along its axis.

We see from (2.47) that the larger the factor f is the larger is the mass moved along the cylinder axis by the screw-like motion of the vortex-core. From (2.58) we find that the vortex-core contains approximately z atoms, that is a cluster of nearest-neighbors, and the mass flow is proportional to the vortex-core size, since (T=0):

$$n_0 = |\Psi_0|^2 = 1/f \simeq 1/z \Rightarrow f \simeq z \tag{2.60}$$

This can be understood if we assume that the same mechanism that depletes n_0 also causes the vortex core to become larger, that is stronger inter-atomic interactions and denser atomic packing. The vortex now has a 'thicker' core and causes more mass flow than a thin, straight vortex.

We are now in a position compare (2.58) with [33] where the following form of the condensate fraction for a hard-core gas is proposed:

$$n_0 = \frac{v}{V} \tag{2.61}$$

where v is the volume from which a particle is not excluded by the presence of the other particles, and V is the total volume. It is clear that the number of nearest neighbors is proportional to the density of the packing in a hard-core gas, so that $z \propto V/v$ which agrees with (2.58).

From the identification (2.58) we see that the condensate fraction at zero temperature is dependent on the internal geometry of the fluid. It has been found that at high pressure there is a rearrangement of the atoms in the liquid and not just a simple dilation. We can therefore estimate the condensate fraction at high pressure by assuming that just below the solidification pressure the number of nearest neighbors approaches the close-pack value of 12 (In [32] it is found that at high densities the number of neighbors approaches this value). We therefore get:

$$z(P = 24atm) \simeq 12 \pm 1 \Rightarrow n_0(T = 0, P = 24atm) \simeq 8 \pm 1\% \tag{2.62}$$

The experimental result is [29]:

$$n_0(T = 0, P = 24atm) \simeq 5.5 \pm 1\% \tag{2.63}$$

The comparison to the experimental ratio gives:

$$\frac{n_0(P = 24atm)}{n_0(s.v.p.)} \simeq \frac{0.055}{0.10} = 0.55 \pm 0.1$$

while from (2.62) and (2.56) we predict a ratio of: 0.67 ± 0.15, in rough agreement.

Further, it is found theoretically [34] that in the surface region of a superfluid droplet the condensate fraction approaches one. This is in accordance with our identification (2.58) since on the surface the density is very much reduced from its bulk value, and so should be the parameter z. A decrease in z will translate to an increase in n_0, approaching the limiting value of one.

2.8 Mapping to an XY-model

Superfluid ^{4}He and 3d XY ferromagnet are in the same universality class and have therefore the same critical exponents. We shall now describe a mapping of the superfluid to an XY-spin problem using the angular-momentum formalism we developed for the cylindrical case.

From (2.55) the reduction of the energy with respect to the superfluid order is:

$$H_{xy} = -\frac{1}{mV^{2/3}z\left|\Psi_0\right|^2}\left(L_{xy}\cdot L_{xy}\right)$$

where: $\langle L_{xy}\rangle = \sqrt{\frac{\rho_s}{\rho}}\left|\Psi_0\right|\hbar$. If the length of the spins is normalized to 1 then the XY Hamiltonian is:

$$H_{xy} = -J\sum_{i,j}\left(S^i_{xy}\cdot S^j_{xy}\right)$$

where i,j are the indices of the nearest-neighbor atomic sites, and the spins of the XY-model map to the vectors of the superfluid velocity times the 'radius' b, with the interaction constant

$$J \equiv \frac{\hbar^2}{mV^{2/3}z}\frac{\rho_s}{\rho} \tag{2.64}$$

Taking into account the z neighbors we get the energy reduction for a perfect ferromagnetic state

$$\Delta E = -\frac{1}{2}Jz \Rightarrow J = 2\frac{\hbar^2}{mV^{2/3}}\frac{1}{z^2}$$

If we take $z \simeq 8$, we get for the ^{4}He (using the experimental energy reduction)

$$J \simeq 0.62 \pm 0.1^oK$$

This gives in the 3D-XY model a critical temperature of

$$T_c = J/K_c \simeq 2.2 \pm 0.5^oK$$

where we have taken $K_c = 0.277$, which is the value at the critical point of a vortex-loop model of the XY-transition [23]. This is in rough agreement with the experimental value of: $T_\lambda \simeq 2.17^oK$.

We note also that in the 3D spin-1/2 XY-model the state of uniform magnetization is not the ground state of the Hamiltonian since the magnetization in the XY-plane does not commute with the Hamiltonian. The ground state has therefore a non-uniform configuration of the spins, which in the superfluid corresponds

to superfluid velocity. The spontaneous circulation in the cylinder is therefore in accordance with the situation in the XY-model.

In the superfluid the atoms synchronize their zero-point-motion in order to reduce the zero-point-energy, and in the presence of some symmetry-breaking external field will spontaneously produce a macroscopic circulation. The symmetry-breaking external field is provided in the wire-limit by the boundary of the container, which is an infinitely long cylinder of finite radius. The geometry of this situation provides a prefered direction ($\hat{z}$), and the circulation is azimuthal. In the equivalent XY-model this condition means that the spins have to be tangent to the boundary since there cannot be a superfluid velocity normal to the walls.

2.9 Path-integral calculations

We have already mentioned the results of the PIMC calculations in section IV.

Here we want to compare the expression found by Ceperley [36] with our expressions for the superfluid component and the condensate fraction. In a Bose system near zero temperature, the ground-state occupation of the zero-energy excitations is:

$$n_0 = \frac{1}{\exp(-\beta\mu) - 1} \rightarrow_{\mu\to 0} -\frac{1}{\beta\mu} \Rightarrow \mu \simeq -k_B T/n_0$$

The energy due to this occupation is therefore:

$$\begin{aligned} \Delta E &= -\mu n_0 = k_B T = \frac{1}{2} n_0 \hbar\omega_0 \\ \Rightarrow \; n_0 &= \frac{b^2}{\lambda_T^2} \end{aligned} \tag{2.65}$$

where the thermal de-Broglie wavelength is: $\lambda_T^2 \equiv \hbar^2/2mk_BT$, and we used the definition $\omega_0 \equiv \hbar/mb^2$. From (2.65) we find for the superfluid fraction (using (2.35))

$$\frac{\rho_s}{\rho} = \frac{1}{(k\lambda_T)^2} \tag{2.66}$$

This result is compared to that derived in [36]

$$\frac{\rho_s}{\rho} = \frac{\langle W^2 \rangle}{\lambda_T^2} \tag{2.67}$$

where $\langle W^2 \rangle$ is the expectation value per atom of the 'winding-length' squared of the path in a periodic system. From (2.66) and (2.65) it appears that at finite temperature the infinite superfluid will spontaneously break-up into finite domains, or vortices, such that the largest k for the calculation of the velocity or vortex excitations (2.40,2.32) is finite. This is seen in the real superfluid, especially near T_λ where the density of the vortices diverges [23],[37] such that

$$T_\lambda : k \to \infty, \left\langle W^2 \right\rangle \to 0 \Rightarrow \frac{\rho_s}{\rho} \to 0$$

Indeed, if the vortex density is given by

$$n_v \propto k^3$$

then using (2.66) we have

$$\frac{\rho_s}{\rho} \propto n_v^{-2/3}$$

Using the result of [24] for the vortex density in 2D, and assuming that it also pertains to 3D, we have:

$$n_v \propto t^{-1} \Rightarrow \frac{\rho_s}{\rho} \propto t^{2/3} \tag{2.68}$$

where $t = |T - T_\lambda| / T_\lambda$. This result is close to the measured critical exponent for the superfluid fraction at T_λ : $\sim 0.674 \pm 0.005$.

It is clear from comparing (2.66) and (2.67), that the paths winding around the system in the path-integral treatment just trace the spontaneous circulation around the vortex.

2.10 Vortex-ring theory of the λ-transition

The theory of the vortex-ring transition provides a natural additional motivation for our proposed spontaneous circulation. In this theory the fluid is filled by a dense collection of vortex-rings at the transition temperature. As the temperature lowers their density diminishes, similar to the density of free vortices in the Kosterlitz-Thouless (KT) transition in two dimensions. It is therefore not unreasonable that in a cylinder there will be a remaining vortex at low temperature. We shall now compare some features of this theory with our treatment.

In the vortex-ring theory of the superfluid transition as proposed by Williams [23], there is a definition of an effective core radius of a vortex ring. This effective core radius is shown to diverge at the transition temperature with the exponent which controls the divergence of the vortex diameter: $\nu \simeq 0.67$. The superfluid fraction and the condensate fraction both vanish near the transition as

$$\rho_s/\rho, n_0 \propto \xi^{-1} \propto a_{eff}^{-1} \propto t^\nu \tag{2.69}$$

where: $t = |T - T_\lambda| / T_\lambda$, ξ is the vortex diameter (coherence length), and a_{eff} is the effective core radius. The individual vortex-core in this model performs a self-avoiding-random-walk in 3D so that it is entangled into an effective core of radius a_{eff}.

We shall now present an aspect of the Vortex-loop model that may is related to our description of the modes of a quantized vortex. In a finite volume [23] the superfluid fraction scales at the transition temperature as

$$\rho_s = 0.484 \frac{m}{\lambda_{T_c}^2 L} \tag{2.70}$$

where: $\lambda_{T_c}^2 = \hbar^2 / 2mk_B T_c$, and L is the system size. On the other hand when looking at the response of the vortex-rings to a superfluid-velocity perturbation of the kind:

$$v_s = v_{s,0} \exp(i(\overrightarrow{k} \cdot \overrightarrow{r} - \omega t))$$

it was found that

$$\rho_s = 0.046 \frac{mk}{\lambda_{T_c}^2} \tag{2.71}$$

The response function of the vortex ring is taken as a square function, falling to zero at: $ka = 8.6$ (a is the atomic radius). We therefore conclude by comparing (2.70) with (2.71) that:

$$k = \frac{1}{L} 10.52 \tag{2.72}$$

The energy of a vortex ring with wavevector k is proportional to f according to (2.40), while here this energy is given by:

$$E \sim \hbar k v_s$$

To get a match with the finite-size effect of L the wavevector needs to be multiplied by f, which is the meaning of the factor in (2.72). From (2.72) we therefore obtain

$$f = \frac{\rho_s/\rho}{n_0} \simeq 10.52$$

If the factor f is constant at all temperatures then we conclude that at zero temperature the condensate fraction is: $n_0 \simeq 9.5\%$. This value is consistent with accepted estimates [29].

2.11 Experimental evidence for spontaneous circulation in a cylinder

There has been some experimental evidence that remanent vorticity exists in all samples of superfluid ^{4}He [37]. It was found that in a planar geometry there is an equilibrium density of vortices that connects the lower and upper plates (Fig.2.5). This density is independent of the surface quality of the plates and of the rate of passing through the superfluid transition temperature. It is given approximately as:

$$L \sim 2\ln(D/a)/D^2$$

where D is the distance between the plates and $a \simeq 1.4 \times 10^{-8} cm$ is the vortex-core radius. In the plane geometry this equilibrium vortex density is a metastable equibrium since at this density the vortices exert no forces on each other, and are loosly pinned to the plates. Any superfluid velocity between the plates will 'wash' them away. They prove, though, that vorticity is spontaneously created at the superfluid transition.

There is an indirect indication that in experiments with long cylinders a more persistent type of remnant vorticity exists. These are critical-velocity or superfluid-turbulence experiments [38] in long capillaries where the superfluid flow becomes resistive at a critical velocity which is temperature-independent but size-dependent. It has been suggested [39] that an initial vortex running along the capillary, but pinned away from it (in a low velocity region) can be a mechanism for the turbulence transition. It is not known at present where this long vortex comes from. We therefore see this calculation as an indication that in cylinders there is a spontaneous vortex along its axis.

2.12 The effect of disorder on the superfluid transition

Following the ideas first discussed by Thouless [40] concerning electron localization in a disordered metal, we are now looking for the critical dimension for the occurance of superfluidity. The critical dimension is understood as the dimension above which there is a well defined transition point from superfluid to some other non-superfluid phase at zero-temperature as a function of the strength of the disorder. We look for the conditions of localization of the superfluid current (velocity) i.e. such that the long-range coherence and superfluid order are destroyed.

Let us rewrite the relation (2.45) as a diffusion equation by rewriting the original Josephson relation:

$$\chi_{\Psi\Psi}(k,\omega) = \frac{|\Psi_0|^2 (m/\hbar)^2}{\rho_s k^2} \Rightarrow \rho_s = \frac{|\Psi_0|^2 (m/\hbar)^2}{k^2 \chi_{\Psi\Psi}} \tag{2.73}$$

We write the equation of motion of the superfluid velocity as

$$\frac{\partial v_s}{\partial t} = i\omega \frac{\hbar}{m} \frac{\nabla\Psi}{\Psi_0} \equiv \frac{F}{m} \equiv A \tag{2.74}$$

The force A represents random fluctuations in space and time in the field Ψ. These random fluctuations result in an effective force on the superfluid component. By analogy with Brownian motion we can add to (2.74) a viscosity term of the form: $m\gamma v_s$, where γ is the viscosity constant. The results are standard

$$m\left\langle v_s^2 \right\rangle = mC/2\gamma \Rightarrow \gamma = \frac{m}{2\hbar\omega} \int \langle A(0)A(t)\rangle \, dt \tag{2.75}$$

where $C \equiv \langle A(0)A(t)\rangle(\omega)/2\pi$, and we have assumed that the average kinetic energy is $\hbar\omega$. The diffusion constant follows

$$\left\langle r^2 \right\rangle = 2\left\langle v_s^2 \right\rangle \frac{t}{\gamma} \equiv D_s t \Rightarrow D_s = 2\left\langle v_s^2 \right\rangle / \gamma = \left(\frac{2\hbar\omega}{m}\right)^2 \left(\int \langle A(0)A(t)\rangle \, dt\right)^{-1}$$

Using (2.74) we finally get:

$$D_s = \left(\frac{|\Psi_0|}{k}\right)^2 \left(\int \langle \Psi(0)\Psi(t)\rangle \, dt\right)^{-1} \tag{2.76}$$

which in the $k, \omega \to 0$ limit is:

$$D_s = \left(\frac{|\Psi_0|}{k}\right)^2 \frac{V}{\hbar\chi_{\Psi\Psi}(k,\omega)} \tag{2.77}$$

where V is the molar volume.
From (2.73) and (2.77) we finally obtain for the superfluid fraction:

$$\frac{\rho_s}{\rho} = \frac{D_s}{D_0} \tag{2.78}$$

where $D_0 \equiv \hbar/m$. We note from (2.78) that large fluctuations in Ψ cause large $\chi_{\Psi\Psi}$ and therefore small diffusion coefficient. The 'superfluid-diffusion' described by D_s represents the ordered superfluid circulation, and therefore decreases if the field is not uniform. From (2.25), ρ_s/ρ represents the ordered circulation around the z-axis so if the superfluid velocity becomes more random then the circulation is decreased (2.44):

$$\chi_{v_s v_s} = {\rho_s}^{-1} \Rightarrow \langle L_z \rangle / \hbar \propto 1/\chi_{v_s v_s}$$

According to Thouless [41] if an eigenstate of a system of size L is extended, i.e. delocalized, then it will broaden upon enlarging the system to infinity. The energy width ΔE of this broadening is given by the curvature of the energy levels when changing the boundary conditions [42]. On the other hand a localized eigenstate will remain localized inside the original box of size L, and in the infinite system will be unaffacted by a change of boundary conditions at infinity. Thouless assumed that there is a single parameter that describes the behavior of the eigenstates and it is the ratio of the energy broadening to the typical level spacing in the original system. If there is localization this ratio should vanish in the thermodynamic limit, otherwise it signals delocalization. For the case of electron conductivity this dimensionless parameter is the conductance written in units of $e^2/\hbar$.

The dimensionless parameter in our case is:

$$g_s \equiv \frac{\hbar/t}{\delta E} \tag{2.79}$$

where $\hbar/t$ is the diffusion energy of the superfluid current over the system (t here is the time), and δE the level spacing for the excitations of the superfluid current. The superfluid-diffusion energy is a measure of the effects of the boundaries on the fluid by creating superfluid currents through the system, while the excitation spectrum is just the level spacing in the system.

Then

$$\hbar/t = \hbar D_s/L^2 = \frac{\rho_s}{\rho}\frac{\hbar^2}{m}L^{-2}$$

We assume that the superfluid transition is driven by the proliferation of vortices both at zero-disorder and finite temperature [23], and at zero-temperature and finite disorder (see the end of this section). The excitations which are therefore dominant near the transition are the natural modes of the vortex (2.40)

$$\delta E = \hbar\omega(k) = \frac{\hbar^2}{m} f L^{-2} \tag{2.80}$$

where $k \sim L^{-1}$.

Then

$$g_s = n_0 \tag{2.81}$$

By comparison, for the electron conductivity we have:

$$\sigma = \frac{De^2}{2(dE/dn)} = \frac{De^2}{2(dE/dN)V} \tag{2.82}$$

And therefore the criterion for metal-insulator transition is:

$$\begin{aligned} \delta E &= dE/dN, \qquad \hbar/t = \hbar D/L^2 \\ \Rightarrow \quad g &= \frac{\hbar/t}{\delta E} = \sigma\left(\hbar/e^2\right) L^{d-2} \end{aligned} \tag{2.83}$$

In order to learn about the critical dimensionality in the metal-insulator transition we must take into account that the conductivity σ might depend on the size L too. If there is no such dependence (when there is no spin-orbit coupling) then the critical dimensionality for conductivity with disorder is found to be 2, since at two or lower dimensions g will vanish in the thermodynamic limit. In this case this critical dimension can be read directly from (2.83). For dimension large enough to have a metal-insulator transition it is found that at the transition point itself the dimensionless parameter g is independent on the system size L.

Similarly from (2.81) we conclude that disorder (of any strength) will prohibit superfluid currents only at zero-dimensions ('dot' geometry), i.e. in a closed geometry. This is since at any dimension large enough to hold a vortex-structure ($d \geq 1$) the ratio g_s does not vanish in the thermodynamic limit and there is therefore no localization (as long as n_0 is non-zero). We note the appearance of the condensate fraction n_0 in (2.81) so it is thus possible to distinguish between different superfluids using the Thouless-like parameter g_s. This would not be possible if instead of n_0 we would get ρ_s/ρ in (2.81), which is always 1 at T=0. By comparing with the metal-insulator transition we find that the superfluid is always at the critical point since g_s is independent of the system size L. We are not sure of the meaning of this specific point at the moment.

By comparing (2.78) with (2.67) we arrive to [36]:

$$D_s = \left\langle W^2 \right\rangle / \tau_T \tag{2.84}$$

where: $\tau_T \equiv \hbar/2k_BT$. We see that for the superfluid diffusion-coefficient only macroscopic, winding paths contribute.

Let us compare the localization transitions for superfluids and metals. Both transitions are signaled by the vanishing of the diffusion constant:

$$\begin{aligned} \sigma &= D/D_0 \to 0 \Rightarrow D \to 0 \\ \rho_s &= D_s/D_0 \to 0 \Rightarrow D_s \to 0 \end{aligned}$$

The essential difference is the following:

Metal-insulator: The electron becomes localized when, even for infinite time, its average diffusion distance squared is finite:

$$D = \left\langle x^2 \right\rangle / \tau \to 0 : \qquad \left\langle x^2 \right\rangle \to const., \tau \to \infty$$

Superfluid-normal fluid: The superfluid 'phase' diffusion ceases when the average winding distance squared is zero, even for finite time:

$$D_s = \left\langle W^2 \right\rangle / \tau_T \to 0 : \qquad \left\langle W^2 \right\rangle \to 0, \tau_T \to const.$$

Although in both cases the diffusion constant vanishes, we see that the mechanisms are 'complementary'.

The critical dimension for disappearance of superfluidity due to any amount of disorder is found from (2.81) to be 0, i.e. this is the dimension at which there is strictly no superfluidity. We understand this result by assuming that the vortex excitations are dominant near the transition, or alternatively that the important disorder is related to vortex creation.

We note that in a recent experiment it was shown that in a quasi-1D system there is superfluidity at finite temperature [43]. This is in accordance with our finding that there is superfluidity in all d¿0 at both finite temperature and disorder.

There is further support for our treatment of the disorder through the spectrum of vortices in the experiments of [44]. In these experiments superfluid ^{4}He fully penetrates an ultralight silica aerogel. It is found that the excitation spectrum is affected by the static disorder in a way that can be explained through the introduction of vortices. The disorder is therefore mainly manifested through the vortices it induces in the superfluid, justifying our treatment.

In the calculations of [45] it is shown that the static disorder potential reduces the superfluid density (or 'stiffness') by allowing large local twists in the phase. These large twists are localized around the 'impurities' (large disorder potential), where they mean localized momentum correlations. This is just the situation around a vortex-core. This is further supports the idea that vortices are driving the superfluid transition both through temperature and disorder.

2.13 Superfluids films and lines

We now consider with the relation between the critical dimension for disorder- and temperature-transition and the absence of condensation in dimension lower than 2 for finite temperature (Hohenberg-Mermin Theorem (HMT)[46]). We note [24] that in the derivation of the HMT we need to use the Boguliubov inequality and the continuity equation. The velocity field of a vortex satisfies, in two dimensions

$$\vec{\nabla} \cdot \vec{J}_{xy} = 0$$

The vortices are therefore not taken into account in the HMT, only the phonon(densi fluctuations) excitations. We therefore assume that the vortex excitations allow a finite condensation in two dimensions and in one dimension at finite temperature, using the following picture:

A 'two dimensional' system with finite condensation and superfluidity needs to have some finite thickness. This is needed to support a vortex of some minimum length. Similarly in a 'one dimensional' configuration. Such a minimum thickness $L_{\min}$ (or radius of the cylindrical-pore) changes the system to an effectively three dimensional on the atomic scale, allowing a finite condensate fraction. The minimum thickness has to be at least larger than the zero-temperature coherence length which is of the order of a few angstroms in ^{4}He. This minimum thickness means that the integrals in k-space that diverge in low dimensions and lead to the conclusion of no-condensation, may have a natural lower cut-off that prevents their

divergence: $k_{\min} \sim 1/L_{\min}$. The conclusion of zero condensate-fraction is therefore not valid anymore, but we now have a 'generalized' condensate fraction which gives the macroscopic occupation of the lowest $k_{\min}$ state (the $k = 0$ state is not available anymore). The superfluid phase was shown to be a 'coherent-ferromagnet' in section II, so that it always needs the two quantities ρ_s/ρ,n_0.

This minimum thickness for the superfluid is found in experiments in thin layers and in microscopic cylindrical pores: In two-dimensional films [47] at least two layers of ^{4}He atoms (above the solid first layer) are needed to show a finite superfluid-fraction. In linear microscopic-pores [43] it is found that below a critical radius of $\sim 10\mathring{A}$, there is no sign of a superfluid fraction. In both these systems the long wave-length phonon modes are two- and one-dimensional respectively [43].

In addition it is found in experiments on thin films that the effective core-size of the vortices changes with the thickness [48] by a factor of ~ 40 from the thick layer to the thinest (critical) layer. We therefore get that the condensate fraction in the thinest layer is (2.58): $n_0(film) \sim \frac{1}{40^2} n_0(bulk)$, and is therefore unobservable. In the limit where the thickness is reduced to the critical thickness the superfluidity disappears, the core radius diverges and the condensate fraction goes to zero.

2.14 Summary

Let us summarize the results of this chapter:

1) We have shown that from the operational definition of the superfluid results a situation (wire-limit) where there is an off-diagonal momentum-momentum response in the thermodynamic limit. This situation is interpreted as the occurance of a spontaneous quantized-vortex (superfluid circulation) along the axis of a long cylinder. By comparing with the case of a two-dimensional charged particle in a magnetic field, we were able to map the condensate-wavefunction (or superfluid order-parameter) to the creation and anihilation operators of circulation. We found that the superfluid fraction ρ_s and the condensate fraction $|\Psi_0|^2 = n_0$ can be written in terms of the angular momentum expectation values. Moreover they are proportional to each other and both are needed to define uniquely the superfluid state. Both vanish at the superfluid transition.

2) We have given physical motivation in favor of a spontaneous circulation relying on the PIMC calculations of Ceperley. The superfluid phase has lower z.p.e. due to macroscopic permutation-cycles of the atoms. The symmetry is broken when they occur along one direction only, which means a specific circulation and broken TRS. We also described the circulating superfluid in terms of an XY-spin problem, and estimated the transition temperature T_λ.

3) Some measurements and numerical calculations do support the possibility of spontaneous circulation along the length of long cylinders. We suggest that ion-motion experiments may be able to check if a spontaneous axial vortex is a feature of long cylinders, especially in the recent microscopic pores of diameter $\sim 25\mathring{A}$ [43].

4) We showed that the vortex has an excitation spectrum similar to the magnon in a ferromagnet (2.40), which compares very well with the spectrum found experimentally. It is shown that this excitation spectrum is directly dependent on the

condensate fraction, unlike the other hydrodynamic modes of the superfluid (first and second sounds).

5) We related the condensate fraction to the internal structure of the fluid (at T=0), showing that it may be simply proportional to the vortex-core cross-section or the number of nearest-neighbors. The short-range correlations in the fluid therefore seem to determine the condensate fraction, similar to what is found from the hybridization scheme of the next chapter. A vortex performing a screw-like motion is shown to produce a longitudinal mass current along the axis, proportional to the vortex-core cross-section. In addition the superfluid wavefunction (order-parameter) Ψ is mapped to the transverse displacement of the spontaneous vortex.

6) Finaly we did show that assuming the vortices' excitations as being dominant near the transition we get the lower critical dimension for the superfluid-normal fluid transition to be zero. We predict this as the critical dimensionality for the zero-temperature disorder-driven transition and for the temperature-driven transition, without disorder. These results are corroborated by experimental and numerical results, where it is found that in one-dimensional (and higher) systems there is still superfluidity, which is destroyed at a finite critical temperature and/or disorder.

7) To explain the discrepancy with the usual treatment where there is a superfluid transition without condensation for dimensions less than 3, we propose that the vortex structure needs a minimum thickness of fluid in order to exist, and the system is therefore an effective three-dimensional one (at least locally). This condition of minimum thickness for superfludity is absent from the phonon (density fluctuation) treatments and is found in experiment. This minimum length introduces a lower cut-off in k-space and allows a finite 'generalized' condensate fraction. This prediction has to be checked experimentally, though we show that the values of n_0 for the thinest films are probably too small to detected.

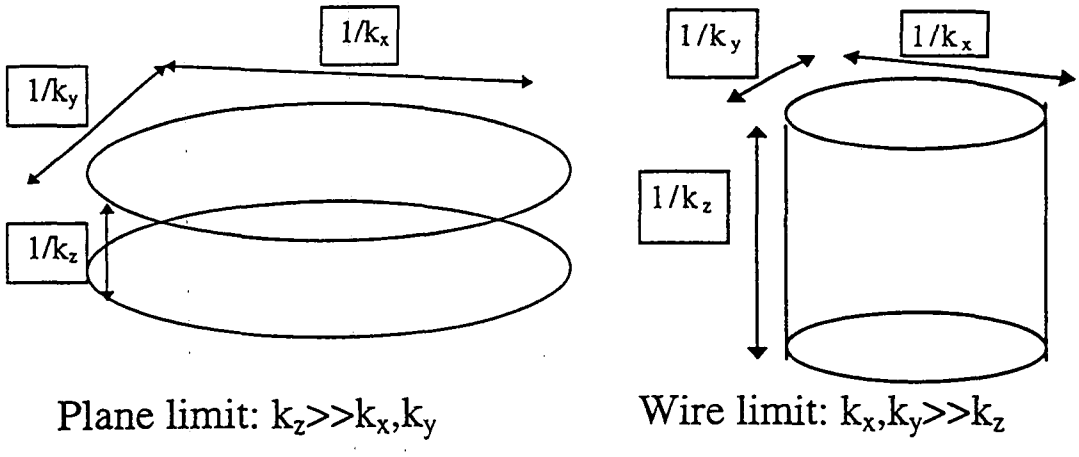

Figure 2.1: The two physically different ways to take the thermodynamic limit $k \to 0$: The plane-limit and the wire-limit.

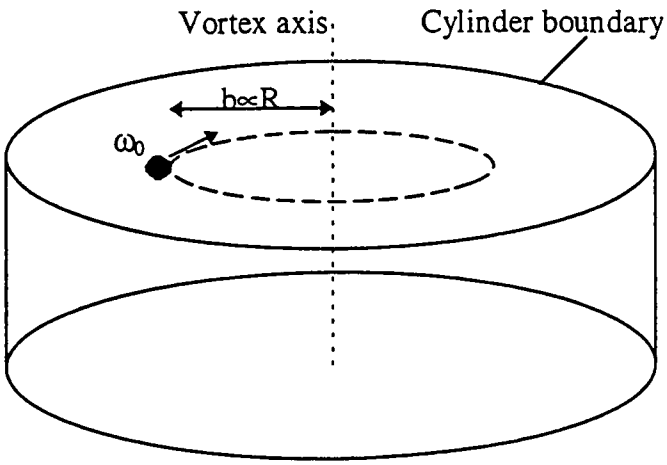

Figure 2.2: The rotational frequency of the superfluid circulation around the axial vortex in a long cylinder.

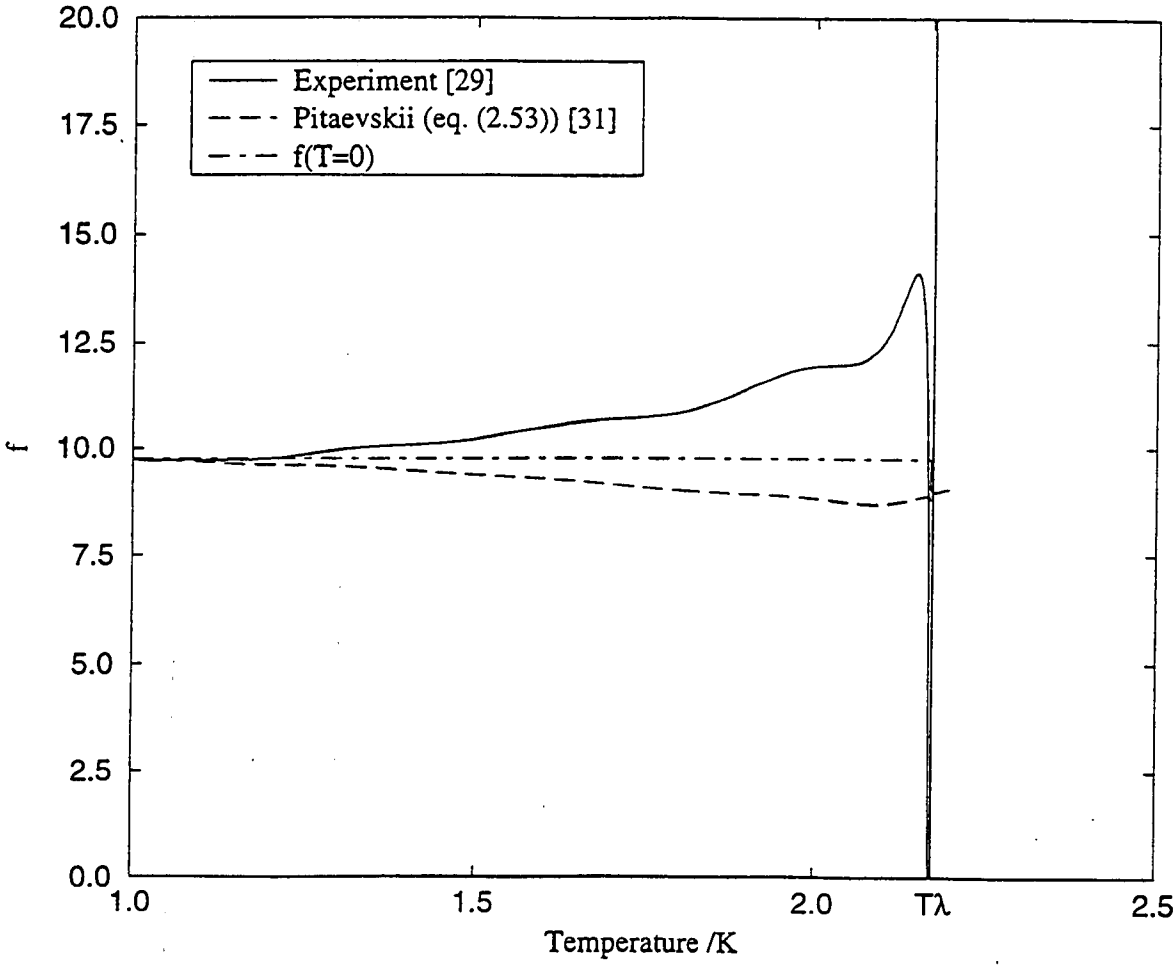

Figure 2.3: The ratio $f = (\rho_s/\rho)/n_0$ as a function of temperature. Comparison between experimental results [29] and eq.(2.53) [31].

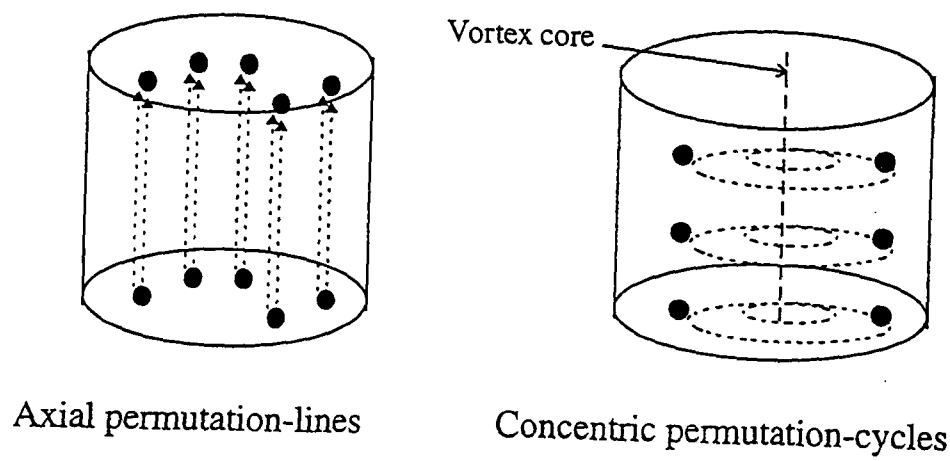

Figure 2.4: The two extreme cases of uniform permutations in a cylinder: Axial lines and concentric cycles.

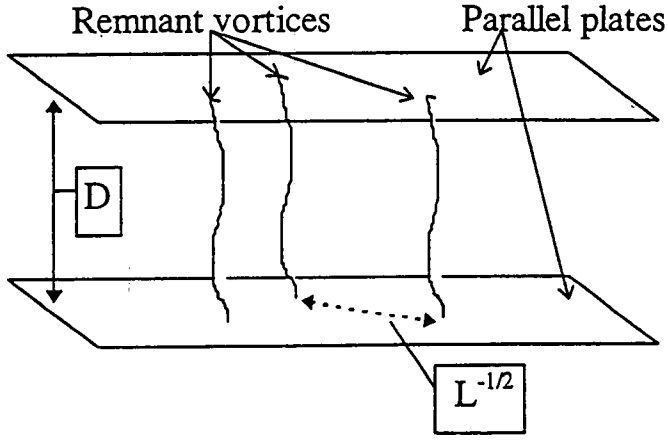

Figure 2.5: The configuration of experiments to detect remnant vortices in stationary superfluid [37].

Chapter 3

A hybrid phonon-exciton model for the spectrum of superfluid ^{4}He

3.1 Introduction

In this section we shall develope a new theoretical approach to the excitation spectrum of superfluid ^4He. In spite of the success obtained with the original wavefunction proposed by Feynman [49], a quantitative agreement with the experimental results has not yet been achieved. Subsequent refinements using more complicated variational wavefunctions were at the expenses of a simple interpretation as a pure density fluctuation. The experimental data compared with the Feynman and later calculations is shown in Fig.3.1.

More recently, new experimental results [50] obtained in high resolution neutron scattering did show puzzling features. One of them is the persistence of the phonon peak which describes the density fluctuations up to temperatures higher than T_λ i.e. in the normal phase. On the other hand, the peaks associated respectively to the maxon and roton excitations sharply decrease at T_λ. Those features tend to indicate that the low momentum phonon mode is marginally related to superfluidity or even to the Bose-Einstein statistics. This point was already noticed by Pines [18] who proposed that this mode is a collective zero sound just like in ^3He and therefore independent of the statistical effects. In contrast, the decrease at the transition of the other modes suggests a connection with quantum exchange effects.

In this section we will show a new way to interpret these features. To that purpose, we assume the existence of two kinds of excitations in the system. At large scales, there are the usual delocalized density fluctuations while at scales of a few interatomic distances, there exist localized excitations associated with exchange rings of atoms [19]. These two kinds of excitations are not independent but instead are hybridized in a way very reminiscent of the case of excitons in dielectric crystals [8]. This analogy will guide us in order to build a phenomenological Hamiltonian. A related point of view has been presented [51, 17] using an effective dielectric formalism. We prefer instead to make directly approximations on the nature of the

localized excitations and to write an effective Hamiltonian we shall subsequently diagonalize. This may be helpful in understanding some of the basic features of the spectrum.

The physical motivation in considering the existence of localized excitations stems from the following remarks. In any attempt to reproduce quantitatively the spectrum, we need to take into account the liquid nature of ^4He. But the interatomic potential responsible for the (short range) nature of the liquid does not account for superfluidity. To that purpose, it is important to consider exchange effects which might be described [19] by localized and closed exchange rings of atoms. Therefore, we view the system as being a liquid at large distances while locally, on the scale of some interatomic distances, there are localized quantum clusters interpreted as the vortex-core elements. Since the helium atoms are all identical, we cannot split them into two such classes (i.e. either embedded in a long range density mode or in a localized cluster) but we suppose instead that each atom retains both characteristics. Then, we assume that these two kinds of excitations are coupled and the spectrum results from this hybridization. From a methodological point of view, our approach is close to that of Hopfield [8] who described excitons in dielectric crystals as localized excitations which interact between themselves via the photons of the electromagnetic field. Here, along the same line, the interaction between the localized excitations is mediated by the density fluctuations. The need for more localized structure to describe the experimental spectrum was already realized by Feynman and Cohen [6]. Recently increasingly elaborate variational expressions are being used in order to reproduce the spectrum [7]. The localized structure in our approach is being introduced in the Hamiltonian and not in the wavefunction directly. This way we do not loose the physical interpretation of the wavefunction as a well defined excitation.

Finally there is the question of the 'multiparticle' excitation spectrum at higher energy (and lower intensity) of the superfluid (see Fig.1.2). This branch is usually interpreted in terms of multi-particle excitations of the phonon-roton quasiparticles. This interpretation, though, does not accurately describe the shape of this high-energy excitation spectrum and it's intensity. The high-energy spectrum has a complicated structure of several higher-energy branches, and disappears above the superfluid transition temperature, signaling its intimate connection with the superfluid order.

We begin by introducing the effective Hamiltonian description of the hybridization scheme in section 3.2. In section 3.3 we compare the resulting spectrum and structure-factor to the experimental data. In section 3.4 we obtain the scattering intensity of the single-excitation branch. In section 3.5 we discuss the new vortex-loop branch. In section 3.6 we calculate the reduction in the ground-state energy of the superfluid and in section 3.7 we calculate the condensate fraction. In section 3.8 we discuss the effect of vortices on the total density due to the effective mass of the vortex-core. In sections 3.9-3.11 we develope a Fermi-Dirac description for the 'multiparticle'-excitation branch at higher energy which is present in the superfluid. We conclude in section 3.12.

3.2 The effective Hamiltonian

The starting point is the Feynman phonon [5], whose spectrum is given by:

$$\varepsilon(k) = \frac{\hbar^2 k^2/2m}{S(k)} \tag{3.1}$$

where: $S(k)$ is the static structure factor, k is the wavevector and $\hbar^2k^2/2m$ is the free atom energy. The wavefunction that describes this single phonon is:

$$\psi = \sum_i e^{ik\cdot R_i}\varphi \tag{3.2}$$

where R_i is the position of atom i and φ is the ground-state wavefunction. This wavefunction describes a single pure density excitation:

$$\psi = \rho_k^\dagger \varphi \tag{3.3}$$

If we compare the experimental spectrum [52] at T=0.5^oK with the result of (3.1) we get only qualitative agreement at both saturated-vapor-pressure (s.v.p.) and high pressure (Fig.3.1). The linear phonon-like spectrum at $k \to 0$ at superfluid temperatures is due to the behavior $S(k) \propto k$. According to the Landau criterion, a linear spectrum is the characteristic that gives the superfluid its finite critical velocity, i.e. the velocity below which a moving object will not create any excitations in the superfluid. This critical velocity is zero in the normal fluid where the quadratic dispersion of free a free particle has zero slope at $k \to 0$.

In order to improve the agreement between the Feynman spectrum and the experimental result, an increasingly elaborate expression for ψ (3.2) is usually used. This is given some physical motivation as 'backflow' effects, but is at the price that the excitation does not describe anymore a pure density fluctuation (3.3).

We first consider the Hamiltonian H_0 describing the pure density modes obtained using the Feynman ansatz. It is given by $H_0 = \sum_k \epsilon(k) {a_k}^\dagger a_k$. The energy $\epsilon(k)$ is obtained from the Feynman expression (3.1). Then, we consider the Hamiltonian H_{loc} of the localized excitations and assume that they can be approximated by two-level systems of energy $\hbar\omega_0$, such that the corresponding free Hamiltonian is ${H^0}_{loc} = \sum_k \hbar\omega_0({b_k}^\dagger b_k + \frac{1}{2})$. The operators a and b obey bosonic commutation relations. But the bosonic character of the b operators is only approximate and holds in the limit of a low density of localized modes [53]. To write down the part describing interactions between the two sets of excitations, we follow the approach of Hopfield and Anderson [8, 53] and assume that the role of the density fluctuations is to induce an effective interaction between the localized modes and as a result to modify their spectrum as well as the spectrum of the Feynman density modes. Using the dipolar approximation, we obtain [53] for the local excitations the effective Hamiltonian

$$\begin{aligned} H_{loc} &= \sum_k (\hbar\omega_0 + X(k))({b_k}^\dagger b_k + \frac{1}{2}) \\ &\quad + \sum_k X(k)({b_k}^\dagger b_{-k}^\dagger + b_k b_{-k}) \end{aligned} \tag{3.4}$$

where $X(k)$ is a (real and negative) matrix element which depends on the microscopic details of the dipolar interaction. As we shall see later, its exact expression is not important at this stage. Finally, the part describing the coupling between the phonons and the localized modes is [8]

$$\begin{aligned} H_c &= \sum_k \left(\lambda(k,\omega_0)b_k + \mu(k,\omega_0)a_k\right)\left(a_k{}^\dagger + a_{-k}\right) \\ &\quad - \left(\lambda(k,\omega_0)b_k{}^\dagger - \mu(k,\omega_0)a_k{}^\dagger\right)\left(a_k + a^\dagger{}_{-k}\right) \end{aligned} \tag{3.5}$$

where, in the dipolar approximation the two functions λ and μ are given by $\lambda(k) = i\hbar\omega_0(-\frac{3X(k)}{2\epsilon(k)})^{\frac{1}{2}}$ and $\mu(k) = -\hbar\omega_0\frac{3X(k)}{2\epsilon(k)}$. The total Hamiltonian is then $H = H_0 + H^0{}_{loc} + H_c$. The part H_{loc} which describes the effective interaction between localized modes can be diagonalized using the Bogoliubov transformation $\beta_k = u(k)b_k + v(k)b^\dagger{}_{-k}$. This gives the spectrum

$$E = \sqrt{\hbar\omega_0(\hbar\omega_0 + 2X(k))} \tag{3.6}$$

The two functions $u(k)$ and $v(k)$ are given by:

$$u^2(k) = \frac{1}{2}(\frac{\hbar\omega_0 + X(k)}{E(k)} + 1), v^2(k) = \frac{1}{2}(\frac{\hbar\omega_0 + X(k)}{E(k)} - 1) \tag{3.7}$$

We now compare the localized excitation Hamiltonian (3.4) with the usual approximation of the superfluid ^{4}He as a Weakly Interacting Bose Gas (WIBG) due o Bogoliubov [14]. The WIBG Hamiltonian is given by

$$H_{WIBG} = \sum_k \left(\varepsilon_k + N_0V_k\right)b_k^\dagger b_k + \sum_k N_0V_k\left(b_k^\dagger b_{-k}^\dagger + b_k b_{-k}\right) \tag{3.8}$$

where $N_0 \equiv |\langle b_0\rangle|^2$ is the condensate fraction, $\varepsilon_k = \hbar^2k^2/2m$, and V_k is the effective potential between the bosons at wave vector k. The operators $b_k^\dagger, b_k$ represent creation/anihilation of a ^{4}He atom, not a localized-mode as in (3.4). The approximation is that the condensate fraction is almost unchanged by the weak interaction from the Ideal Bose Gas (IBG) value of one.

The excitation spectrum of (3.8) is the well-known Bogoliubov linear spectrum in the limit $k \to 0$:

$$E = \sqrt{\varepsilon_k\left(\varepsilon_k + 2N_0V_k\right)} \to \hbar kc \tag{3.9}$$

where the velocity of sound is defined by $c \equiv \sqrt{N_0V_0/m}$ such that $N_0V_0 = mc^2$.

The physics of the two Hamiltonians is very different. The WIBG has as a non-interacting limit the IBG which at T=0 describes a fully Bose condensed system and has a broken gauge symmetry. The interaction slightly depletes the condensate fraction and changes the spectrum from quadric spectrum to linear at low momentum.

On the other hand the localized excitation Hamiltonian describes in the non-ineracting limit($X(k) = 0$) a (non-condensed) collection of independent localized modes. This state has no broken symmetry. In order to obtain a linear spectrum

at low momentum, condensation and broken-symmetry the interaction needs to be large ($X(k \to 0) = -(\hbar\omega_0)/2$), which shows that this is not a small perturbation to the non-interacting case. In that sense it is a strong-coupling description of the superfluid.

The total Hamiltonian H is quadratic and can be diagonalized using the canonical transformation:

$$\begin{aligned} \alpha_k &= Aa_k + Bb_k + Ca^\dagger{}_{-k} + Db^\dagger{}_{-k} \\ \tilde{\alpha}_k &= Ba_k + Ab_k + Da^\dagger{}_{-k} + Cb^\dagger{}_{-k} \end{aligned} \tag{3.10}$$

where these operators describe the lower and upper branch of the energy spectrum respectively.

The corresponding dispersion relation is

$$\frac{\epsilon^2(k)}{E^2(k)} = 1 - \frac{6}{\hbar\omega_0} \frac{X(k)}{1 - (\frac{E(k)}{\hbar\omega_0})^2} \tag{3.11}$$

We first notice that taking the coupling $X(k)$ between the two sets of modes to zero, we obtain, as expected, the two solutions $E(k) = \epsilon(k)$ describing the pure density mode and $E = \hbar\omega_0$ for the localized two-levels. A non zero coupling hybridizes the two sets of excitations. We choose now for the energy $\hbar\omega_0$ the highest value of the phonon-roton spectrum namely $\hbar\omega_0 = 2\Delta$ where the energy Δ corresponds to the roton minimum (at this energy the phonon-roton spectrum terminates). To solve the dispersion relation we use (3.6) into (3.11). This procedure means that we demand a self-consistent interaction: the direct dipole-dipole interaction H_{loc} gives the same spectrum as the phonon-mediated interaction appearing in H. The sources of the field are the localized dipole moments, and their interaction is through the dipole-field.

This gives $E(k) = \frac{1}{2}\epsilon(k)$ i.e. an expression independent of the matrix element $X(k)$. Using now this latter expression into (3.11), we obtain the other solution describing the energy of the hybridized local modes as $E = 2\hbar\omega_0$ which is as well independent of $X(k)$. Therefore, as a result of the hybridization, the energy spectrum of the delocalized density fluctuations is shifted by a factor two towards the lower energies and the localized modes still have a constant energy but equals to four times the roton minimum Δ.

The transformation functions $u(k), v(k)$ and $A(k), B(k), C(k), D(k)$ can be calculated using the spectrum we derive from the self-consistent procedure. We point out that the roles of the phonons and localized-modes are interchanged between the two branches.

The ground state of the total hamiltonian H is defined by

$$\alpha_k |0\rangle = 0, \tilde{\alpha}_k |0\rangle = 0 \tag{3.12}$$

We write the ground state as:

$$|0\rangle \equiv |0_1\rangle |0_2\rangle , |0_{1,2}\rangle = \prod f_{1,2}(a_k, a^\dagger_{-k}) g_{1,2}(b_k, b^\dagger_{-k}) |vac\rangle$$

where the index $1,2$ stands for the two branches and rewrite (3.12) for each component:

$$\begin{aligned}
\alpha_k|0\rangle &= 0: \quad \left(A\frac{d}{da_k^\dagger}+Ca_{-k}^\dagger\right)f_1(a_k,a_{-k}^\dagger)=0, \left(B\frac{d}{db_k^\dagger}+Db_{-k}^\dagger\right)g_1(b_k,b_{-k}^\dagger)=0 \\
\tilde{\alpha}_k|0\rangle &= 0: \quad \left(B\frac{d}{da_k^\dagger}+Da_{-k}^\dagger\right)f_2(a_k,a_{-k}^\dagger)=0, \left(A\frac{d}{db_k^\dagger}+Cb_{-k}^\dagger\right)g_2(b_k,b_{-k}^\dagger)=0
\end{aligned}$$

The final result is:

$$\begin{aligned}
|0_1\rangle &= \prod \exp\left(\frac{A}{C}a_k^\dagger a_{-k}^\dagger\right)\exp\left(\frac{B}{D}b_k^\dagger b_{-k}^\dagger\right)|vac\rangle \\
|0_2\rangle &= \prod \exp\left(\frac{B}{D}a_k^\dagger a_{-k}^\dagger\right)\exp\left(\frac{A}{C}b_k^\dagger b_{-k}^\dagger\right)|vac\rangle
\end{aligned} \tag{3.13}$$

where the ratios of the coefficients can be written in a simple form:

$$\frac{A}{C}=-\frac{\varepsilon(k)+E}{\varepsilon(k)-E}, \frac{B}{D}=\frac{\hbar\omega_0+E}{\hbar\omega_0-E} \tag{3.14}$$

The hybridization coefficients can be written as well

$$\begin{aligned}
|A|^2 &= \frac{9\left(1-\left(\varepsilon(k)/2\hbar\omega_0\right)^2\right)}{8\left(4-\left(\varepsilon(k)/2\hbar\omega_0\right)^2\right)} \\
|B|^2 &= \frac{3\left(\varepsilon(k)+2\hbar\omega_0\right)^2}{8\hbar\omega_0\varepsilon(k)\left(4-\left(\varepsilon(k)/2\hbar\omega_0\right)^2\right)} \\
|C|^2 &= \frac{1\left(1-\left(\varepsilon(k)/2\hbar\omega_0\right)^2\right)}{8\left(4-\left(\varepsilon(k)/2\hbar\omega_0\right)^2\right)}=\frac{1}{9}|A|^2 \\
|D|^2 &= \frac{3\left(\varepsilon(k)-2\hbar\omega_0\right)^2}{8\hbar\omega_0\varepsilon(k)\left(4-\left(\varepsilon(k)/2\hbar\omega_0\right)^2\right)}
\end{aligned} \tag{3.15}$$

The values of the coefficients at various special momenta can be calculated:
$\underline{k\to 0:}$

$$\begin{aligned}
|A|^2 &\to \frac{9}{32}, |C|^2 \to \frac{1}{32} \\
|B|^2, |D|^2 &\to \frac{\hbar\omega_0}{\varepsilon(k)}\frac{3}{8}
\end{aligned} \tag{3.16}$$

$\underline{\text{Roton minimum } (E=\Delta=\hbar\omega_0/2):}$

$$|A|^2=\frac{9}{40}, |C|^2=\frac{1}{40}, |B|^2=\frac{9}{10}, |D|^2=\frac{1}{10} \tag{3.17}$$

3.3 Comparison with experimental results

The above results are quite appealing since we know that the Feynman ansatz alone gives a spectrum for the density fluctuations which is too high in energy by about a factor two. To compare our results with the experimental data we shall consider two independent sets of results namely the measurements of the energy spectrum and of the structure factor $S(k)$. We obtain from (4) the relation

$$E(k) = \frac{\hbar^2 k^2}{4mS(k)} \tag{3.18}$$

for the lower branch which we compare to the experimental results [72, 73, 52, 71] obtained at two different pressures (Fig.3.2). The main discrepancy is obtained at the saturation vapor pressure in the low momentum region ($k \leq 1\mathring{A}^{-1}$). In the same way (Fig.3.3), comparing for $S(k)$ our results agree with the experimental structure factor to within the experimental uncertainty, in the above range of momentum. Our calculations become meaningless when the phonon-roton branch terminates i.e. for $k \simeq 2.5\mathring{A}^{-1}$ where the spectrum becomes that of a free particle. In the low momentum limit $k \to 0$, the structure factor is linear with the momentum k, and the expression (3.18) gives

$$\lim_{k\to 0} S(k,\omega) = \frac{\hbar k}{4mc}\delta(\hbar\omega - 2\hbar kc) \tag{3.19}$$

where c is the sound velocity. The experimental data are not accurate enough in order to prove this conclusively. Nevertheless, for a neutral system, we expect both from the f-sum rule and the compressibility sum rule that:

$$lim_{k\to 0} S(k,\omega) = \frac{\hbar k}{2mc}\delta(\hbar\omega - 2\hbar kc) \tag{3.20}$$

instead of (3.19). The discrepancy comes from the effective long range interactions which result from the dipolar coupling in the hybridized system. We can therefore define, just like in a dielectric medium [18], an effective dielectric constant given here by $\left(\frac{\epsilon(k)}{E(k)}\right)^2 = 4$. In a dielectric medium, the ratio of the density-density response function over its bare (unscreened) value is given by the dielectric constant. Then, the compressibility sum rule is modified into

$$\lim_{k\to 0} 4\int \frac{d\omega}{\omega} S(k,\omega) = \frac{N}{2mc^2} \tag{3.21}$$

Using (3.21) and the f-sum rule we recover our result (3.19).

The experimental data at small momenta is shown in Fig.3.4. The structure factor tends to a constant as $k \to 0$ given by [54]

$$\lim_{k\to 0} S(k,\omega) = k_B T/mc^2 \tag{3.22}$$

We find that our expression seems to agree with the slope of the experimental structure-factor above $k \simeq 0.5\mathring{A}^{-1}$.

3.4 Scattering intensity

The neutron scattering intensity is a direct measure of the density fluctuations in the liquid and may be described in terms of the dynamic structure factor $S(k,\omega)$. It is usually accepted since the work of Miller, Pines and Nozieres [55] that we can split the total contribution to $S(k,\omega)$ into two parts,

$$S(k,\omega) = NZ(k)\delta(\hbar\omega - \epsilon_k) + S^{(1)}(k,\omega) \tag{3.23}$$

where the first term accounts for single quasi-particle excitations while the second describes multiparticle excitations. This separation is quite easy to justify at low temperature and low momentum, typically for $k \leq 0.5\mathring{A}^{-1}$. In this regime, integrating (3.23) over the energy and noticing that $S^{(1)}(k,\omega)$ vanishes in the low momentum limit we obtain $Z(k) = S(k)$, which results also from the Feynman theory. The comparison with the experimental data [52] shows that although it works in the low momentum regime mentionned above, it fails to describe the non linear portion of the spectrum, except perhaps for the position of the maximum.

In contrast to this approach, we do not consider here a precise decomposition of the structure factor. But, since the density fluctuations result from the hybridization with the localized modes, we expect the differential cross-section $Z(k)$ for the excitation of a single quasi-particle to be proportional to the expectation value of the localized modes calculated in the ground state of the Bogoliubov pairs namely, $\langle {b_k}^\dagger b^\dagger_{-k}\rangle = u_k v_k$. This result follows from looking at the ground-state wavefunction of the hybridized Hamiltonian (3.4) [56]:

$$|\Psi_0\rangle = \prod_k \exp\left(\frac{v_k}{u_k}{b_k}^\dagger b^\dagger_{-k}\right)|vac\rangle \tag{3.24}$$

The ground-state contains pairs of localized modes and the creation or anihilation of an excitation is the destruction of such a pair. The probability of the neutron scattering is therefore proportional to the occupation density of these pairs, and we have:

$$Z(k) = 4\pi k^2 I_0 u_k v_k$$

where I_0 is a normalization constant. Using our previous expression for u_k and v_k (3.7) we obtain $u_k v_k = \frac{1}{2}\frac{|X(k)|}{E(k)}$ which gives:

$$Z(k) = \pi k^2 I_0 \frac{\hbar\omega_0}{E(k)}\left|\left(\frac{E(k)}{\hbar\omega_0}\right)^2 - 1\right| \tag{3.25}$$

From the two independent measures of $E(k)$ and $S(k)$ we obtain using (3.25) a theoretical expression of the differential cross-section which fits well the experimental results as shown in Fig.3.5. Moreover, in the low momentum limit, we recover the Feynman result namely the proportionality between $S(k)$ and $Z(k)$. It is important to emphasize that the shift by a factor two between the Feynman and hybridized spectra determines both the maximum of the $Z(k)$-curve and the momentum k_0 at which $Z(k)$ vanishes. In the framework of our approach it is not an adjustable

parameter, i.e. in order to describe quantitatively the scattering intensity curves, the ratio $\frac{\epsilon(k)}{E(k)}$ cannot be adjusted independently. Indeed by choosing any good fitting parameter λ ($\neq 2$) such that $E(k) = \frac{1}{\lambda}\epsilon(k)$ we do not obtain a solution of the dispersion relation (3.11).

3.5 Vortex loops

We found a second branch of excitations at the constant energy $E = 4\Delta$. It describes localized excitations of energies which are twice the bare vortex core energy. It is suggestive to interpret this mode as a single vortex loop which is made of a vortex-core pair. In support of this interpretation we notice that for this branch the Feynman-phonons condense at $k \to 0$ in pairs, just as the localized-modes do for the lower-branch (section I). Such a macroscopic occupation by opposite-momentum phonons is expected for the dipolar velocity field around a vortex-loop.

The vortex-loop radius can be calculated using a Feynman-type formula for the energy of the circulating current of a vortex-loop [49]

$$E_{vortex} = 2\pi^2\rho\frac{\hbar^2 R}{m^2}ln(\frac{R}{a}) \tag{3.26}$$

where at $T = 0$, we take the density of the superfluid i.e. $\rho = \rho_s$ and a is the core size equal to the atomic radius namely $a \simeq 2.8\mathring{A}$. The radius R is obtained taking $E_{vortex} = 4\Delta = 34.4K$. This gives $R \simeq 7.1\mathring{A}$ which is the expected size for the smallest vortex-loop i.e. about twice the size of the vortex core. A further experimental evidence for our interpretation of the hybridized localized state at $E = 4\Delta$ as an intrinsic excitation of the fluid is provided by critical velocity experiments [21]. In phase-slippage studies of the critical velocity through an orifice, the critical velocity is driven by the thermal nucleation of vortex-loops. The corresponding energy E_v is determined by the nucleation rate Γ which using a Arrhenius law can be written $\Gamma = \Gamma_0 exp(\frac{-E_v}{k_B T})$. It is found [21] that $E_v \simeq 33 \pm 5K$ which is indeed very close to our result $4\Delta = 34.4K$. Moreover, the upper critical velocity v_c may be estimated as being given by the velocity of the vortex-loop itself [49] i.e. $v_c = \frac{\hbar}{2mR}ln(\frac{R}{a}) \simeq 20m/s$, a value close to the largest measured critical velocity [21].

Another relevant set of experiments we consider is provided by the Raman scattering around $k = 0$ (Fig.3.6). It has been found that besides a peak at $E = 2\Delta$, there is an additional contribution at $E = 4\Delta$ [57] which we associate to the vortex-loop. The peak at 2Δ is usually interpreted as a two-roton excitation and therefore the additional contribution is viewed as a four-roton excitation. This interpretation suffers nevertheless from the fact that there is no three-roton peak. In our model, the lowest excitation energy of a vortex-core is given by 2Δ and not by Δ so that we do not expect any contribution at 3Δ. The peak at 2Δ which does not appear in the hybridized spectrum will be discussed in the last subsections of this chapter [58].

We also point-out that at high-energy and momentum transfer where the scattering peak is along the free-atom spectrum [17], there is a marked broadening of the width of this peak where the free-atom spectrum crosses the second branch,

i.e. around energy 34.4^oK (Fig.1.2). If a neutron scatters a free-atom then at the crossing point the free-atom can create a vortex-loop and loose the corresponding energy and momentum:

$$E_{new}(k) = \frac{\hbar^2}{2m}(k - k_x)^2, \text{fork} \geq \mathrm{k_x} \tag{3.27}$$

where k_x is the momentum of the free-atom at the crossing point of the vortex-loop level: $k_x = \sqrt{4m\Delta}/\hbar$. The remaining energy of the free-atom will therefore be below the original free-atom spectrum and the scattering peak will broaden (Fig.1.2). This result is a possible further indication for the existence of the second branch with energy 2Δ.

3.6 Ground-state energy

Following [53] we can calculate the reduction in the ground-state energy of the hybridized system compared with the non-hybridized one:

$$\Delta E_0 = \sum_k \frac{1}{2}\left(E(k) - (\hbar\omega_0 + X(k))\right) = V\int \frac{k^2 dk}{4\pi^2}\left(E(k) - (\hbar\omega_0 + X(k))\right) \tag{3.28}$$

where V is the specific volume. The results at s.v.p. and at P=24atm are:

$$\Delta E(s.v.p.) \simeq 5^oK \pm 1.0^oK, \qquad \Delta E(P = 24atm) \simeq 3.0^oK \pm 1.0^oK \tag{3.29}$$

where we used $V(s.v.p.) \simeq 45.8\mathring{A}^3, V(P = 24atm) \simeq 38.6\mathring{A}^3$. The integration is done numerically for momenta $0 \leq k \leq k_m(\simeq 2.5\mathring{A}^{-1})$. The calculations were done using the experimental phonon-roton spectrum. These values can be compared with the experimental data [29]:

$$\Delta E_{ex}(s.v.p.) \simeq 2.8 \pm 2.0^oK, \qquad \Delta E_{ex}(P = 24atm) \simeq 1.3 \pm 3.0^oK \tag{3.30}$$

The large experimental uncertainty makes exact comparison difficult but we see that the theory predicts well the difference between the two pressures. The theoretical values are consistently larger than the experiment, but they do not include a small increase in the potential energy due to the reduced density of the superfluid compared with the normal fluid. This increase of approximately $\simeq 2^oK$ will lower the total reduction in the ground-state energy and make the theory agree more with the experiment. This calculation (3.28) is the first analytic calculation of the reduction in the ground-state energy of the superfluid.

As explained in [53] this reduction of the zero-point-energy (z.p.e.) of the atoms is due to the interaction between them. Compared with the path-integral calculations [19] we find that in both cases it is the kinetic z.p.e. which is reduced, compared with the normal fluid, and drives the superfluid transition.

3.7 Condensate fraction

When the occupation diverges at a certain k there is a condensation. From (3.7) we find that at $k \to 0$ the occupation by the localized modes diverges:

$$v_k^2 \to_{k\to 0} \equiv \frac{1}{2}\frac{\hbar\omega_0}{\varepsilon(k)} = \frac{n_0}{n}\frac{mc}{2\hbar k} \Rightarrow \frac{n_0}{n} = \frac{1}{2}\frac{\hbar\omega_0}{mc^2} = \frac{\Delta}{mc^2} \tag{3.31}$$

where we used: $\varepsilon(k)|_{k\to 0} = 2\hbar kc$ and the definition of the condensate fraction from the usual treatment [17]. We point out that (3.31) gives the condensate fraction in terms of the parameters of the phonon-roton spectrum. We also find that the order-parameter which is usually identified with the condensate-fraction is here identified with the value of the matrix-element function $|X(k)|$ at $k = 0$, i.e. Δ.

From (3.31) we get:

$$S.V.P. : \frac{n_0}{n} \simeq 30 \pm 1\%, P = 24atm : \frac{n_0}{n} \simeq 11.8 \pm 0.3\%$$

These values are higher than the experimental results [29] by a factor of ~ 2. This factor may be explained by noting that we have a condensation of localized-modes. These excitations may have an effective mass: $m_{loc} \sim 2m_{He}$. This effective mass is in accord with the results of path-integral Monte-Carlo (PIMC) calculations of the effective mass of a ^{4}He atom that is not participating in the Bose-permutation [19]. This atom therefore represents a localised excitation similar to our vortex-core element and has a similar effective mass.

We can plot the condensate fractions at different pressures and compare with the experimental values for n_0/n [29](Fig.3.7). We use eq. (3.31) and renormalize the result to fit with the experiment (we use experimental values for Δ and c at different pressures [10]). The agreement with experiment is reasonable, considering the small number of points, and experimental uncertainty.

3.8 Vortex-core density

As proposed in the last section it is possible that the vortex-core (localized-mode) can be treated as having an effective mass twice that of the bare ^{4}He atom. This may be the explanation of the result that a rotating ^{4}He when cooled below T_λ has a jump in its density [59]. It is known that in a rotating fluid the superfluid will form a dense array of vortices so as to move with the normal solid-body rotation. We propose that these vortices will cause an increase in the density due to the higher density of the cores. If we treat the vortex core of radius a as having twice the mass of the surrounding fluid then the change in density is:

$$\Delta\rho = \rho n_v a^2 \tag{3.32}$$

where n_v is the vortex areal density. In order to get the measured change in density: $\Delta\rho \sim 3 \times 10^{-5} gr/cm^3$ (at rotation velocity: $\omega = 30\,\mathrm{sec}^{-1}$) we need: $n_v \simeq 2.5 \times 10^{11} cm^{-2}$. This value is much higher than that needed to create a solid-body rotation:

$$n_v \simeq \omega\frac{m}{\hbar} = 1.9 \times 10^5 cm^{-2} \tag{3.33}$$

but it is closer to the density of vortices that are spontaneously created on passing through the transition [60]. This is estimated form experiments as: $n_v \geq 10^9 cm^{-2}$. This density usually quickly decays in a non-rotating superfluid, and this estimate is therefore a lower limit on the vortex density created at the transition. It is possible that in a rotating superfluid the initial vortex density created at the transition is stabilized and becomes the array that maintains the superfluid solid-body rotation. We predict that the density of vortices created at the transition is therefore of the order of: $n_v \simeq 10^{11} cm^{-2}$. This density means an average distance between vortices of: $L_v \sim 200\mathring{A}$. This is the order of magnitude of the distance between elementary vortex-loops thermally activated at the transition temperature:

$$N_v = \frac{V}{4\pi^2}\frac{k_m^3}{3}\frac{1}{\exp(E_v/k_B T_\lambda) - 1} \simeq 1.3 \times 10^{-6} \Rightarrow V_{vort} \simeq V/N_v \equiv L_v^3 \Rightarrow L_v \simeq 328\mathring{A}$$

where: $V \simeq 45.8\mathring{A}^3$ is the atomic volume, $E_v = 34.4^o K$ is our vortex-loop excitation energy and $k_m \simeq 2.5\mathring{A}^{-1}$ is the maximum wave-vector for which the hybridized Hamiltonian is applicable. This is of the same order of magnitude as the estimate from the density jump. Vortex-loop models of the superfluid transition [23] predict that at the transition temperature the superfluid is filled with thermally excited vortices.

The increase in the density due to superfluid turbulence ('vortex-tangle') was also confirmed experimentally in [61].

We therefore conclude that it is possible that the vortex-cores have a higher density then the surrounding superfluid, even up to twice the normal density. This is in contrast to most description that use a non-linear Schrodinger equation to describe the vortex, and find a reduced (even zero) density at the core [62].

3.9 Dirac Hamiltonian for the 'multiparticle'-branch of superfluid ^{4}He

Following the previous sections on the phonon-roton spectrum we propose here a new treatment of the high-energy branch. We showed that the phonon-roton branch results from the resonant hybridization of localized-modes (vortex-cores) and delocalized density fluctuations (Feynman). Here we propose that the elementary, non-hybridized vortex-core can be treated as a fermion described by a many-body Dirac Hamiltonian. We show that the 'multiparticle'-branch is therefore an excitation of free non-hybridized vortex-cores, moving in a back-ground of vortex-antivortex core pairs. To calculate the high-energy spectrum we only need the phonon-roton spectrum and the bare vortex-core energy as inputs.

The ground-state of the superfluid was shown before to have a condensate of localized-modes which are treated as bosons and condense in pairs of opposite momentum. The localized-modes have a bare non-hybridized energy of $E_0 = 2\Delta$, where Δ is the roton energy. The quantum statistics of the localized-modes is determined by their local phase with respect to the global superfluid-phase. The localized-modes are treated as localized oscillating dipoles which are whose individual oscillations are synchronized by the dipolar interaction into a coherent-state

(the superfluid phase) with uniform phase. Every localized-mode is symmetric with respect to the others and Bose-Einstein statistics result. It is possible though to excite a localized-mode which is in anti-phase (phase difference π) with respect to the global phase of the coherent ground-state. In this case it is anti-symmetric with respect to the localized-modes which are in the coherent ground-state and Fermi-Dirac statistics are appropriate. The statistics of the localized-modes is therefore defined in the superfluid state depending on their phase relative to the global phase (broken gauge-symmetry).

An anti-phase localized-mode (a fermion) will not be hybridized into the coherent field of the ground-state, but nevertheless will feel the effect of the Bose excitations (phonon-roton) as they interact with it and cause interactions between the localized fermions. The effective Hamiltonian should therefore contain a term describing the creation and anihilation of pairs of fermions from the ground-state by a phonon. This is an off-diagonal term that describes the fluctuation caused by a phonon-roton of energy ε_k: it changes a fermion 'particle' into a 'hole' and vice versa. In addition there should be a term that describes the energy of the free unpaired fermion, that is E_0. The many-body 'Dirac' Hamiltonian that we therefore propose is

$$H_D = \sum_k \varepsilon_k \left(c_k^\dagger c_{-k}^\dagger + c_k c_{-k} \right) - \sum_k V_k \left(c_k^\dagger c_k c_{-k}^\dagger c_{-k} \right) \tag{3.34}$$

where $c_k^\dagger, c_k$ are the creation and annihilation operators of the anti-phase (Fermi) localized mode (vortex-core element). The first term in (3.34) is the 'kinetic' term due to the phonon-roton branch, where the localized-modes come in pairs. The energy ε_k is just the phonon-roton spectrum. In addition there is finite 'potential' energy if there is a finite density of unpaired fermions, which we take as E_0.

We linearize the equations of motion that follow from (3.34), similar to the BCS method:

$$i\hbar\, \dot{c}_k = -\varepsilon_k c_{-k}^\dagger + \Lambda_k c_k \qquad i\hbar\, \dot{c}_{-k}^\dagger = -\varepsilon_k c_k - \Lambda_k^* c_{-k}^\dagger \tag{3.35}$$

where we used:

$$\left\{ c_k, c_k^\dagger \right\} = 1 \qquad \left\{ c_k, c_{-k}^\dagger \right\} = 0 \tag{3.36}$$

and where

$$\Lambda_k = \Lambda_k^* \equiv E_0 \equiv \sum_k V_k \left\langle c_k^\dagger c_k \right\rangle \tag{3.37}$$

and we normalize the density as:

$$\sum_k \left\langle c_k^\dagger c_k \right\rangle \equiv 1 \tag{3.38}$$

and take the potential as a constant for all wavevector k:

$$V_k = E_0 \tag{3.39}$$

The equations (3.35) are identical to Dirac's equation for a single particle, if we insert: $\varepsilon_k = \hbar k c, E_0 = mc^2$ (m particle mass, c velocity of light). We can write the equations of motion (3.35) in matrix form and compare them with the Dirac equations where we disregard the spin degree of freedom:

Helium:

$$i\hbar\frac{\partial}{\partial t}\begin{pmatrix} c_k \\ c_{-k}^\dagger \end{pmatrix} = \varepsilon_k \begin{pmatrix} 0 & 1 \\ 1 & 0 \end{pmatrix}\begin{pmatrix} c_k \\ c_{-k}^\dagger \end{pmatrix} + E_0 \begin{pmatrix} 1 & 0 \\ 0 & -1 \end{pmatrix}\begin{pmatrix} c_k \\ c_{-k}^\dagger \end{pmatrix} \tag{3.40}$$

Dirac:

$$i\hbar\frac{\partial}{\partial t}\begin{pmatrix} \varphi \\ \chi \end{pmatrix} = c(\overrightarrow{p}\cdot\overrightarrow{\sigma}) \begin{pmatrix} 0 & 1 \\ 1 & 0 \end{pmatrix}\begin{pmatrix} \varphi \\ \chi \end{pmatrix} + mc^2 \begin{pmatrix} 1 & 0 \\ 0 & -1 \end{pmatrix}\begin{pmatrix} \varphi \\ \chi \end{pmatrix} \tag{3.41}$$

where φ, χ are the particle/antiparticle two-component spinors, and $\overrightarrow{\sigma} = (\sigma_x, \sigma_y, \sigma_z)$. In order to get rid of the extra dimensions in the Dirac equation in 3 dimensions we can write the 2x2 Dirac equation in 2 dimensions, with momentum in the $\hat{x}$-direction:

Dirac 2D:

$$i\hbar\frac{\partial}{\partial t}\begin{pmatrix} \varphi \\ \chi \end{pmatrix} = c\begin{pmatrix} 0 & -i\hbar\partial_x \\ -i\hbar\partial_x & 0 \end{pmatrix}\begin{pmatrix} \varphi \\ \chi \end{pmatrix} + mc^2 \begin{pmatrix} 1 & 0 \\ 0 & -1 \end{pmatrix}\begin{pmatrix} \varphi \\ \chi \end{pmatrix} \tag{3.42}$$

where now the φ, χ are the particle/antiparticle scalar wavefunctions. There is now complete identity between (3.40) and (3.42). This identity has implications on the kind of symmetry-breaking described by the (3.34) hamiltonian, which we shall describe later.

The equations of motion have the following eigenvalues:

$$\begin{vmatrix} E_k - E_0 & -\varepsilon_k \\ -\varepsilon_k & E_k + E_0 \end{vmatrix} = 0 \Rightarrow E_k = \pm\sqrt{E_0^2 + \varepsilon_k^2} \tag{3.43}$$

The above spectrum is identical to the BCS spectrum but originates from a completely different Hamiltonian. We can solve the equations using the Bogoliubov-Valatin transformation for superconductivity [63]:

$$c_k = u_k\alpha_k + v_k\alpha_{-k}^\dagger \qquad c_{-k}^\dagger = -v_k\alpha_k + u_k\alpha_{-k}^\dagger \tag{3.44}$$

The condition that the operators $\left(\alpha_k^\dagger, \alpha_k\right)$ are fermions gives:

$$u_k^2 + v_k^2 = 1 \tag{3.45}$$

Using (3.44) in (3.35) we get:

$$E_k u_k = -\varepsilon_k v_k + E_0 u_k \Rightarrow 2E_0 u_k v_k = \varepsilon_k\left(v_k^2 - u_k^2\right) \tag{3.46}$$

We now substitute:

$$u_k = \cos(\theta/2), v_k = \sin(\theta/2) \Rightarrow \tan\theta = -\varepsilon_k/E_0 \tag{3.47}$$

to obtain

$$u_k^2 = \frac{1}{2}\left(1 + \frac{E_0}{E_k}\right), v_k^2 = \frac{1}{2}\left(1 - \frac{E_0}{E_k}\right) \tag{3.48}$$

The ground state is the same as for BCS:

$$\alpha_k |0\rangle = 0 \Rightarrow |0\rangle = \prod \alpha_{-k}\alpha_k |vac\rangle = \prod \left(u_k + v_k c_k^\dagger c_{-k}^\dagger\right) |vac\rangle \tag{3.49}$$

And the diagonalized Hamiltonian is:

$$H = \sum E_k \alpha_k^\dagger \alpha_k \tag{3.50}$$

We see from (3.48) that when there is no free-fermion present (i.e. if we put $E_0 =$ 0in (3.37)) the ground state has equal numbers of fermions and holes, that is vortex and anti-vortex core pairs. The symmetry between particles and holes is broken by the free fermion (or hole), and the sign of the symmetry-breaking parameter E_0 determines which kind is present. The hole is with respect to the equilibrium occupation by pairs of fermions in the ground-state as we describe previously for the phonon-roton branch. The symmetry-breaking parameter E_0 is identical to the mc^2 parameter in the 2D Dirac equations-of-motion (3.42). The symmetry that is broken by choosing a non-zero mc^2 in two-dimensions is the time-reversal symmetry (TRS) [64]. This is in agreement of our interpretation of the free fermion as a free element of a vortex-core. A vortex core has a defined sense of vorticity which is reversed under time-reversal, therefore breaking TRS.

We again mention the fact that had we used Bose operators in the Hamiltonian (3.34) the energy spectrum would be:

$$E_k = \pm\sqrt{E_0^2 - \varepsilon_k^2} \tag{3.51}$$

which has energy reduced compared with the bare energy E_0, unlike the experimental spectrum and again justifying our choice of fermi-statistics.

In Fig.(4.1) we plot the functions u_k^2, v_k^2 using the experimental phonon-roton spectrum for ε_k and: $E_0 = 2\Delta$. We see that for all momenta the excitation is almost a pure fermion (or hole) with the maximum mixing at the termination of the phonon-roton branch, where we have:

$$k_m \simeq 2.5\mathring{A}^{-1}, \varepsilon_{k_m} \simeq E_0 \Rightarrow v_{k_m}^2 = \frac{1}{2}\left(1 - \frac{1}{\sqrt{2}}\right) = 0.146$$

At low momenta the fermion will behave like a relativistic particle with the sound-velocity as the limiting velocity.

The excited state can be written as:

$$|1\rangle = \alpha_k^\dagger |0\rangle \tag{3.52}$$

A single excitation of a state k is therefore just a destroyed fermion-pair and a free fermion. This has energy E_k (3.43), unlike the case of BCS where the excitation has twice this energy.

The excited states can form a wavepacket:

$$|\Psi_{ex}\rangle = \sum \beta_k \alpha_k^\dagger |0\rangle \tag{3.53}$$

where β_k are general coefficients. The resulting density fluctuation caused by the wave-packet (3.53) is:

$$\begin{aligned} \langle \Psi_{ex} | \rho(r) | \Psi_{ex} \rangle &= \sum \left\langle c_k^\dagger c_k \right\rangle e^{ikr} = \sum e^{ikr} \left[2v_k^2 + \left(u_k^2 - v_k^2 \right) \alpha_k^\dagger \alpha_k \right] \quad (3.54) \\ &= 1 + \sum e^{ikr} \left(u_k^2 - v_k^2 \right) |\beta_k|^2 \end{aligned}$$

The first term of (3.54) is just the uniform background density (which we normalized to 1). The second term is due to the excitation. We can plot the function $(u_k^2 - v_k^2)$ to see the nature of the excitation at each wavevector k (Fig.4.1). We see that at $k = 0$ the excitation is a single fermion but that at higher wavevectors the excitation is slightly mixed and the density is reduced from 1.

In the absence of symmetry-breaking we have $u_k^2 = v_k^2 = 1/2$ and the excitation causes no density fluctuation.

3.10 Comparison with experimental results

In Fig.4.2 we plot the spectrum of (3.43) using for ε_k the experimental phonon-roton spectrum [52] and: $E_0 = 2\Delta$. We also plot the position of the peaks in the experimental scattering profile, collected from various sources [65]. There is a large uncertainty in the results due to insufficient resolution. We see that in the range of momenta $k \leq 1.2\mathring{A}^{-1}$ the calculated and experimental spectrums agree extremely well. At high pressure there is less data, but the agreement is also very good, even up to $k \sim 1.5\mathring{A}^{-1}$. At higher momenta the isolated peaks in the scattering tend to disappear and change to broad distributions. It is possible that the disappearance of the sharp peak above $k \sim 1.5\mathring{A}^{-1}$ is due to the crossing of the spectrum by the free-particle spectrum, which becomes the dominant feature at high momenta.

It is noticable that there is a second distinct line of peaks above our calculated spectrum. We can estimate this spectrum by assuming it to be two free-vortex-cores, superimposed or a twice excited vortex-core. The energy of this excitation can be approximated as:

$$E_2 \simeq 2E - E_0 \quad (3.55)$$

where we substracted the energy of a bare-core since it is included twice in the first term. In fig. (2) this spectrum is also plotted, and is seen to correspond very well to the second peak in the experimental results.

In Fig.4.3 we show the results of [66] for the structure-factor $S(k, \omega)$ at s.v.p. and compare them with the theoretical expressions of (3.43) and (3.55). The agreement between the peaks' position in the experimental contours and the theory is very good except at momenta approaching the crossing of the free-particle spectrum, which dominates at high momentum transfers.

As for the phonon-roton branch we took the density of fermion-pairs at each momentum as proportional to the scattering intensity of neutrons:

$$I = I_0 n_k^{pair} k^2 \quad (3.56)$$

where I_0 is a normalization factor. This is due to the ground-state having a finite population of fermion-pairs (3.49). The pair-number density is given by:

$$n_k^{pair} = \left\langle c_k^\dagger c_{-k}^\dagger \right\rangle = v_k u_k = \frac{1}{2}\frac{\varepsilon_k}{E_k} = \frac{1}{2}\frac{1}{\sqrt{(E_0/\varepsilon_k)^2+1}} \tag{3.57}$$

Putting (3.57) in (3.56) we plot in Fig.4.4 the theoretical intensity compared with the experimental results [52]. The theoretical calculation was normalized to agree with the experiments by having in (3.56): $I_0 \simeq 0.7$. The agreement is very good except at momenta higher than the termination point of the phonon-roton spectrum: $k_m \simeq 2.5\mathring{A}^{-1}$. It must also be remembered that the experimental results give the strength of the entire high-energy spectrum and not just the distinct 'multiparticle'-branch. For most momenta there appears to be good correlation between the strength of the sharp peak and the entire high-energy tail, but they are not identical.

3.11 Equivalent magnetic Hamiltonian

In comparison with the BCS problem we see that here the symmetry-breaking parameter is a finite density of unpaired fermions: $\left\langle c_k^\dagger c_k \right\rangle \neq 0$. The ground-state without unpaired fermions is a 'vaccum' of pairs of particle-holes in equal numbers. In the BCS problem the symmetry-breaking parameter is a finite pair-density: $\left\langle c_k^\dagger c_{-k}^\dagger \right\rangle \neq 0$. The ground-state in the absence of electron pairing is just a finite density of electrons below the fermi-energy and zero above. In this respect the two problems are 'complementary'.

Similar to the Anderson [67] transformation of the BCS problem to a magnetic Hamiltonian we can transform (3.34) using:

$$\begin{aligned} n_k &= c_k^\dagger c_k \qquad c_k^\dagger c_{-k}^\dagger = \sigma_k^-/2 \qquad c_k c_{-k} = \sigma_k^+/2 \\ &\Rightarrow \quad n_k n_{-k} = \begin{pmatrix} 1 & 0 \\ 0 & 0 \end{pmatrix} = \frac{1}{2}\left(\sigma_k^z + 1\right) \qquad c_k^\dagger c_{-k}^\dagger + c_k c_{-k} = \sigma_k^x \end{aligned} \tag{3.58}$$

where the σ_k are Pauli spin-1/2 operators. The basis is such that an up-spin in the $\hat{z}$-direction represents an empty pair, while a down-spin represents an occupied pair.

The resulting Hamiltonian is:

$$H_{mag} = \sum \varepsilon_k \sigma_k^x - \frac{1}{2}\sum V_k \left(\sigma_k^z + 1\right) \tag{3.59}$$

This Hamiltonian describes a fictitious magnetic field acting on the spin $\overrightarrow{\sigma}$:

$$\overrightarrow{B} = \varepsilon_k \hat{x} - \frac{1}{2} V_k \hat{z} \tag{3.60}$$

We can replace the potential energy with the constant: $V_k = E_0$, for all $k \leq k_m$. The magnetic field (3.60) can be compared with the BCS result:

$$\overrightarrow{B}_{BCS} = \varepsilon_k \hat{z} + \frac{1}{2} V \sum \left(\sigma_k^x \hat{x} + \sigma_k^y \hat{y}\right) \tag{3.61}$$

The alignment of the spins in the ground-state is shown for the two cases in Fig.4.5.

In the BCS problem the sign of the symmetry-breaking field in (3.61) has to be positive and to induce a ferro-magnetic interaction between the spins, otherwise there will not be any rotation of the spins. Only when the spins rotate do they go through the point where the spin is entirely in the xy-plane. At this point the state has no defined occupation number but a well defined phase, while on both sides of the domain-wall there is well defined occupation and no phase. The phase is just the angle of the spin in the xy-plane, and the broken-symmetry is therefore U(1).

In the Dirac case the symmetry-breaking field in (3.60) is a constant external field. It can have both signs, which control the direction along the z-axis that the rotated spin has in the middle of the domain-wall. This spin describes if a particle or a hole is occupied, while away from the $\varepsilon_k = 0$ point the spins are more in the xy-plane, with well defined phase. The symmetry that is broken is therefore the binary $\pm$ symmetry.

This again shows the complementary nature of the two Hamiltonians.

3.12 Conclusion

We have shown that the excitation spectrum of superfluid ^4He can be described quantitatively by assuming the existence of two kinds of excitations. A first one is provided by the delocalized density fluctuations whose energies are given by the Feynman variational ansatz. Those excitations describe the long range properties of the liquid and depend weakly on the quantum statistics. There are in that sense analogous to the zero sound in normal ^3He as emphasized by Pines [18]. In contrast, the second set of excitations describes the short range order in the system resulting from the exchange of atoms, a situation where the Bose-Einstein quantum statistics is relevant. We have assumed that these excitations instead of being independent are coupled in a way reminiscent from the case of excitons in dielectric systems. By writing a phenomenological Hamiltonian together with the dipolar approximation to describe this coupling, we obtained as a result of the diagonalization of the total Hamiltonian an excitation spectrum which involves two sets of hybridized modes. One corresponds to renormalized phonons of energy given by the Feynman result shifted by a factor of two to lower energies. The second set can be interpreted as vortex-loop modes which as a result of the coupling to the phonons do have a dipolar interaction. This picture describes quantitatively the experimental results obtained either from the energy spectrum, the neutron or Raman scattering data or critical velocity experiments. In addition, it may help understanding the persistence of the phonon peak above T_λ which appears to be shifted upwards in energy together with a sharp drop of both the maxon and roton peaks. Since the localized excitations depend on the superfluid order, they will vanish at the transition to the normal state, while the Feynman density modes will remain unaffected and only shifted upwards in energy in the abscence of dipolar coupling $X(k)$.

We propose therefore that the superfluid state is characterized by the appearance of a coherent-state of localized modes due to the dipolar coupling $X(k)$. The

order parameter which is usually taken as the condensate fraction can therefore be identified with this function as we showed. This function is reminiscent of the superconducting gap-function $\Delta(k)$, which in both cases indicate an interaction that reduces the ground-state energy, leading to the phase-transition and symmetry breaking. At the transition temperature T_λ the coupling $X(k)$ vanishes along with the condensate-fraction. We therefore predict that the roton minimum Δ should vanish at the transition. There are indications that this is indeed the case [68].

In comparison with the description of the excitation spectrum put forth by Griffin and Glyde [17], we treat the spectrum not as a combination of two distinct excitations that replace each other at a certain momentum, but as a continuous single excitation. In this respect we support the position that the spectrum is describable as a single excitation-mode along its entire length.

We shall now comment on the connection with the PIMC calculations of the superfluid done by Ceperley et. al [19]. In those calculations a small number of atoms are calculated using path-integral method, taking into account the real inter-atomic potential between two Helium atoms. The results for the specific heat, superfluid fraction and internal energy are very close to the experimental values. What is the relation between our work and the PIMC calculations ?

The superfluid phase in our picture is a phase where we have a coherent field of dipoles which oscillate in resonsnce. Such a coherent state has a specific phase at each point in space, and in the ground-state the phase is everywhere the same.

In the path-integral calculations it is found that the superfluid phase is characterized by having long-range permutation cycles. Due to the repulsive hard-core interaction the lowest energy (and largest weight) configuration is such that the permutation cycles are parrallel straight lines. In these configurations the atoms in the same 'time-slice' can always be in the minimum of their inter-atomic potntial so that the energy is minimized. The direction of the lines is arbitrary in a homogeneous system, but once chosen by some external field it breaks the gauge invariance. It is these macroscopic cycles which span the entire system that define the superfluid fraction and condensate fraction. We therefore find that both pictures assign the superfluid state with a coherent field in a particular direction in space. In one case the coherence is of vortex-core pairs which condense at $k = 0$, while in the second case it is the Helium atoms themselves. We see that the permutation-cycles is the necessary ingredient in the PIMC calculation, analogous to the synchronous dipole interaction $X(k)$ in the localized-mode case.

We also give analytical expressions for the reduction in the ground-state energy and the condensate fraction. Both compare well with the experimental results. These results show that the superfluid order is the coherent state of the fluid where there is a long-range dipolar hybridization of the localized motion of the atoms. This allows the reduction in the zero-point energy of the fluid through the macroscopic condensation of the atoms, leading to superfluidity.

In addition we have shown that a Fermi-like anti-phase vortex-core excitation can describe the high-energy 'multiparticle'-branch of the spectrum of superfluid ^{4}He. The comparison with experiments for both the energy spectrum and the scattering-intensity is very good and we also describe the multi-peak structure seen in the

spectrum. Our work departs from the usual interpretations of this spectrum which ascribe it to multi-particle excitations of the phonon-roton branch. These interpretations cannot describe the shape of the excitation spectrum or it's scattering intensity. We treat it is a continuos branch of elementary excitations unique to the superfluid phase. The anti-phase localized-mode is treated as a fermion, while in the begining of this section it was treated as a boson . The statistical description of this excitation depends on its phase relation with the coherent superfluid background. The resulting effective Hamiltonian produces Dirac's equations of motion for a single particle. This Hamiltonian is diagonalized using the mean-field technique and compared to the BCS result for superconductivity. It is shown that the two Hamiltonians are complementary.

The free vortex-core has therefore some of the properties of a free massive fermion in a vacuum. At small momenta where the phonon spectrum is linear it behaves like a sound-relativistic particle, i.e. the sound velocity replaces the velocity of light in the relativistic expression for the energy.

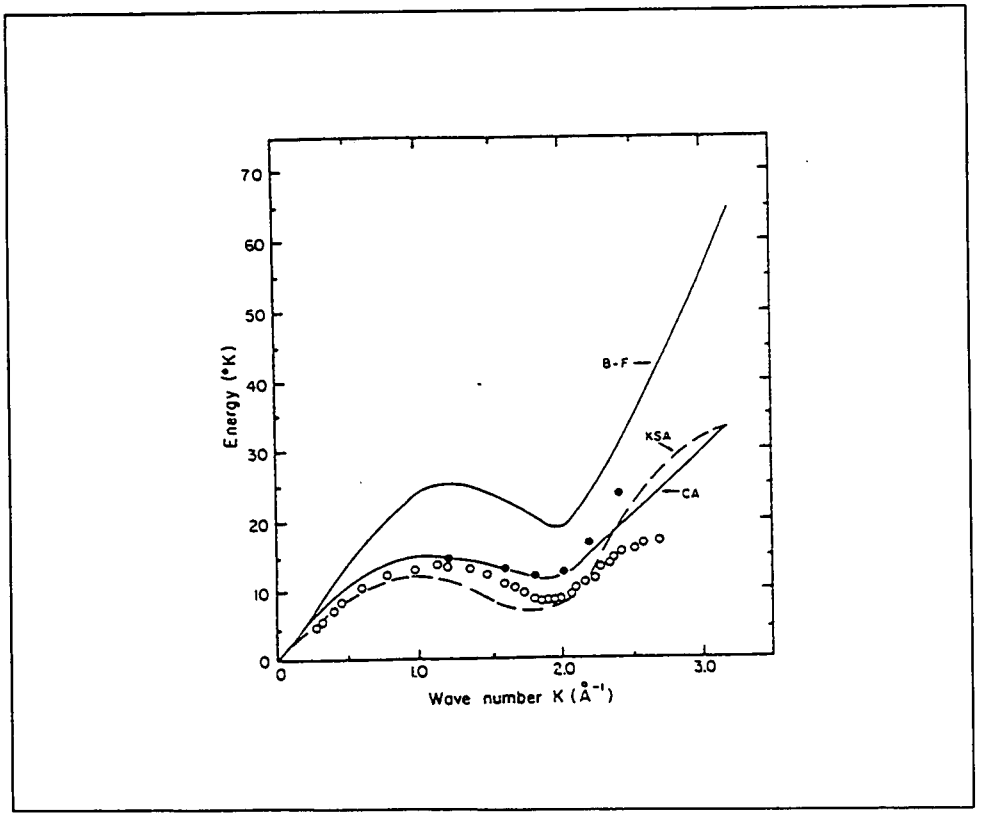

Figure 3.1: The experimental spectrum compared with the Feynman spectrum (eq. (3.1)) and more elaborate calculations [70].

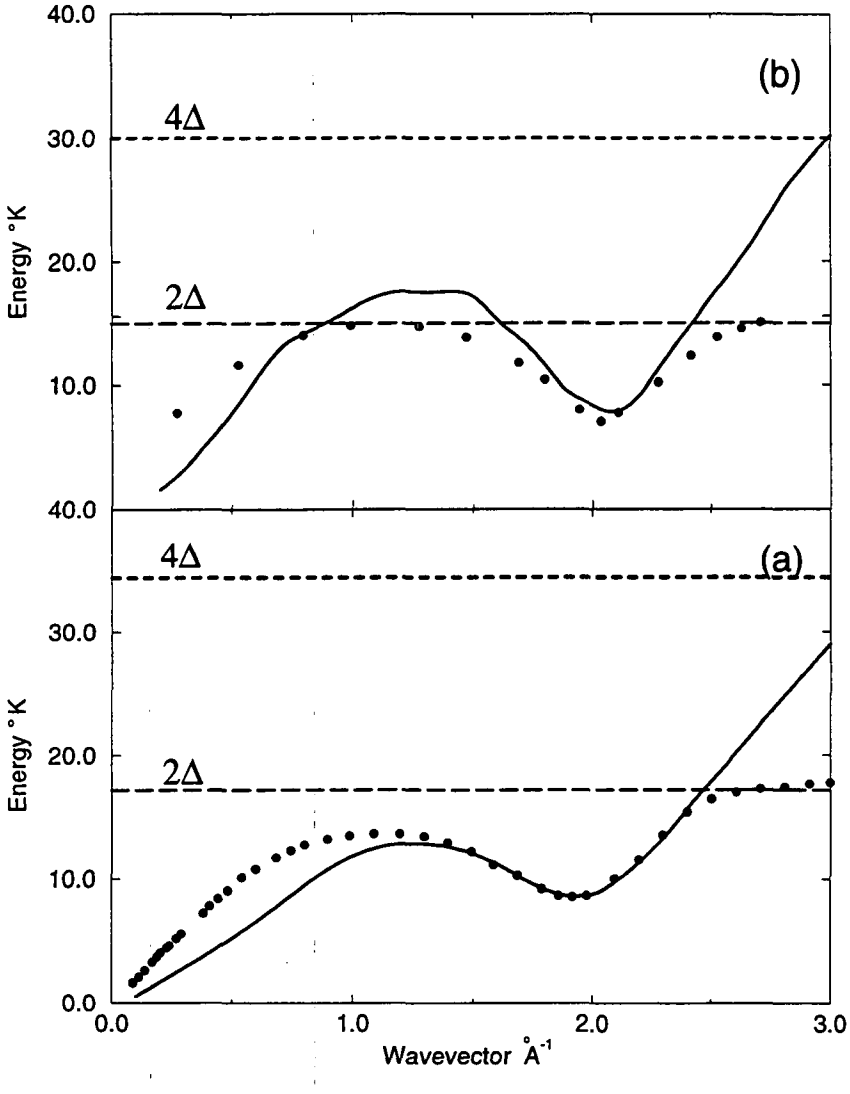

Figure 3.2: Comparison between the experimental energy spectrum [52,71](points) and the theoretical expression (3.18)(solid line) where the structure factor $S(k)$ is obtained from independent measurements [72,73]. (a) and (b) correspond respectively to the saturation vapor pressure and to P= 24 atm. The dashed line at 4Δ indicates the position of the branch of the vortex-loop excitations.

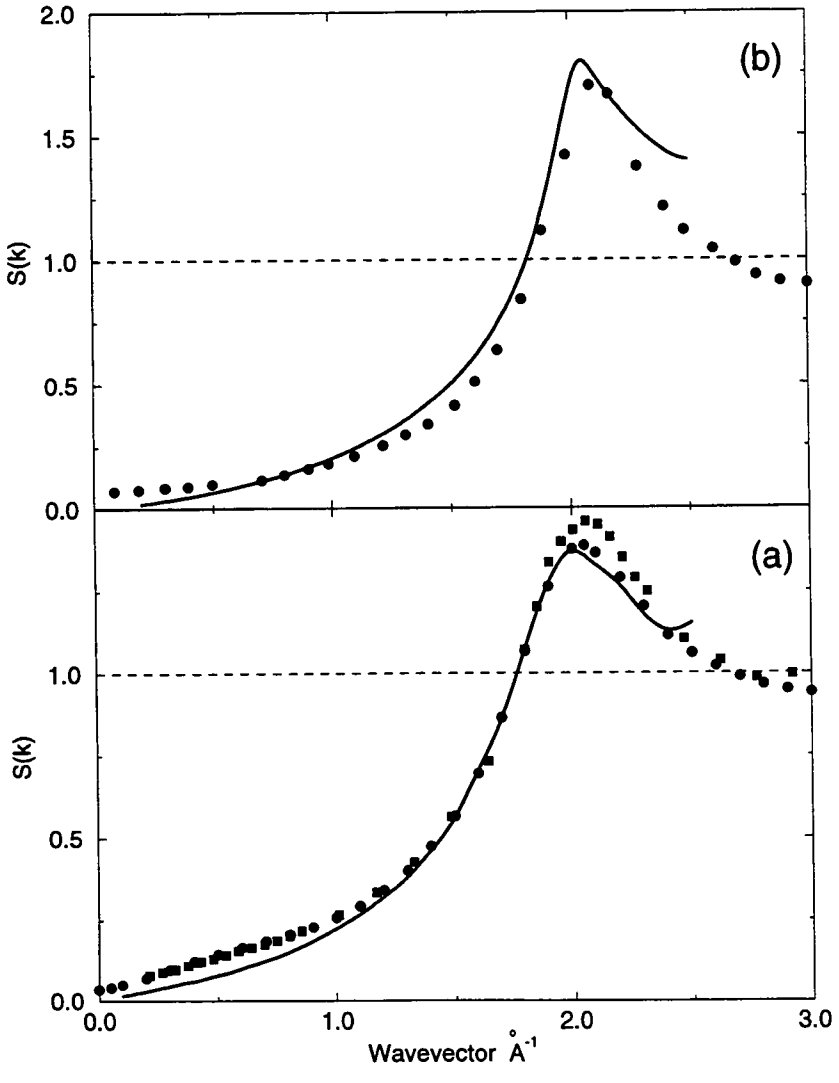

Figure 3.3: Comparison between the experimental structure factor $S(k)$ [72,73,54](points) and the expression (3.18) (solid line) for the same two pressures as in fig.(3.2) where the energy $E(k)$ is obtained from independent measurements [52,71].

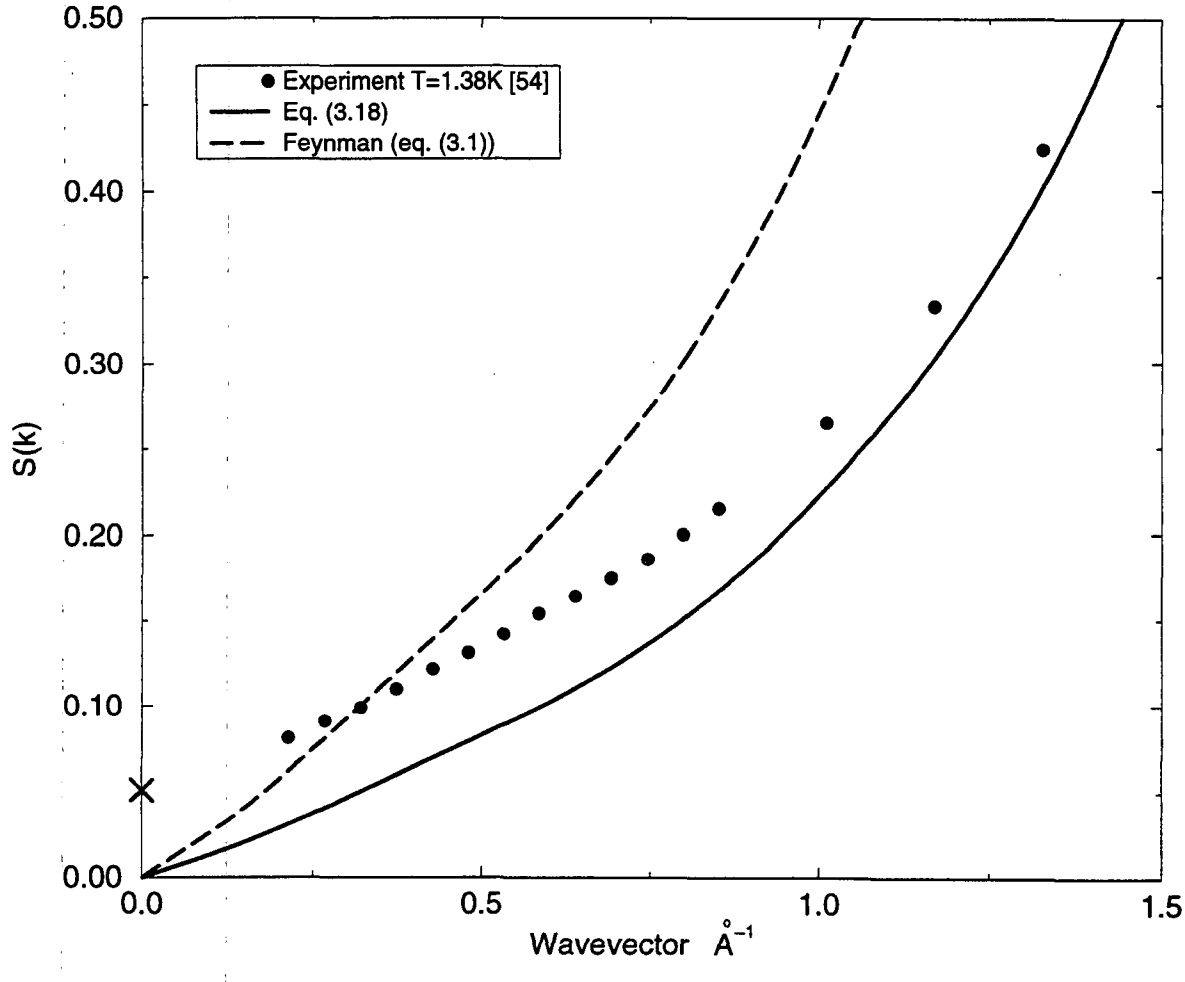

Figure 3.4: Comparison between the experimental structure factor $S(k)$ [54] (points) and the expression (3.18) (solid line) at $k \to 0$ for $T = 1.38^{o}K$ and $T = 1.1^{o}K$. The dashed line is from the Feynman relation (3.1) using the experimental energy spectrum [52]. The star and X mark the theoretical $S(k = 0)$ at the respective temperatures according to (3.22).

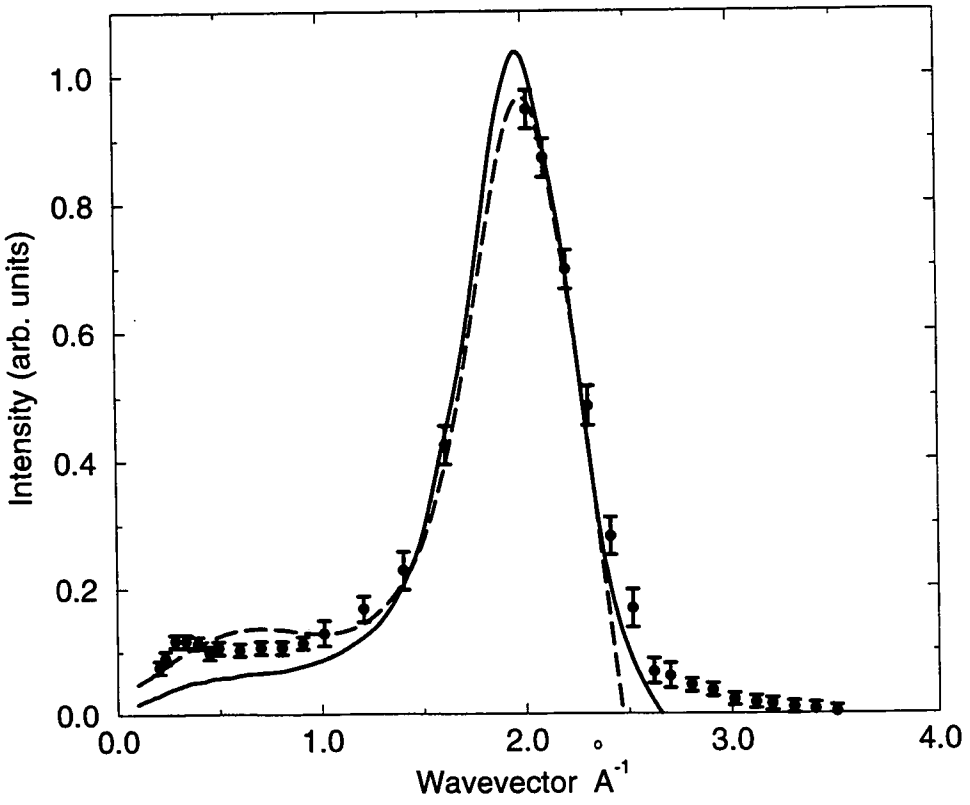

Figure 3.5: Comparison between the experimental scattering cross-section [52] $Z(k)$ of single quasi-particle excitations (points) at 1.1 K and the theoretical expression (3.25). The two curves are obtained using respectively in (3.25) the experimental results for $S(k)$ [54](solid line) and for the energy $E(k)$ [71](dashed line).

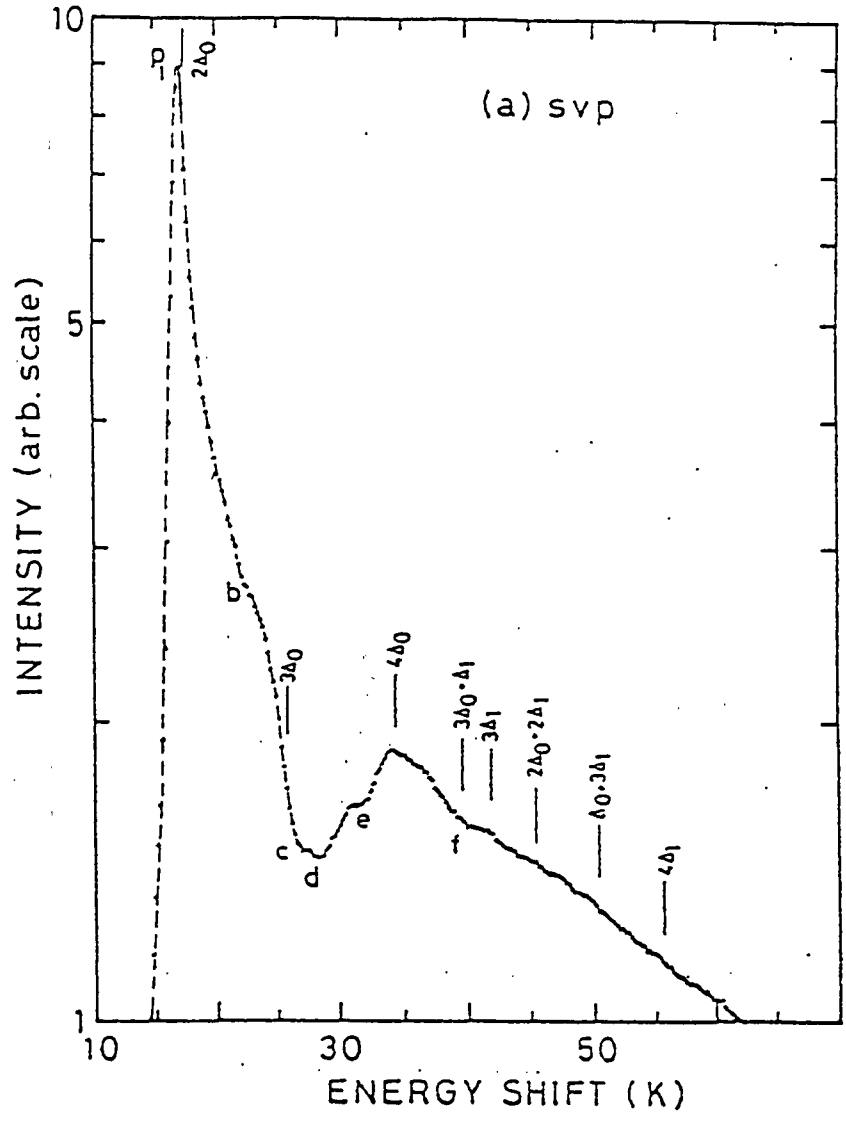

Figure 3.6: The experimental Raman scattering around $k = 0$ [20]. The peaks at energies 2Δ and 4Δ are marked. There is no 3Δ peak.

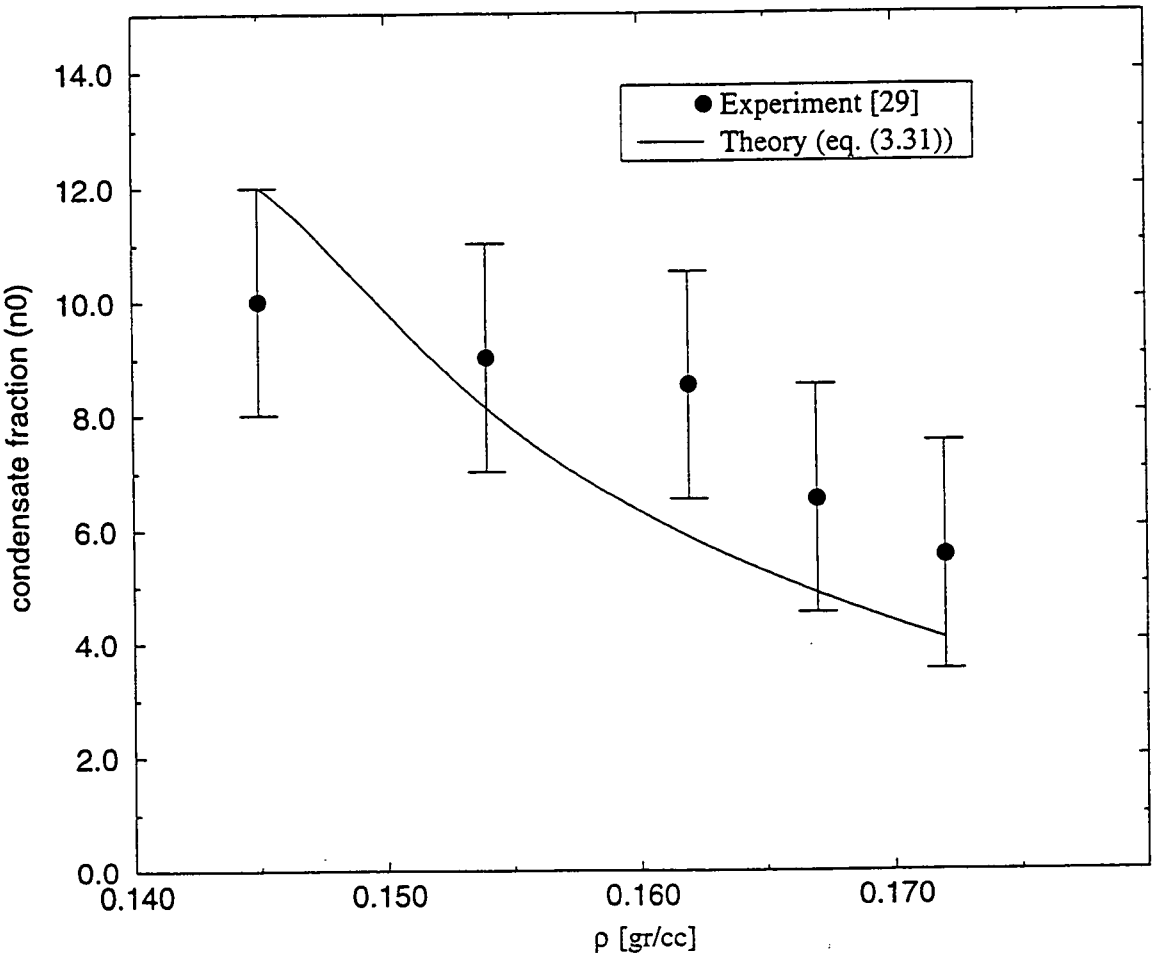

Figure 3.7: Comparison between the experimental condensate fraction at different pressures [29] and the relation (3.31) suitably normalized.

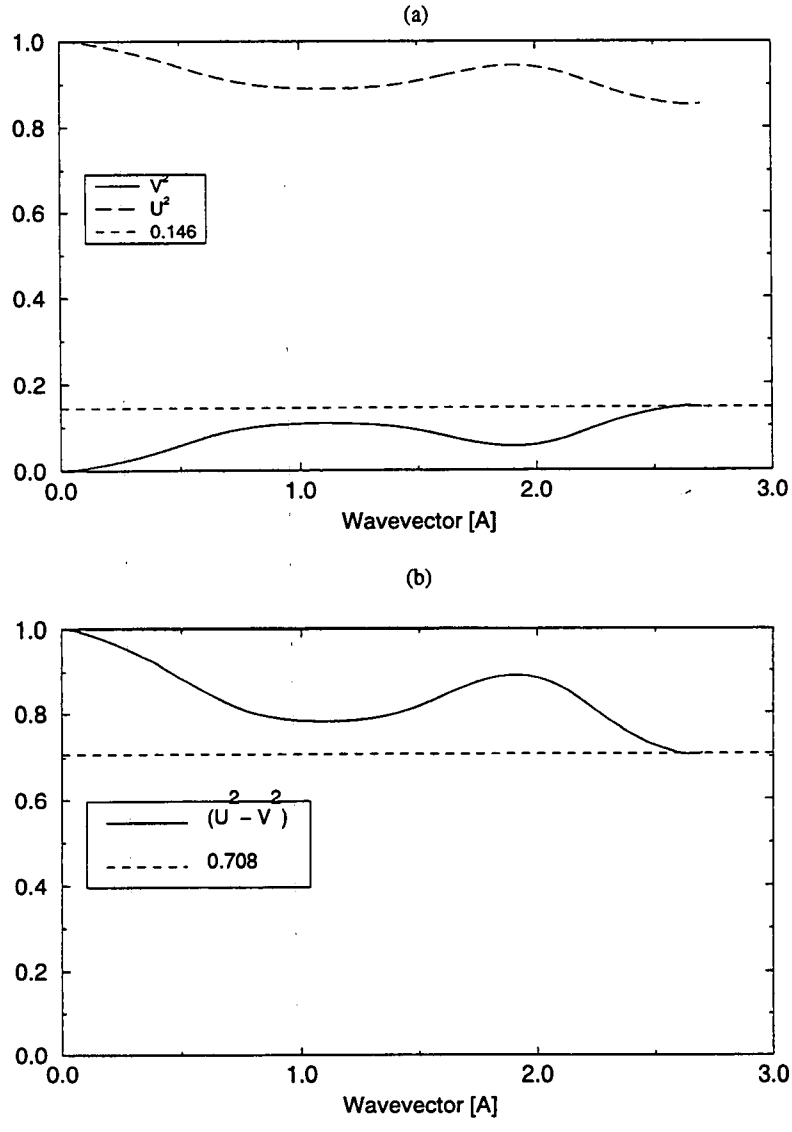

Figure 3.8: The Bogoliubov factors of the diagonalization $u(k)^2, v(k)^2$ (3.48), and the density of an excited state $u(k)^2 - v(k)^2$ (3.54).

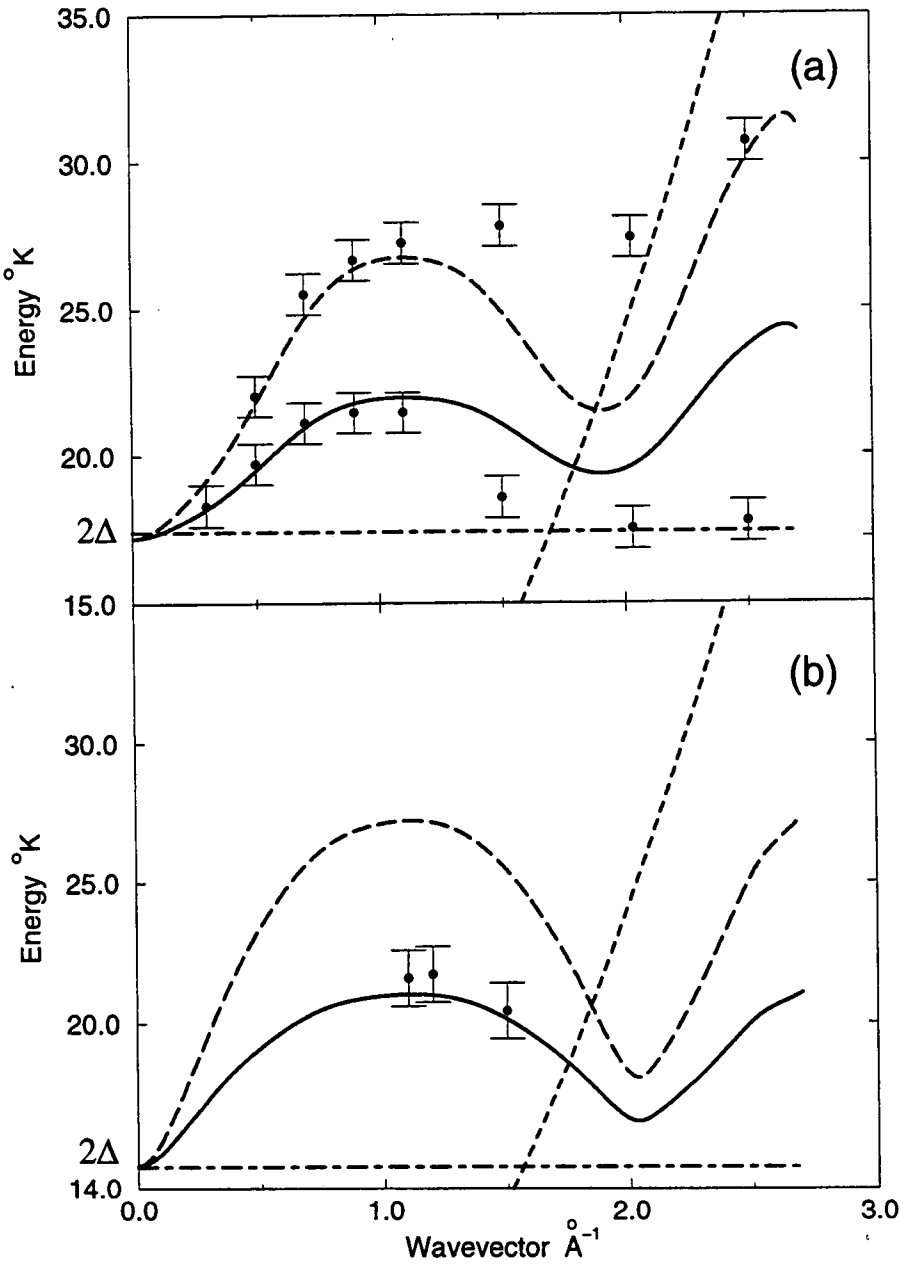

Figure 3.9: Theoretical spectrum compared with experimental peak position [65]: (a) S.V.P. (b) P=24atm. Solid line: eq.(3.51), dashed line: eq.(3.55), short-dashed: free particle.

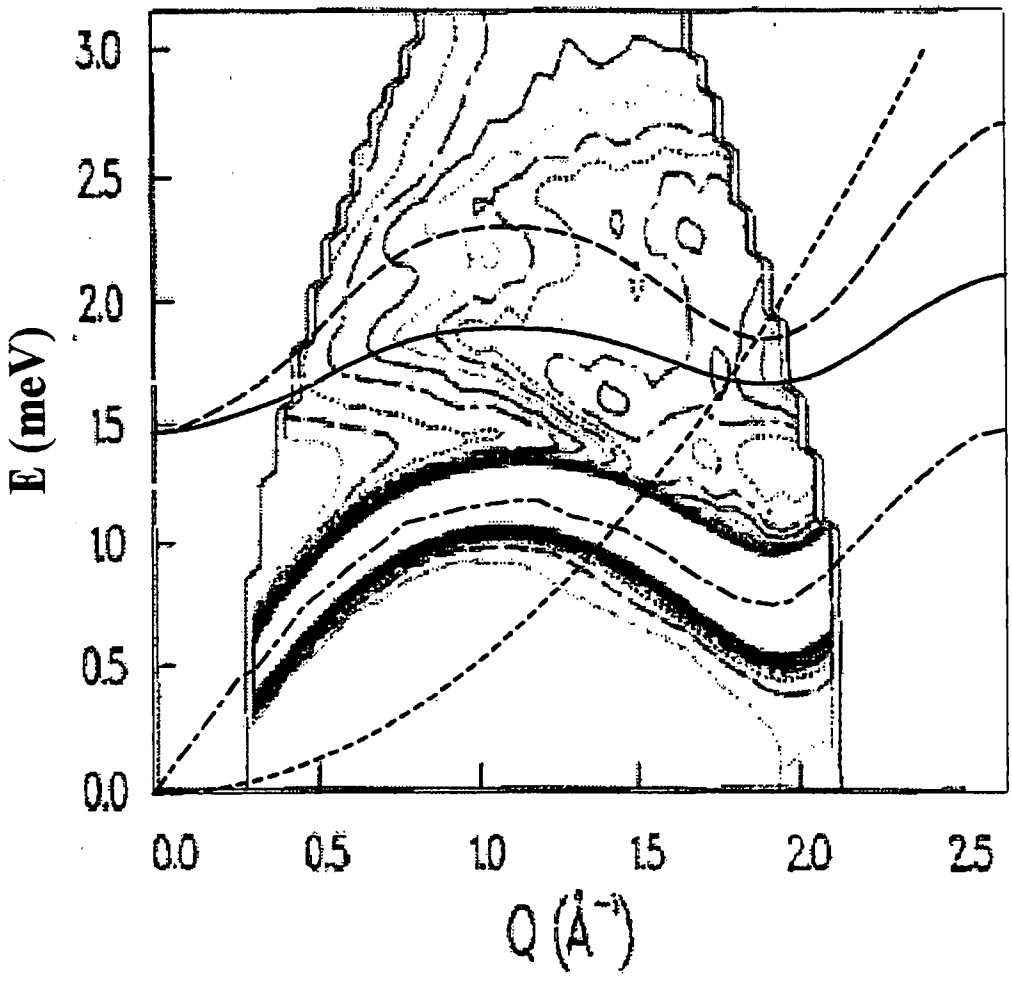

Figure 3.10: Contours of the experimental scattering intensity [67] compared with theoretical calculations. Solid line: eq. (3.51),long dashed: eq.(3.55),dash-dot: phonon-roton spectrum, short dashed: free particle.

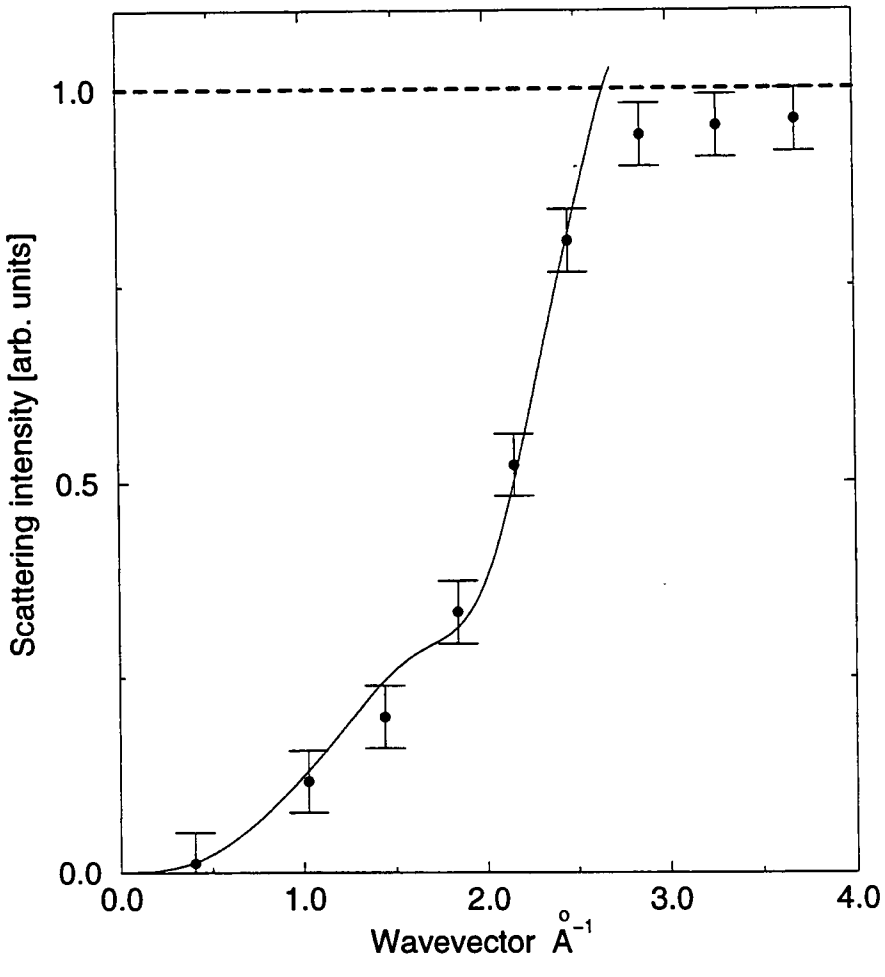

Figure 3.11: Scattering-intensity of the 'multiparticle'-branch. Theory (solid line) from eq.(3.56,3.57) compared with experiment [52].

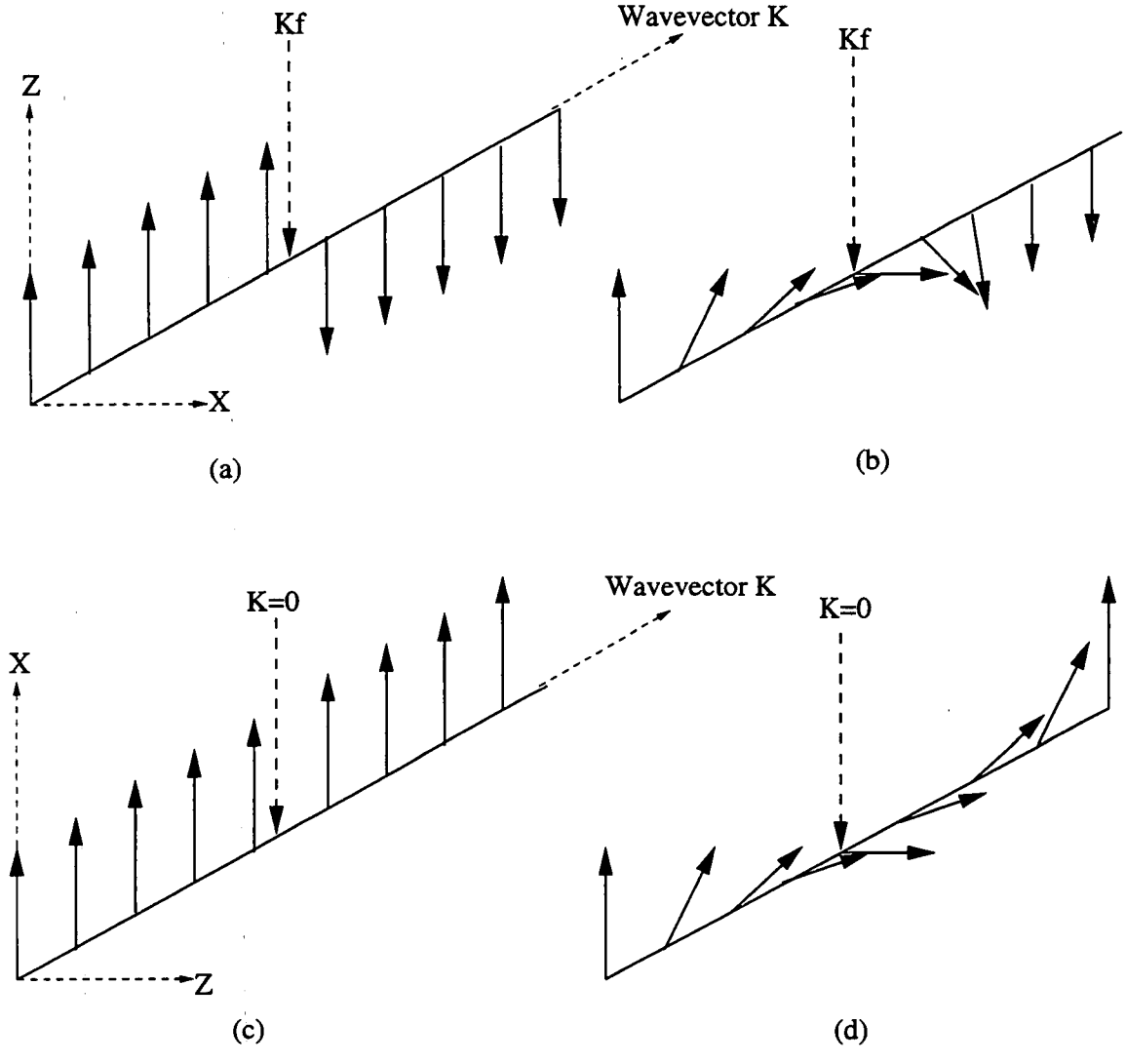

Figure 3.12: Arrangement of the spins in the magnetic-analogue-Hamiltonian. BCS: (a) without pairing, (b) with pairing. Dirac: (c) without unpaired fermion, (d) with unpaired fermion.

Appendix A: Comparison with the Klein-Gordon Hamiltonian

We would like to point out that the Hamiltonian describing excitons (localized-modes (3.4)) is actually the same as the Klein-Gordon (KG) Hamiltonian for a single spinless boson, written in its first-order form [69]:

Klein-Gordon:

$$H_{KG} = \varepsilon_k \left(\sigma_z + i\sigma_y\right) + mc^2\sigma_z + e\Phi\hat{1} \tag{A.1}$$

Localized-mode (3.4):

$$H_{loc} = X(k)\left(\sigma_z + i\sigma_y\right) + \hbar\omega_0\sigma_z \tag{A.2}$$

where σ_i is the Pauli matrices, $\varepsilon_k = \hat{p}^2/2m$, e is the electric charge, Φ is the electrostatic potential. The two-component wavefunction of the KG Hamiltonian is:

$$\Psi_{KG} = \begin{pmatrix} \varphi \\ \chi \end{pmatrix}, \varphi = \frac{1}{2}\left(\psi + \frac{i\hbar}{mc^2}\psi^0\right), \chi = \frac{1}{2}\left(\psi - \frac{i\hbar}{mc^2}\psi^0\right) \tag{A.3}$$

where ψ is the original wavefunction of the second-order KG equation, and $\psi^0 = \left(\frac{\partial}{\partial t} + \frac{ie}{\hbar}\Phi\right)\psi$. The two-component "wavefunction" of the localized-mode is: $\Psi_{loc} = \begin{pmatrix} c_k^\dagger \\ c_{-k} \end{pmatrix}$. The definition (A.3) is the same as the Bogoliubov transformation (3.7), as we now show (for the simple case $\Phi = 0$):

Klein-Gordon:

$$\begin{aligned} \varphi &= \frac{1}{2}\left(1 - \frac{E}{mc^2}\right)\psi, \chi = \frac{1}{2}\left(1 + \frac{E}{mc^2}\right)\psi \\ \Rightarrow \tilde{u} &= \frac{1}{2}\left(1 + \frac{E}{mc^2}\right), \tilde{v} = \frac{1}{2}\left(1 - \frac{E}{mc^2}\right) \\ &\Rightarrow \tilde{u}^2 - \tilde{v}^2 = E/mc^2 \end{aligned} \tag{A.4}$$

We see that the KG density is not normalized to 1 but to: $\langle\rho\rangle = E/mc^2$, describing the relativistic increase in the density with velocity. In order to compare with (3.7) we will normalize the KG density to 1, and identify from (A.1) and (A.2): $\hbar\omega_0 \leftrightarrow mc^2$, $x(k) \leftrightarrow \varepsilon_k$. The result is:

$$\begin{aligned} u^2 &= \frac{1}{2}\left(\frac{\hbar\omega_0 + x(k)}{E} + 1\right) = \frac{1}{2}\left(\frac{mc^2 + p^2/2m}{E} + 1\right) = \frac{mc^2}{2E} + \frac{p^2}{4mE} + \frac{1}{2} \\ &= \frac{mc^2}{2E} + \frac{E}{4mc^2} + \frac{1}{2} = \frac{mc^2}{4E}\left(1 + \frac{E}{mc^2}\right) = \tilde{u}^2\frac{mc^2}{E} \end{aligned}$$

The peculiarities of the KG equation appear when there is a potential $V = e\Phi$ (the Klein paradox for example). The equation for the momentum in the KG case:

$$2mc^2\varepsilon_k = \hbar^2c^2k^2 = (E - V)^2 - \left(mc^2\right)^2 \Rightarrow k = \frac{\sqrt{(E - V)^2 - \left(mc^2\right)^2}}{\hbar c} \tag{A.5}$$

becomes the equation for $x(k)$ in the exciton case:

$$x(k) = \frac{(E-V)^2 - (\hbar\omega_0)^2}{2\hbar\omega_0} \tag{A.6}$$

We see from (A.6) that there is a region of energies where the interaction parameter $x(k)$ is positive and a region where it is negative, depending on the potential V. We saw in section I that the superfluid is characterized by a negative $x(k)$ which enables the localized-modes to condense and causes the reduction in the ground-state energy which drives the transition to superfluidity. The excitations with $E > V + \hbar\omega_0, E < V - \hbar\omega_0$ have a positive $x(k)$ and are therefore not contributing to the superfluid order. Such a destruction of the superfluid order is expected in the core of a vortex. A free non-hybridized vortex-core is such an excitation, and we see that it indeed costs at least $|\hbar\omega_0|$ to create [58].

Just as in the KG case the destruction of the vacuum occurs when there are particle-antiparticle pairs created with energy $2mc^2$. In the superfluid case this is $2\hbar\omega_0$ which is the energy of the second branch in (3.5) identified as the intrinsic vortex-loop excitation of the superfluid.

The density of the KG equation is identified as charge density with the particle and antiparticle having opposite charge. If we look at the density for the excitons we get:

$$\rho_{KG} = \frac{E-V}{mc^2} \rightarrow \frac{E-V}{\hbar\omega_0} \tag{A.7}$$

What is the meaning of the different signs of the density (A.7) in the superfluid case ? A possible meaning is that the field of resonating dipoles (excitons) can have two configurations shifted by π. These two configurations are identical with respect to the energy spectrum. We can therefore identify two "charges" for the superfluid to distinguish between the two shifted phases.

If we compare the KG Hamiltonian (A.1) and the WIBG Hamiltonian (3.8) we have simply that the roles of mc^2 and ε_k are interchanged. In this sense these two Hamiltonians are complementary.

Bibliography

[1] D. Forster, 'Hydrodynamic Fluctuations, Broken Symmetry, and Correlation Functions', 1975.

[2] G. Baym, in 'Mathematical Methods in Solid State and Superfluid Theory', p. 121, 1969.

[3] I.M. Khalatnikov, 'An Introduction to the Theory of Superfluidity', 1965.

[4] R.A. Cowley and A.D.B. Woods, Can. J. Phys. **49** (1971) 177.

[5] R.P. Feynman , Phys. Rev. **94** (1954) 262.

[6] R. P. Feynmann and M. Cohen, Phys. Rev. **102** (1956) 1189.

[7] L. Reatto and G.V. Chester, Phys. Rev. **155** (1967) 88.

[8] J.J. Hopfield, Phys. Rev. **112** (1958) 1555.

[9] S.J. Putterman, 'Superfluid Hydrodynamics', Series in Low Temperature Physics Vol.3,1974,Ed. C.J. Gorter, R. De Bruyn Ouboter and D. De klerk.

[10] J. Wilks, 'The Properties of Liquid and Solid Helium', 1967.

[11] M.P.A. Fisher, P.B. Weichman, G. Grinstein and D.S. Fisher, Phys. Rev. B, **40** (1989) 546.

[12] R.T. Scalettar, G. G. Batrouni and G.T. Zimanyi Phys. Rev. Lett. **66** (1991) 3144; W. Krauth, N. Trivedi and D. Ceperley Phys. Rev. Lett. **67** (1991) 2307; M. Makivic, N. Trivedi and S. Ullah Phys. Rev. Lett. **71** (1993) 2307.

[13] P. Lee and T.V. Ramakrishnan, Rev. Mod. Phys. **57** (1985) 287.

[14] N.N. Bogoliubov ,J. Phys. U.S.S.R. **11** (1947) 23.

[15] E.M. Lifshitz and L.P. Pitaevskii, 'Statistical Physics, Part 2, (1980).

[16] C.N. Yang, *Rev. Mod. Phys.*, **34** (1962) 694.

[17] A. Griffin, 'Excitations in a Bose-Condensed Liquid', Cambridge Studies in Low Temperature Physics, Cambridge University Press (1993).

[18] D. Pines and P. Nozieres,'The Theory of Quantum Liquids',Vol. I: Normal Fermi Liquids, (Addison-Wesley,1966).

[19] Ceperley, Rev. Mod. Phys. **38,** 567 (1995).

[20] K. Ohbayashi, 'Elementary Excitations in Quantum Fluids', 1989, p.32.

[21] E. Varoquaux, W. Zimmermann Jr. and O. Avenel, 'Excitations in Two-Dimensional and Three-Dimensional Quantum Fluids', A.G.F.Wyatt and H.J.Lauter ed. (Plenum 1991).

[22] C. Cohen-Tannoudji, B. Diu and F. Laloe, 'Quantum Mechanics', Vol I,p.648 (1977).

[23] G. Williams, Phys. Rev. Lett. **59** (1987) 1926.

[24] A. D. Speliotopoulos and H.L. Morrison, J. Phys. A: Math. Gen. **24** (1991)

[25] K.O. Friedrichs, 'Special Topics in Fluid Dynamics', 1966.

[26] J.E. Avron, Phys. Rev. Lett., **75** (1995) 697.

[27] M.D. Girardeau, J. Math. Phys. **6** (1965) 1083.

[28] H.E. Hall, Proc. R. Soc. A **245,** 546 (1958).

[29] P.E. Sokol and W.M. Snow, J. of Low Temp. Phys., **101**, 881 (1995).

[30] C.E. Campbell, 'Excitations in Two-Dimensional and Three-Dimensional Quantum Fluids',p.159, (1991).

[31] S. Giorgini, L. Pitaevskii and S. Stringari, J. of Low Temp. Phys. **89** (1992) 449.

[32] D.G. Henshaw, Phys. Rev. **119** (1960) 14.

[33] J. Mayers, J. Low Temp. Phys., **109**, 135 (1997).

[34] A. Griffin and S. Stringari, Phys. Rev. Lett. **76** (1996) 259.

[35] Domb and Green, 'Phase Transitions and Critical Phenomena',**3**, 570 (1974).

[36] E.L. Pollock and D.M. Ceperley, Phys. Rev. B **36** (1987) 8343.

[37] D.D. Awschalom and K.W. Schwarz, Phys. Rev. Lett.**52** (1984) 49.

[38] E. Varoquaux, W. Zimmermann and O. Avenel, 'Excitations in Two-Dimensional and Three-Dimensional Quantum Fluids',p.343, (1991).

[39] K.W. Schwarz, Phys. Rev. Lett. **64** (1990) 1130.

[40] P. Lee and T.V. Ramakrishnan, Rev. Mod. Phys. **57** (1985) 287.

[41] D.J. Thouless, Phys. Rev. Lett., **39** (1977) 1167.

[42] E. Akkermans, J. Math. Phys. **38** (1997) 1781.

[43] S. Miyamoto and Y. Takano, Czech. J. Phys. **46** (1996) 137-140.

[44] R.M. Dimeo, P.E. Sokol, D.W. Brown, C.R. Anderson, W.G. Stirling, M.A. Adams, S.H. Lee, C. Rutiser, and S. Komarneni, Phys. Rev. Lett. **79** (1997) 5274.

[45] A. Paramekanti, N. Trivedi and M. Randeria, cond-mat/9801053 (1998).

[46] P.C. Hohenberg and P.C. Martin, Ann. Phys. **34** (1965) 291.

[47] P.A. Crowell, F.W. Van Keuls and J.D. Reppy, Phys. Rev. Lett. **75** (1995) 1106.

[48] H. Cho and G.A. Williams, Phys. Rev. Lett. **75** (1995) 1562.

[49] for a review see P.Nozieres and D. Pines, The Theory of Quantum Liquids, Volume II: Superfluid Bose Liquids, Addison-Wesley, 1990.

[50] A.D.B. Woods and E.C. Svensson, Phys.Rev. Lett.**41**, 974 (1978), E.F. Talbot, H.R. Glyde, W.G. Stirling and E.C. Svensson, Phys.Rev. **B38**, 11229 (1988) and W.G. Stirling and H.R. Glyde, Phys.Rev. **B41**, 4224 (1990).

[51] H.R. Glyde and A. Griffin, Phys.Rev.Lett. **65**, 1454 (1990).

[52] R.A.Cowley and A.D.B.Woods, Can.J.Phys. **49**,177 (1971).

[53] P.W. Anderson, 'Concepts In Solids', 1963, p.132-148.

[54] H.N. Robkoff and R.B. Hallock, Phys. Rev. B**24**,159 (1981).

[55] A.Miller, D.Pines and P.Nozieres, Phys. Rev. **127**,1452 (1962).

[56] K. Huang, 'Statistical Mechanics',1987, John Wiley and Sons,Inc..

[57] K.Ohbayashi, in "Elementary Excitations in Quantum Fluids" , K.Ohbayashi and M.Watabe ed. (Springer-Verlag 1989).

[58] N.Gov, unpublished results.

[59] Andronikashvili and Malmaladze, *Rev. Mod. Phys.* **38** 567 (1966).

[60] Zurek, *Phys. Rep.* **276** 177 (1996).

[61] Erben and Pobell, *Z. Physik* **49** 177 (1968).

[62] A.L. Fetter, Annals of Phys. **70** 67 (1972); Q. Niu, P. Ao and D. J. Thouless, Phys. Rev. Lett. **72** 1706 (1994). density=0.

[63] C. Kittel, 'Quantum Theory of Solids', p. 165.

[64] M.V. Berry, F.R.S. and R.J. Mondragon, Proc. R. Soc. Lond. A**412** 53 (1987).

[65] H.R. Glyde, 'Excitations in Liquid and Solid Helium', Oxford University Press,1994.

[66] K.H. Andersen, W.G. Stirling, R. Scherm, A. Stunault, B. Fak, H. Godfrin and A.J. Dianoux, *Physica B* **180 & 181** 851 (1992).

[67] P.W. Anderson, *Phys. Rev.* **112** 900 (1958).

[68] E.C. Svensson, W. Montfrooij and I.M. Schepper, Phys. Rev. Lett. **77**,4398 (1996)

[69] G. Baym, 'Lectures On Quantum Mechanics',p. 499, 9th edition 1981.

[70] G.D. Mahan, 'Many-Particle Physics',p. 883, 2nd edition 1990.

[71] R.J. Donnelly, J.A. Donnelly and R.N. Hills, *J. Low Temp. Phys.* **44**,471 (1981).

[72] E.C. Svensson, V.F. Sears, A.D.B.Woods and P. Martel, *Phys. Rev.* **21**,3638 (1980).

[73] D.G. Henshaw, *Phys. Rev.* **119**,9 (1960).

לוקלים (Localized-modes). עירורים לוקלים אלו מייצגים מרכז של מערבולת קוונטית ונובעים מאופי הסטטיסטיקה הקוונטית של האטומים שהם בוזונים ויוצרים מעגלי-החלפה (Permutation-cycles) ביניהם. שני סוגי העירורים אינם בלתי-תלויים אלא קשורים (Hybridized) בצורה הזהה לקשר בין אקסיטון ופוטון בחומר דיאלקטרי. התאור של הקשר אקסיטון-פוטון פותח ע"י הופפילד ואנדרסון ומאפשר לנו לכתוב המילטוניאן אפקטיבי עבור האינטראקציה בין העירורים הלוקלים והפונון של פיינמן. באמצעות קירוב דיפולי של האינטראקציה וע"י הנחה של התאמה-עצמית (Self-consistent) אנו מקבלים את התוצאה הפשוטה הבאה עבור ספקטרום האנרגיה:

הענף הפונוני-רוטוני ניתן ע"י:

$$E(k) = \varepsilon(k)/2 \qquad (4)$$

כאשר $\varepsilon(k)$ היא האנרגיה של פיינמן (3). התוצאה (4) מתאימה באופן טוב ביותר לתוצאות ניסויים בלחץ-רווית-אדים (Saturated-Vapor-Pressure SVP) ובלחץ גבוה.

בנוסף אנו מנבאים קיומו של ענף נוסף באנרגיה של: $E_{vortex-loop} = 2E_0$ כאשר E_0 היא האנרגיה של העירור הלוקלי הערום (bare) ללא אינטראקציות. מכיון שזיהינו את העירור הלוקלי כמרכז מערבולת קוונטית טיבעי לזהות את הענף השני כעירור של לולאה-קוונטית (Vortex-loop). את האנרגיה E_0 טבעי לבחור כאנרגיה שבה מסתיים ספקטרום האקסיטציות הפונון-רוטון ז"א היכן שההיברידיזציה מסתיימת והספקטרום הופך לזה של חלקיק חופשי. אנרגיה זו הינה בערך 2Δ כאשר Δ היא האנרגיה של המינימום הרוטוני ($\Delta \approx 8.6^oK$ ב- T=0 ובלחץ SVP) מכאן שאנרגיית הלולאה הקוונטית היא: $E_{vortex-loop} = 4\Delta \approx 34.4^oK$. אנרגיה זו מתאימה לתוצאות ניסויים של מהירות קריטית דרך מיקרו-חורים שנשלטת ע"י יצירה תרמית של לולאות קוונטיות. בניסויים של פיזור ראמאן נמצא פיזור חזק באנרגיה של 4Δ ואנו מזהים זאת כעדות נוספת לעירור של לולאות קוונטיות באנרגיה של $2E_0$.

בנוסף אנו מקבלים ביטוי אנליטי לתלות עוצמת הפיזור של ניוטרונים בוקטור-הגל k עבור ענף הפונון-רוטון. הביטוי הינו קשר פרופורציה בין עוצמת הפיזור או חתך-הפעולה הדיפרנציאלי וצפיפות הזוגות של עירורין לוקלים במצב היסוד. ההתאמה בין הביטוי שקיבלנו ותוצאות ניסיוניות טובה מאד. זהו ביטוי אנליטי ראשון לעוצמת הפיזור.

התאור הנ״ל מאפשר חישוב של הירידה באנרגיית מצב היסוד של העל-נוזל בהשוואה לנוזל הנורמלי. הערכים שמתקבלים ב- SVP ובלחץ גבוה מתאימים לתוצאות ניסויים. ירידה זו באנרגיה היא שמוליכה למעבר הפאזה מנוזל נורמלי לעל-נוזל. בנוסף מתקבל ביטוי עבור אחוז העיבוי n_0 במונחים של מאפייני ספקטרום האקסיטציות הפונון-רוטון: $n_0 = \frac{\Delta}{mc^2}$ כאשר c היא מהירות הקול (שיפוע הספקטרום ב- $k\to 0$). בהשוואה לתוצאות הניסיוניות הביטוי הנ״ל נותן תוצאה הגדולה בפקטור של 2~ . יש לזכור שבתאור שלנו העיבוי הוא של עירורים-לוקלים והמסה האפקטיבית שלהם במונחים של מסת אטום ^4He יכולה להסביר את הפקטור החסר.

בנוסף לאקסיטציות בענף הפונוני-רוטוני ישנו בעל-נוזל ענף עם אנרגיה גבוהה יותר שבד״כ נקרא ענף רב-חלקיקי (Multiparticle-branch). שמו נובע מהאינטרפרטציה שלו כענף של עירור מספר עירורים בסיסיים של הענף הפונוני-רוטוני. הסבר זה אינו נותן את צורת הספקטרום של הענף ה-׳רב-חלקיק׳ וגם לא את עוצמתו כפונקציה של התנע k. אנו מציעים להתייחס לענף זה כאל עירור של אופן לוקלי כך שהוא באנטי-פאזה ביחס לשדה הזוגות הלוקלים שבמצב היסוד. מכאן שטיבעי להניח סטטיסטיקה פרמיונית עבור עירור זה. אנו מניחים המילטוניאן דירק לתאור הענף ומלכסנים אותו ע״י שדה ממוצע. הספקטרום המתקבל מתאים מאד לתוצאות הניסוי. בנוסף אנו מקבלים ביטוי אנליטי עבור תלות עוצמת הפיזור של העירור כפונקציה של k, וגם כאן ההתאמה לניסוי טובה מאד.